



universität
wien

DISSERTATION

Titel der Dissertation

The Use of Remote Sensing to Evaluate and Detect Desert
Regions

Verfasser

Chooghi Bairam Komaki MSc.

angestrebter akademischer Grad

Doktor der Naturwissenschaften (Dr. rer.nat.)

Wien, im February 2011

Studienkennzahl lt. Studienblatt: A 091 455

Dissertationsgebiet lt.
Studienblatt: Kartographie und Geoinformation

Betreuerin / Betreuer: Univ.-Prof. Dipl.-Ing. Dr. Wolfgang Kainz

This collection is dedicated to

My dear family,

Parents,

My country,

All with peace and love!

Acknowledgements

First of all, I would like to thank Prof. Kainz, my supervisor, for his kind efforts and guidance in helping me to complete my thesis. I sincerely acknowledge all the valuable assistance he has given me throughout this project, and the positive environment his faculty has provided during my four years at the university. His overall expertise in the field of fuzzy systems in geography has been invaluable, his instruction in fuzzy logic, and innovative ideas, essential in the scientific formulation of my thesis. Prof. Kainz has throughout been central to the creation, quality and fulfilment of this paper.

I would also like to thank the staff at Vienna University, for the provision of their facilities, their support, as colleagues and friends, and for making the overall working environment both pleasant and efficient, especially Prof. Wohlschlägl and Dr. Voit.

I express my sincere appreciation to Prof. Alavipanah for his continuous support, fruitful encouragement and generous guidance during my research period in Vienna, and I am deeply indebted to him for his scientific advice during my education.

I must also acknowledge my gratitude to Dr. Matinfar and Dr. Shamsipour for their contributions and accompaniment in my field work and for spending their valuable time in forwarding suggestions, and allowing me access to their own work. Additionally, I appreciate the cooperation and friendship of my immediate colleagues, Mr. Jokar and Miss Thitirat Panbamrunkij, with whom it was a pleasure to work alongside.

Throughout my studies I have had the unstinting support of my family, without whom the nature of this work would have been entirely different. During the past four years they have given moral and filial encouragement and together made possible the adjustment to a culture entirely different to our own. We have been especially blessed with the birth of our beloved daughter, Ilkai, during my education in Vienna.

Furthermore, I acknowledge the General Office of Scholarship and Overseas Students, Ministry of Science, Research and Technology (MSRT) in Iran, which provided the financial aid and total grant for the four initial years of my research programme – and, of course I would like to pay my respects to the Austrian government for making my stay in Vienna such a pleasant and memorable one.

In closing I would also like to express my gratitude to Mr Alan Jones for his practical assistance as a proof-reader on this project.

Finally I give my greatest thanks to God, who has given me the opportunity to complete my doctorate in Natural Science in Cartography and Geoinformation using remote sensing methods in desert studies.

Abbreviations

Abbreviation/Acronym	Series of Words
AMS	American Meteorological Society
AVHRR	Advanced Very High Resolution Radiometer
BT	Brightness Temperature
CDF	Cumulative Distribution Function
CN	Curve Number
CoA	Centre of Area
CoG	Centre of Gravity
EC	Electrical Conductivity
EOS	Earth Observing System
ERTS	Earth Resources Technology Satellite
ET	Evapotranspiration
ETM	Enhanced Thematic Mapper
FAO	Food and Agriculture Organization
FB	Function Block
FBD	Function Block Diagram
FCL	Fuzzy Control Language
FFC	False Colour Composite
FIS	Fuzzy Inference System
FisPro	Fuzzy Inference System Professional
FL	Fuzzy Logic
GDAL	Geospatial Data Abstraction Library
GIS	Geographic Information Systems
GIScience	Geographical Information Science
HDF	Hierarchical Data Format
HFP	Hierarchical Fuzzy Partitioning
HSG	Hydrologic Soil Groups
IEC	International Electrotechnical Commission
IRMO	Islamic Republic Of Iran Meteorological Organization
ISDR	International Strategy for Disaster Reduction
K	Kelvin
KBCT	Knowledge Base Configuration Tool
km	kilometre
LM	Left most Maximum
LOM	Law Of Minimum
LOT	Law Of Tolerance
LS	Length and Steepness
LST	Land Surface Temperature
MF	Membership functions
MLE	Maximum Likelihood Estimation
MODIS	Moderate-Resolution Imaging Spectroradiometer

Abbreviations (contd.)

Abbreviation/Acronym	Series of Words
MoM	Mean of Maxima
NASA	National Aeronautics and Space Administration
NDVI	Normalized Difference Vegetation Index
NEMA	National Electrical Manufacturers Association
NGO	Nongovernment Organization
NIR	Near Infrared
NOAA	National Oceanic Atmospheric Administration
NRCS	Natural Resources Conservation Service
P	Precipitation
PAR	Photosynthetically Active Radiation
PDF	Probability Distribution Function
PDSI	Palmer Drought Severity Index
PET	Potential Evapotranspiration
PMU	Photomorphic Unit
PPF	Percent Point Function
RM	Right most Maximum
RS	Remote Sensing
RUSLE	Revised Universal Soil Loss Equation
SAR	Sodium Absorption Ratio
SciPy	Scientific Tools for Python
SCS	Soil Conservation Service
SPI	Standardized Precipitation Index
ST	Structured Text
TCI	Temperature Condition Index
TM	Thematic Mapper
UNCCD	United Nations Convention to Combat Desertification
UNCED	United Nations Conference on Environment and Development
UNEP	United Nations Environment Program
UNESCO	United Nations Educational, Scientific and Cultural Organization
USDA	USA Department of Agriculture
USLE	Universal Soil Loss Equation
VCI	Vegetation Condition Index
VHI	Vegetation Health Index
VI	Vegetation indexes
WMO	World Meteorology Organization
WRI	World Resources Institute

Abstract

Remote sensing plays a significant role in providing up-to-date data for the estimating of empirical indices in studying the environment, especially in drylands. The spectral and thermal bands in satellite images are also applied to calculate the indices to detect, identify, and evaluate the natural phenomena in drylands such as land degradation and desertification.

In this project, for the identification of desertification in the Kashan-Qom region in Central Iran, five main indicators of desertification are used as follows: vegetation, land surface temperature, erosion, drought, and flooding; therefore, these indices are selected as Vegetation Condition Index (VCI), Temperature Condition Index (TCI), Revised Universal Soil Loss Equation (RUSLE), and Standardized Precipitation Index (SPI), and runoff (Q), respectively. The multi-spectral satellite images of MODIS are used for the calculation of remotely sensed indices such as Vegetation Condition Index (VCI) and Temperature Condition Index (TCI). Furthermore, the ancillary data-based indices, Revised Universal Soil Loss Equation (RUSLE), and Standardized Precipitation Index (SPI), and runoff (Q), are also estimated. Then several desertification maps are produced in two models: conventional method and fuzzy model. The result of each model is also evaluated, that is, the results are assessed by the supplying of field sampling as ground truth references and the defining of error matrix.

In the fuzzy modelling, a rule-based system is built by expert knowledge and data-induction method. According to the obtained results, even though the accuracy of the fuzzy model is lower than the conventional method, the fuzzy model represents the uncertainty in the classes of resulted desertification by providing a map for each class.

Zusammenfassung

Die Fernerkundung spielt eine signifikante Rolle bei der Bereitstellung von aktuellen Daten zur Schätzung von empirischen Indizes bei Untersuchungen der Umwelt, insbesondere in Trockengebieten. Spektral- und thermische Kanäle in Satellitenbildern werden auch zur Berechnung von Indizes verwendet, um natürliche Phänomene in Trockengebieten – wie etwa Bodendegradation und Desertifikation – aufzuspüren, zu bestimmen und zu evaluieren.

In dieser Arbeit wurden zur Identifikation von Desertifikation in der Kashan-Qom Region im Zentraliran fünf Desertifikationsindikatoren verwendet: Vegetation, Oberflächentemperatur, Erosion, Trockenheit und Überflutungen. Diese Indikatoren wurden dargestellt mit Hilfe von: Vegetationsindex (VCI), Temperaturindex (TCI), Revidierte Universelle Bodenverlustgleichung (RUSLE), standardisierter Niederschlagsindex (SPI) und Abfluss. Multispektrale Bilder des MODIS Satelliten wurden für die Berechnung von VCI und TCI herangezogen. Des Weiteren wurden RUSLE, SPI und Abfluss bestimmt. Schließlich wurden mehrere Desertifikationskarten anhand von zwei Modellen – einem konventionellen Modell und einem unscharfen Modell – erstellt. Die Ergebnisse der Modelle wurden mit Hilfe von Feldproben und der Erstellung einer Fehlermatrix analysiert.

Im unscharfen Modell wurde ein regelbasiertes System aufgrund von Expertenwissen und einer induktiven datengetriebenen Methode erstellt. Obwohl das unscharfe Modell weniger genau als die konventionelle Methode ist, zeigt es die Unbestimmtheit in den Desertifikationsklassen der erstellten Karten.

Table of Contents

Acknowledgements.....	ii
Abbreviations.....	iii
Abstract.....	v
Zusammenfassung.....	vi
Table of Contents.....	vii
List of Figures.....	x
List of Tables.....	xiii
Chapter 1 General Introduction.....	1
1.1 Problem Statement.....	1
1.2 Land Degradation.....	3
1.2.1 Desertification; Terminology and Concepts.....	3
1.2.2 Extent of Desertification in Iran and its Importance.....	8
1.3 Remote Sensing and Desert.....	10
1.4 Research Hypotheses.....	12
1.5 Research Questions.....	12
1.6 Research Objectives.....	12
1.7 Research Approach.....	13
1.8 Dissertation Framework.....	14
Chapter 2 Desertification Indices.....	17
2.1 Empirical Indices.....	18
2.2 Vegetation Indices (VI).....	19
2.2.1 Normalized Difference Vegetation Index (NDVI).....	21
2.3 Land Surface Temperature (LST).....	22
2.4 Flooding (Overland Flow).....	23
2.4.1 Climate Factor.....	24
2.4.2 Watershed Properties.....	24
2.5 Soil Erosion.....	26
2.6 Drought.....	28
Chapter 3 Fuzzy Logic.....	33
3.1 Introduction.....	33
3.2 Uncertainty.....	34
3.3 Linguistic Variables.....	36

3.4	Fuzzy Set.....	36
3.5	Fuzzy Inference System	39
3.5.1	Fuzzification	40
3.5.2	Operators.....	41
3.5.3	Fuzzy Rule Inference	42
3.5.4	Defuzzification.....	44
3.6	Rule-Based System Improvement.....	44
3.6.1	Simplification.....	46
3.6.2	Data Base Reduction.....	47
3.7	Decision-making Principle in Rule-based systems	47
3.7.1	Expert Rules.....	48
3.7.2	Data-based Rule Learning.....	49
3.8	Fuzzy Control Language (FCL)	50
Chapter 4	Description of Study Area.....	55
4.1	Introduction	55
4.2	Qom (Namak Lake) Watershed.....	58
4.3	Geomorphology Characteristics.....	58
4.3.1	Highlands	60
4.3.2	Plains.....	62
4.4	Climate	65
4.4.1	Temperature	66
4.4.2	Precipitation	67
4.4.3	Climate classification.....	70
4.5	Vegetation	73
4.6	Water Resources.....	74
4.7	Soil Characteristics.....	75
Chapter 5	Data Acquisition and Processing.....	77
5.1	Introduction	77
5.2	Data Sources.....	78
5.2.1	Satellite Data Acquisition	79
5.2.2	Vegetation Index.....	80
5.2.3	Thermal Index.....	83
5.2.4	Standardised Precipitation Index (SPI).....	86
5.2.5	Flooding (Overflow Method).....	91

5.2.6	Revised Universal Soil Loss Equation.....	94
5.2.7	Vegetation Health Index (VHI)	98
5.3	Desertification Map.....	100
5.3.1	RS-GIS-based Crisp Method	100
5.3.2	Conventional Multi-Criteria Method of FAO.....	103
5.4	Evaluation of the Accuracy of Results Using Error Matrix	109
5.4.1	Sample Size.....	110
5.4.2	Confusion Matrix	110
Chapter 6	Fuzzy Expert System for Desertification	113
6.1	Introduction	113
6.2	Fuzzy Expert System.....	114
6.2.1	Step I-Identifying Variables and Indices	117
6.2.2	Step II-Fuzzification or Fuzzy Partition	118
6.2.3	Step III -Rule Block (Rule Base).....	122
6.2.4	Step IV - Defuzzification and Output	127
6.3	Fuzzy Map.....	128
Chapter 7	Conclusion and Recommendations	131
7.1	Introduction	131
7.2	Vegetation Indicators and Drought	132
7.2.1	Land Surface Temperature (LST) Condition.....	136
7.2.2	Vegetation Health Index (VHI) Analysis	139
7.2.3	Standardised Precipitation Index (SPI) Analysis.....	140
7.3	The Extent and Severity of Desertification	144
7.4	Accuracy Evaluation of the Desertification Map.....	148
7.5	Conclusion.....	149
7.6	Research Limitations.....	150
7.7	Recommendations	151
	Bibliography	153

List of Figures

Figure 1.1: General mapping of the project	14
Figure 2.1: Desertification criteria	20
Figure 2.2: The intensity and severity of droughts	29
Figure 3.1: Set of “hot months” in crisp set theory; the data are the monthly average temperature of synoptic, meteorological station at Kashan, Iran, 1967-2008.	38
Figure 3.2: Crisp and fuzzy membership representation for “hot months”	38
Figure 3.3: Membership functions; trapezoidal (a), triangular (b), and bell- shaped (c) forms.....	41
Figure 3.4: Possible linguistic terms and operators (AND, OR, and NOT) for a fuzzy partition with two linguistic terms (A, B).....	41
Figure 3.5: The principles of aggregation (National Electrical Manufacturers Association, NEMA 2005).	43
Figure 3.6: Linguistic conflicts (Alonso Moral 2007)	45
Figure 3.7: Fuzzy control elements in FCL (after http://ffll.sourceforge.net/fcl.htm , 2010).....	51
Figure 3.8: Fuzzy control elements in FCL for Erosion.....	52
Figure 3.9: An example of fuzzy rule inference with two rules	53
Figure 4.1: The study area located in Qom catchment and Esfahan Province, Iran (a); the darker grey rectangle in the map of Iran and (b); satellite image derived from False Colour Composite (FCC) image of Landsat satellite.....	56
Figure 4.2: Land cover map of the study area.....	57
Figure 4.3: A view of the mountain region near Kashan.....	60
Figure 4.4: The eroded hills near Kashan.....	60
Figure 4.5. Relief map of the study area from the U.S. Geological Survey (USGS)	61
Figure 4.6: Salt polygons and "cracked-mud" clay and salt materials in Salt Lake (Matinfar 2005)	64
Figure 4.7: Sand field in the study area: nebkha (a), sand dune near Aran (b).....	65
Figure 4.8: Time series of precipitation (1967-2008) in Kashan meteorological station; dash points shows annual rainfall (mm), the moving average of 3, 6, and 9 yearly scale in red, blue, and green, respectively.....	68

Figure 4.9: The spatial mean of precipitation trend in the study area (2000-2008).....	69
Figure 4.10: Precipitation spatial distribution (2006).....	70
Figure 4.11: The ombrothermic diagram of a normal year, recorded at Kashan meteorological station.....	72
Figure 4.12: Vegetation type in the study area	74
Figure 4.13: Abandoned Qanat, the underground irrigation system between an aquifer and cropland in lowland, near the city of Aran	75
Figure 4.14: Sandy soil in Band-e-rig	76
Figure 4.15: A sample of the soil profile near Aran town.....	76
Figure 5.1: The MOD13A3 image from MODIS/Terra Vegetation Indices Monthly L3 Global 1 km resolution; the pseudo-coloured NDVI as the biomass health in Kashan region (July, 2002).81	
Figure 5.2: VCI distribution in the study area (2006)	82
Figure 5.3: Spatial distribution of TCI in the study area (2006).....	85
Figure 5.4: SPI maps for December 2001 (left), and December 2006 (right)	89
Figure 5.5: Interpolated SPI map for 12-month timescale SPI from January 2005 to December 2006.....	90
Figure 5.6: Flood map (Q) for 2006.....	93
Figure 5.7: Areas affected by water erosion according to RUSLE (2006)	98
Figure 5.8: Vegetation Health Index in 2006.....	99
Figure 5.9: Desertification map according to the frequency of VCI and TCI.....	101
Figure 5.10: Desertification map according to the frequencies of five factors (VCI, TCI, Q, RUSLE, and SPI).....	102
Figure 5.11: The overall desertification map (FAO Method).....	108
Figure 6.1: Fuzzy Expert System Model.....	116
Figure 6.2: The knowledge base (Rule Base, RB) for the desertification process.....	117
Figure 6.3: Linguistic variables declared in FCL.....	118
Figure 6.4: Membership function for VCI with three linguistic terms	120
Figure 6.5: Membership function for SPI with four linguistic terms	120
Figure 6.6: Membership function for soil erosion (RUSLE) with three linguistic terms	121

Figure 6.7: Membership function for flooding (Q) with three linguistic terms.....	121
Figure 6.8: Fuzzy model of VHI (RB1).	122
Figure 6.9: The scatter plot of feature values in TCI and VCI	123
Figure 6.10: Relationship of TCI and VCI in rule base	124
Figure 6.11: Desertification rule bases according to three indicators (Q, RUSLE, and SPI).....	126
Figure 6.12: Membership function for output with five linguistic terms	127
Figure 6.13: Fuzzy model with multiple fuzzy outputs.....	128
Figure 6.14: Different layouts of fuzzy model of desertification map according to the fuzzy sets	129
Figure 7.1: The monthly mean NDVI in land cover (2000-2009).....	133
Figure 7.2: VCI variation over land units: vertical blue lines shows the standard deviation of VCI	135
Figure 7.3: The trend of LST in different classes, in the study area, between 2000 and 2009.	137
Figure 7.4: The trend of TCI between 2000 and 2009 according to different classes in the study area.	137
Figure 7.5: Mean of TCI in land units of the study area (2006); vertical blue lines shows standard deviation	138
Figure 7.6: Time series of spatial mean monthly VCI, TCI, and precipitation in the study area between 2000/3 to 2008/12.....	140
Figure 7.7: The diagrams of Standardised Precipitation Index (SPI) for Kashan meteorology station, from top to bottom for 1, 3, 6, 9, 12, and 24-monthly timescale periods, respectively, from 1967 to 2008.....	142
Figure 7.8: SPI frequency for the Kashan meteorology station.....	143
Figure 7.9: Desertification map based on fuzzy modelling.....	146
Figure 7.10: Desertification percentage based on fuzzy modelling.....	147

List of Tables

Table 1.1: Classification of the regions based on aridity index (in percent) (Murray et al. 1999).	4
Table 3.1: Fuzzy and crisp values of monthly mean temperature of synoptic, at the meteorological station Kashan, Iran, 1967-2008	39
Table 4.1: Land cover in the study area	59
Table 4.2: The properties of landform.....	59
Table 4.3: Monthly mean precipitation and temperature of a normal year (1967 to 2008); P and T represent precipitation (mm) and mean temperature (°C, Celsius), respectively.....	67
Table 4.4: Main species of vegetation in the study area (Matinfar 2005)	73
Table 5.1: Database sources	79
Table 5.2: Classification of SPI and its probability (McKee et al. 1993).....	86
Table 5.3: CN values for land use and soil type in soil moisture condition II (Werner et al. 2004, 2007)	92
Table 5.4: Hydrologic soil group according to soils run-off, producing characteristics as used in the NRCS Curve Number Method (Werner et al. 2004).	92
Table 5.5: Profile permeability class (P) and soil structure code (S) (Renard et al. 1996)	96
Table 5.6: Land cover classification and C, P factors (Sepaskhah and Sarkhosh 2005).	97
Table 5.7: Thresholds for desertification indicators.....	100
Table 5.8: Desertification severity classes.....	104
Table 5.9: Desertification status criteria (DC) (Feiznia et al. 2001).....	105
Table 5.10: The effective criteria in land degradation (potential desertification map) (Feiznia et al. 2001)	106
Table 5.11: Hydrology and desertification classes; Electrical Conductivity (EC) and the Sodium Absorption Ratio (SAR) (Feiznia et al. 2001).....	107
Table 5.12: Criteria in man-made desertification and the severity classes of desertification (Feiznia et al. 2001)	107
Table 5.13: The characteristics of severity classes	109
Table 6.1: The characteristics of features	123

Table 6.2: Rule base (1) by expert (E=Expert) and Induction Wang-Mendel (I= Induction) after consistency analysis	125
Table 6.3: Rule base (1) after simplification (E=Expert, I= Induction)	125
Table 6.4: Rules for Flood-Erosion (FE) from erosion index (RUSLE) and flooding (Q) ...	126
Table 6.5: Rule base (RB2) for Flood-Erosion (FE) and SPI.....	126
Table 6.6: The final Rule base (RB)	127
Table 7.1: the average of VCI value in land units (2006).....	135
Table 7.2: The percentage of TCI classes in land units of the study area (2006)	139
Table 7.3: Drought frequency recorded by Kashan meteorology station, from 1967 to 2008	143
Table 7.4: Percentage of affected area according to Erosion (RUSLE), flooding (Q), drought (SPI), Vegetation Condition Index (VCI), and Thermal Condition Index (TCI)	145
Table 7.5: Severity of desertification based on fuzzy modelling.....	146
Table 7.6: The percentages of desertification severity in land units of the study area	148
Table 7.7: Confusion matrix result of the FAO model; errors and accuracies are shown in percent	149
Table 7.8: Confusion matrix result of the fuzzy model; errors and accuracies are shown in percent	149

Chapter 1

General Introduction

The main purpose of this chapter is to review the problem, importance and definition of land degradation and to introduce a methodology to study drylands in Central Iran.

1.1 Problem Statement

Drylands are prevalent in central Iran and occupy over two-thirds of the country as a whole. In addition to drought, land degradation is one of the most serious problems facing the country. Recently, the following factors have worsened these problems:

- Population is highly concentrated in drylands, especially in the margin of desert lands.
- Human activities, such as inappropriate land management, overgrazing, land clearing and deforestation have put serious pressures on the environment.
- Natural hazards such as drought, flooding and erosion have increased.

In the past, Iranians have established some solutions to maintain soil productivity with the following approaches (Moameni 2000):

- A management system based on well-planned crop rotations.
- Landowners and tenants, who inherited their expertise within the social structures

from their ancestors, governed land tenure, resulting in less intense cultivation.

- Population growth was modest, with no demand for extra sources.

Nowadays, landowners, land tenants, program planners, and local authorities prefer short-term benefits rather than methods in accordance with sustainable land management policies and productivity optimization. The overexploitation of land resources threatens productivity and may lead to land degradation (Moameni 2000).

Indeed, society creates indirect impact on drylands, with high population growth rate and the invasive effects of deforestation, cultivation, and the georgic land extension. Furthermore, drylands are the most fragile ecosystems in the world, where any adverse pressure might influence land quality and its productivity. Consequently, continual land degradation might lead to economic deprivation and famine.

Natural disasters, such as drought and soil erosion can eradicate fertile soil; additionally they diminish land productivity. Inappropriate extensions, such as land use changes or abuse of pastureland, increase the risk of land degradation, especially near the affected areas. In addition, poor irrigation causes salt accumulation.

Recently many considerations have focused on desertification processes in national, regional, and local scales. Different methods hereof exist to evaluate desertification, such as direct observations and field measures, using mathematical models or parametric equations by remote sensing indicators. Nonetheless, there is no satisfactory land evaluation system adapted for the historical and specific characteristics of Iran's ecosystems, especially in regard to the problems of desertification.

Previous methodologies, such as field survey models are time-consuming and expensive. Despite their valuable results, the reliability of the method is unique only to a specific area. Nonetheless, few methods exist on how to assess the affected areas in new approaches, such as with integrated remote sensing and fuzzy models. Moreover, a comprehensive study of desertification requires more than a year to collate and process, by applying recent developments and data availability in remote sensing models, which make the surveying of desertification trends possible as well as drought early warning systems on yearly, monthly, or weekly scale.

1.2 Land Degradation

For centuries, land degradation has been one of the most important global problems, especially in drylands. Therefore, land degradation indirectly influences food security and the quality of life and has an adverse impact on land quality. These problems are manifested in the upland and lowland regions, from its source to its destination, resulting in the decline of productivity and land quality in the affected areas, as well as sedimentation and contamination deposited in the lowlands and its approaches.

There are two viewpoints concerning the rate of land degradation. The first group includes ecologists, soil scientists, and agronomists, who believe land degradation presents a serious global threat; whereas the other view, held by economists, does not take any serious consideration about the problems of land degradation (Eswaran et al. 2001).

1.2.1 Desertification; Terminology and Concepts

In general, the commonly held view was that most regions consisting of arid lands were simply regarded as desert; however, from a climatology aspect, only hyper-arid regions are accounted for as desert. For climatologists, drylands and hyper-arid zones cover approximately half of the world's earth surface, the largest and the most extensive biome (bio-climatic regions). Worldwide, there exist variant types of desert. For this reason, in defining the term 'desert' we realise that in the general sense, it is a non-quantified application to the term.

For instance, the definition of 'a desert' in the Webster Encyclopaedia is given as "*arid land with usually sparse vegetation; especially : such land as having an unusually warm climate and receiving less than 25 centimetres (10 inches) of sporadic rainfall annually*"; likewise, in the Britannica Encyclopaedia, 'desert' is "*any large, extremely dry area of land with sparse vegetation. It is one of the Earth's greatest types of ecosystems, supporting a community of distinctive plants and animals specially adapted to the harsh environment*".

The term "desertification" is first mentioned in Aubreville's report entitled "Climats, forêts et désertification de l'Afrique tropicale" in 1945 to describe land clearing, and deforestation by converting tropical rainforest (with mean annual precipitation about 700 - 1500 mm) to savana and croplands (Glantz and Orlovsky 1983). Later, taking into account human activities and

climate change, such as prolonged or frequent droughts (which aggravate land degradation), desertification is officially defined as “*land degradation in arid, semi-arid, and dry sub-humid areas resulting from various factors, including climate change and human activities*”(Geist and Lambin 2004). This attribution is used for the basis of the United Nations Convention to Combat Desertification (UNCCD), which embraces a definition that takes into account land degradation, climate changes, and human activities (Kassas 1995; Rasmussen et al. 2001).

Aridity index is the ratio of mean annual precipitation (P) as moisture input to mean annual Potential Evapotranspiration (PET, potential evaporation from soil plus transpiration by plants) as moisture loss, which UNEP applied this index to classify arid regions. Accordingly, the world is divided into six aridity zones (Table 1.1): hyper-arid, arid, semi-arid, dry sub-humid, moist sub-humid and humid zones.

Table 1.1: Classification of the regions based on aridity index (in percent) (Murray et al. 1999)

Climate zone		Ratio	World	Iran
Desert	Hyper-arid	<0.05	7.5	-
Dry land	Arid	0.05-0.20	39.9	12.5
	Semi-arid	0.20-0.50		17.5
	Dry sub-humid	0.50-0.65		9.9
Moist sub-humid		0.65-1	39.2	-
Humid		>1		

Arid, semi-arid, and dry sub-humid areas, which comprise drylands, refer to regions with an aridity index of between 50 to 65 percent, excluding highlands, and the semi-polar or polar regions.

According to the United Nations Convention to Combat Desertification (UNCCD), drylands cover almost 90 percent of Iran (Table 1.1), where more than half of drylands are arid lands, followed by semi-arid areas and then dry sub-humid zone, respectively (Murray et al. 1999).

Affected areas mean that the damaged or threatened areas by the desertification processes in arid, semi-arid and dry sub-humid lands.

Combating desertification includes all activities of comprehensive sustainable land development in order to prevent or reduce land degradation and the reclamation of partially degraded lands, or fully affected areas in arid, semi-arid, and dry sub-humid zones. In other words, the combating of desertification is all activities in the framework of comprehensive development projects in drylands, which are based on the principles of sustainable land development, including inhibiting, improvement, and reclamation activities. The inhibitory factor includes creating environmental awareness, modes of encouragement and dealing out punishment to land abusers where necessary. Improvement is the developing of cultivation methods, the reform of irrigation systems, the setting up of fallow crop rotation schedules, and the improvement of fertilizing methods.

Reclamation is typically used in those areas which are seriously damaged, which is an attempt to restore the previous normal ecological conditions through the implementation of technical projects such as windbreaks or shelterbelts, and water supply.

In general literature, there are many terms where definitions overlap with regard to soil degradation, land degradation, and desertification. Even though land and soil are clearly defined, there is uncertainty and vagueness over degradation and desertification. According to the United Nations Environment Program (UNEP), the term “desertification” refers to land degradation in arid, semi-arid, and sub humid area, due to human activities (Eswaran et al. 2001).

In the past, the idea of desert extension (desertification) considered as a physically dynamic, dangerous and rampant phenomenon that rendered ecosystems useless or, at best, areas of low valuable ecosystems without efficiency or capability. Consequently, in order to eradicate deserts, or to vegetate and make deserts green, several radical endeavours were executed, especially in the central drylands of Iran. Some of these ideas were realised in the levelling and stabilizing of sand dunes for use as croplands, the establishment of green belts on the desert margins, and the biological and mechanical conservation of slopes. These efforts and approaches were mostly of a mechanistic nature. Later, following more advanced scientific research in the variant realms of desertification, and the re-evaluation of past research, opinions changed, deeming drylands or hyper-arid lands as natural ecosystems.

Despite the importance of the impact of desertification on the environment and society, there has been little research in the development of diagnostic techniques and criteria for studying the

status and trend of desertification; and most of these studies have been done in developing countries (Rubio and Bochet 1998).

There are two provisions to evaluate land degradation studies: The first addresses inadequate and unnecessary lands or badly affected areas, where their capability and suitability is less than the minimum threshold productivity; in other words, its suitability class must not be below the least determined threshold. The second provision concentrates on the high quality lands, where there is a high potential for productivity, where this land must not exceed the determined threshold class for suitability.

For this reason, the unproductive hyper-arid lands (the first condition) and the humid regions of high productivity (the second condition) cannot be subjected to issues of desertification. Nonetheless, these conditions and classifications can alter according to external factors, such as climate change or the impact of human activities on the ecosystem.

1.2.1.1 Soil Desertification

There are many types of soil desertification such as physicochemical deterioration, erosion, and water-logging (Mbagwu 2003). In the study area, Kashan and Qom regions, the biophysicochemical deterioration and erosion are active soil desertification. The most common types of chemical deterioration in farmlands are nutrient losses and secondary salinization (secondary salinity of soil by over-irrigation). In soil, the physical deterioration occurs mainly through compaction by agricultural machinery and industrial vehicles, resulting partly from mismanagement and partly from natural processes.

The physicochemical characteristics of soil are the most decisive factors in the evaluation of desertification. In this regard, salinization, known as alkalisation or sodification, is one of the uttermost desertification indicators in drylands, especially in lowlands and arable areas. Poor irrigation systems in aggravated areas and the rise of groundwater in lowlands, accompanied by drought and high evaporation, increase the risk of desertification (JRC, Joint Research Centre, 2010). Water-logging is also a prime cause of soil degradation associated with potential salinity hazards that might occur through mismanagement in lowlands.

Soil erosion is such a key factor in land capability, and land suitability evaluation, that often in eroded lands, productivity decreases and destructive flooding increases. The removal of soil, which leads to the exposure of bare land and biodiversity elimination, threatens and impacts upon human life, and forces people to migrate.

1.2.1.2 Status of Soil Desertification in the Irrigated and Dry farms

In irrigated and rain-fed farms, some parts of land degradation are related to natural factors, while other parts are subject to land use policies. Therefore, land management schemes, irrigation systems, tillage methods and crop rotation are central to the degradation of agricultural lands.

In the study area, most sloping lands have been ploughed in the same direction of the gradient and are eventually abandoned after destruction or loss of fertility. Generally, slope, soil depth, and soil susceptibility to erosion, are crucial factors in soil degradation, especially in agricultural lands. These problems are compounded by inappropriate land management and policymaking, ignorant of the technical procedures in ploughing and harvesting, which hasten land degradation.

In Iran, irrigation serves about one-half of the total cultivated areas in the country, which equals 8 million hectares (ha). Most arable and cultivatable land suffers from the absence or shortage of water, meaning there is an abundance of available land for potential development without water. The main causal factors of soil desertification in croplands or rangelands are overexploitation and mismanagement (Moameni 2000).

1.2.1.3 Status of Soil Desertification in Forest and Pastureland

In drylands, the quality and quantity of vegetation are naturally affected by climate and soil conditions, due to the harsh climate and extreme conditions in desert-like regions; therefore, there exist only few plants which have adapted to this environment. Mismanagement and the overuse of lands are other reasons integral to desertification; in drylands wood-burning, overgrazing and cultivation decrease the extent of green land cover. In addition, the spread of aggressive plants and low-graded grasses affects the quality of vegetation in pasturelands, already affected by overgrazing by livestock.

According to some reports and field studies, pasture and rangelands in Kashan areas are showing negative trends. Such reports reveal that the most aggressive soil erosion and land

degradation occurs in pasturelands, suggesting that human-induced desertification is the main causative factor, while natural and climatic factors are next in rank (Shamsipour, 2007).

The recognition of the factors involved in forest and pastureland degradation helps eliminate or control these adverse effects. The most significant deficiencies in rangeland policies are lack of ownership or beneficiary in the tenure system; early and premature grazing in spring; overgrazing by livestock; and converting pasturelands to dry farms.

Land degradation in semi-dense forest is brought on by deforestation, the removal of wood and overgrazing. Yet for all the available evidence, land degradation remains a matter of little concern at national level in Iran (Moameni 2000).

1.2.2 Extent of Desertification in Iran and its Importance

The phenomenon of desertification was first defined by Aubreville (1949), who, at the time, could not have imagined the extent to which it would adversely affect the ecosystem. Nowadays this phenomenon is not only limited to the expansion or movement of sands, but the problem of desertification is also land degradation, which occurs even outside of so-called desert lands. Land degradation includes the decrease of soil productivity, the decline of groundwater quality and its quantity, the increase of land's sensitivity to erosion, the increase of floods, and sedimentation in reservoir water, salinization and inundation (Dregne and Chou 1992). Even in European countries, land degradation occurs. The continent has lost more than one quarter of its soil from the total European lands, of which 60 percent is due to increasing vegetation degradation (van Lynden 2004). Therefore, considering the importance of desertification as a substantial global problem, it is not possible to solve desertification problems without reliable methods for the evaluating and exploring of variant forms of degradations (Lal et al. 2003).

Iran is over the horse latitudes, the hot and dry belt latitudes. Therefore, as the tenth driest country in the world, the hyper-arid and arid climate zones cover most of the country. In fact, Iran is such a susceptible country that every year disasters such as erosion, flood, drought, and landslide bring many economic, social, and natural problems.

According to International Strategy for Disaster Reduction (ISDR) reports:

“In Iran due to a drought in 2001, about 37 million people were affected. Water reserves in the country were reduced by 45 percent; about 800,000 head of livestock were lost in 2000, and 2.6 million hectares of irrigated land and 4 million hectares of rain-fed agriculture were affected. Damage to agriculture and livestock was estimated by the United Nation (UN) about US\$ 2.5 billion in 2001 and US\$ 1.7 billion in 2000” (United Nations & International Strategy for Disaster Reduction 2004).

In the last decades, the woes of desertification and drought have heavily influenced development planning in Iran, for which the allocation of the national budget in the Second Five-Year Development Plan (1995-1999) spent about 51 million US dollars. Simultaneously, NGOs (non-governmental organisations) have invested about five million US dollars; additionally the conservative activities of infrastructures such as residential and industrial lands, as well as route systems against sand dune movement have taken up additional shares in the national budget.

In the late 1980s, the amount of irrigated land damaged by salinization (as secondary salinity by irrigation), brought about by rising water levels of groundwater and the mobilization of salts, reached 17,000 sq km, which is 30 percent of irrigated land in Iran. As the majority of irrigated lands in Iran are saline, productivity fell due to the toxicity of salt.

Because of varying definitions in the literatures, there are differences about the extent of drylands in Iran. According to aridity index (Table 1.1 in Section 1.2.1), the area of drylands in Iran is about 1.466 million sq km (out of 1.624 million sq km) about 90.3 percent of the country (Murray et al. 1999).

Meanwhile, according to the De Martonne index (which indicates the ratio of precipitation to temperature), the area of drylands reaches 53.9 percent, and hyper-arid area and humid zones cover 35.2 percent and 8.9 percent, respectively (Khalili 1992). According to the United Nations Convention to Combat Desertification (UNCCD), the affected areas cover more than 43 percent of the country. The area affected by soil erosion reaches 37 percent of the country; water erosion in Iran is about 26.4 million hectares, and wind erosion is about 35.4 million hectares - 16 and 21 percent of the country, respectively. Therefore, the rate of land degradation is extremely severe (Dregne and Chou 1992; Lal 2001).

Drylands in Iran support half of the population and contain large cities such as Mashhad and Tehran. Therefore, decision-makers and researchers are concerned with solutions, management systems and environmental policy (Pakparvar 1998).

1.3 Remote Sensing and Desert

The emergence of aerial photogrammetric and remote sensing methods has brought about many advantages; there have also been many interests in the study and investigation of natural phenomena. Most of these interests are oriented towards the mapping and understanding of landform variations and geomorphic processes.

Remote sensing includes a wide spectrum of utilities to explore the natural environment and to identify the occurrence of phenomena such as land change and degradation. Sensors are capable of determining land surface temperature and the status of vegetation, help explore and observe environmental disasters such as drought, and to map desertification. The development of thermal sensors makes it now possible to provide thermal maps easily.

Thermal data make possible the capability to investigate and assess the natural resources on a global, national and regional scale, especially in drylands. Principally, these capabilities are remarkably useful in places without climatology stations or little accessibility such as in central Iran, where desertification is one of the most pressing social, ecological, and environmental problems, especially where public and scientific observation has been lacking.

In fact, in order to achieve sustainable development and better decision-making we need proper up-to-date information about phenomena as well as the realizing of inter-relationships of environmental variables.

High usability, temporal accessibility, and extensive coverage of images acquired by remote sensing have been the subject of many studies used to investigate the processes and phenomena. In Iran, there have been many remote sensing studies; the most accessible areas are studied more frequently; however, inhospitable and remote areas are generally neglected.

Before the 18th century, maps were based on Ptolemy's geography, and there are few documents about the importance of environmental issues except for scant reports about

droughts and famines, in which people perished because of mismanagement, starvation and the shortage of food production. Latterly, more focus has been paid to these neglected areas in Iran with the advent of western approaches in education.

The 19th century marked as the beginning of advanced scientific researches and the introduction of aerial photographs. About 1870s, Bladford provided a map of southwest Asia including some salient features of central Iran such as the Great Kavir in central Iran and the Lut desert of eastern Iran. In the beginning the 20th century, Huntington explored the historical stratigraphic evidence, and interpreted the beginning of arid climate at the end of the Tertiary period, followed by a wet epoch. He concluded that south-eastern Iran had experienced a change from a humid climate to its present arid climate. Later, Walther's studies also showed the relationship of climate to surface morphology and genesis; Desio, Bobek, and Wright through land surveying and exploration provided geological maps in 1943, 1963, and 1961 respectively, specifically in the Zagros Mountains; glacial deposits of the Würm (Wisconsin) age were examined. Furthermore, Bobek and Wright found some evidences for a pre-Würm glaciation of the Zagros and Elburs Mountains (Kransley 1970).

In 1960, Huber by performing seismic sounding and drilling in Qom Playa, revealed a secondary section approximately 350 meters thick and upper sections with 46 meters thick near the centre of the playa (salt lake). The lower section consists of a basal layer of medium to coarse-grained sand, gypsum and andesitic grit. This is covered with brown and green clays with 10 to 25 percent of visible salt crystals. The larger upper part of the lower section contains brown clay and silt; the upper section consists of alternating five salt beds with intercalated layers of brown and green clay and silt and two sand horizons. The upper section pinches out at the margins of the playa. Huber also concluded that the lower section, depositing under a permanent water cover, was not relatively saturated salt water and was not precipitating any salty particles. He reasoned that the upper section represented alternative true evaporite and temporary lake sediments under conditions compatible with the real climate (Kransley 1970).

After launching the Landsat satellite (in 1972), the first mission of the Earth Resources Technology Satellite (ERTS) series, a new era of remote sensing appeared. Its utilities in land survey and land management helped researchers to utilize digital images to explore a much larger

environment; especially launch of Terra with Moderate-Resolution Imaging Spectroradiometer (MODIS) in 1999 helped the researcher with exploring land (Hemphill and Estes 2003).

1.4 Research Hypotheses

In order to develop a new algorithm, and to evaluate the utility of remotely sensed data in drylands, the following hypotheses are chosen in the study as follows:

- Desertification is possible to be parameterized based on tools such as satellite data and ancillary spatial data, through which can be extracted some useful indices to evaluate desertification conditions based on thermal and reflective bands.
- A remote sensing integrated fuzzy inference system is helpful to acquire knowledge about desertification models and land evaluation.

1.5 Research Questions

For the aim of this study, the following research questions have been addressed:

- How desertification occurs in response to vegetation and soil index over a long-term period of time?
- What is the spatial and temporal pattern of desertification in the study area?
- Is there any association and relationship among vegetation, soil and climate indexes?
- How desertification risk can be evaluated by the combination of satellite images and ancillary data in a fuzzy inference system?
- How remote sensing integrates with a fuzzy system in the evaluation of desertification?

1.6 Research Objectives

The purpose of the project is to present certain utilities of satellite data in the monitoring of dry land, substantially in the estimating of the causes of natural disasters such as desertification and drought. The challenge consists of studies about climate, vegetation and soil degradation based on

the reflective and thermal indexes of remote sensing. In this research, we attempt to demonstrate semi-linguistic methods in earth science to find out how to improve the analysis of desertification principles by incorporating ancillary data, remote sensing with a fuzzy expert system model.

Despite some limitations, with regard to the inaccessibility of the study area, this research aims to develop an assessment strategy for a desertification model using remote sensing and ancillary data, coupled with expert knowledge. In other words, the objective of the project is to apply the integrated remote sensing and fuzzy system to improve the decision-making process in land evaluation, especially in drylands. Therefore, the following objectives are considered:

- To develop a methodology to assess the sustainability of drylands through the integrated spatial remote sensing data and fuzzy model.
- To determine the areas prone to degradation by the integration of expert and data knowledge base model, by combining satellite data and other thematic information. In other words, this research looks at the applications of remote sensing images in drylands, by using a fuzzy rule-based approach.

In this project, the main objectives are firstly the evaluation of certain criteria to establish the relationship of these indices; secondly the construction of a knowledge-base model for desertification phenomena by using remote sensing data.

1.7 Research Approach

The research approach is comprised of the following steps. First, multi-temporal data will be prepared to acquire knowledge. Then, by the designing of the fuzzy expert systems and the analyses of data, the knowledge about parameters will be extracted and validated. For this reason, the main parameters in desertification (Chapter 2) are introduced; the basic information about fuzzy logic is defined (Chapter 3); then, to find out the environment circumstance of the study area, its main environmental characteristics are described (Chapter 4).

According to Figure 1.1, two kinds of data are used: remote sensing and ancillary data. The vegetation and thermal properties of land surface are calibrated in image processing as indices for desertification. Additionally, a land cover map is digitized by the visual interpretation of satellite images, which is used as a base map for other polygon maps, such as land cover and soil map.

From ancillary data, three indices of desertification are calculated for soil erosion, flooding, and drought, supported by maps (Chapter 5). In the same chapter, some auxiliary analyses, such as time series and spatial analysis in Geographic Information System (GIS) are presented. In the following chapter (Chapter 6), the analysis of the derived indexes and the designing of fuzzy inference system lead to the preparation of the final desertification map.

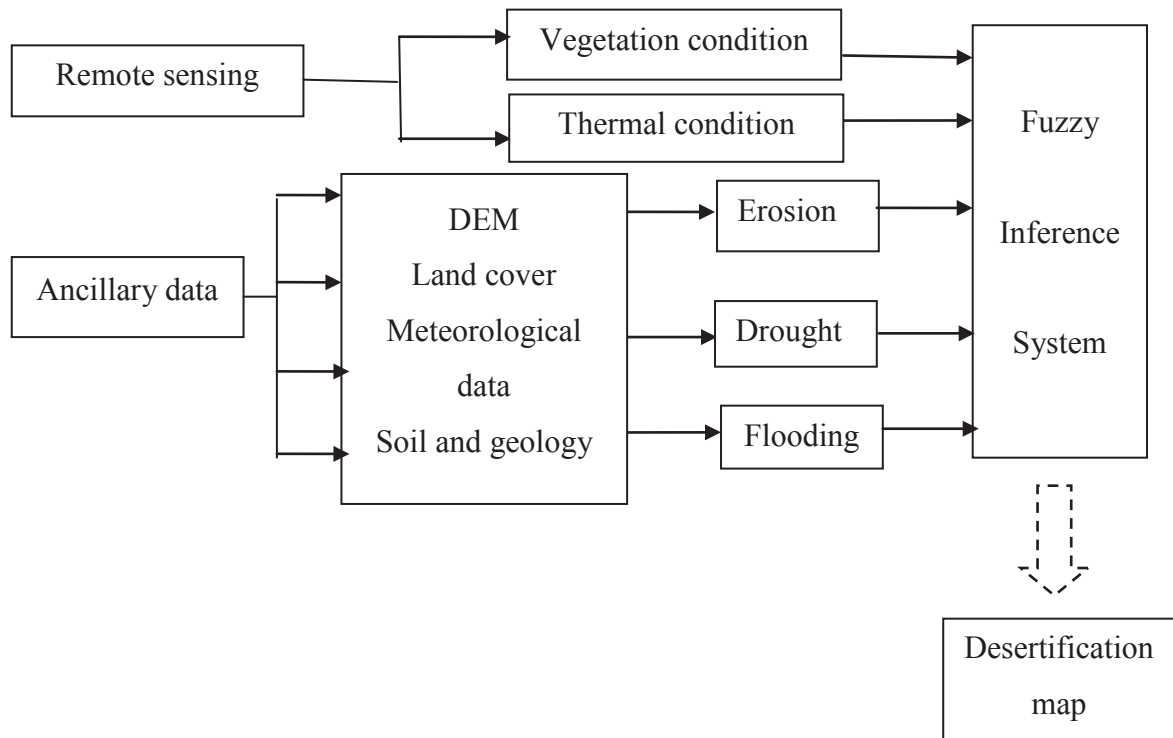


Figure 1.1: General mapping of the project

1.8 Dissertation Framework

This project comprises seven chapters according to the successive divisions listed below:

Chapter 1, General Introduction, contains a brief definition of concepts such as hypotheses, questions, research questions and objectives.

Chapter 2, Desertification Indexes, discusses the main indices used in this research to prepare the desertification map.

Chapter 3, Fuzzy Logic, in this stage, we discuss the fuzzy inference system and its components to construct intelligible fuzzy systems.

Chapter 4, Description of Study Area, gives a brief overview of the study area properties such as introducing land cover types and climate condition in the Qom-Kashan watershed, Iran.

Chapter 5, Data Acquisition and Processing, deals with implementation of data and their characteristic, so this chapter covers the materials and the description about data, image processing, and spatial analyses.

This chapter also gives some description about calculating indexes, which are derived from remote sensing data or ancillary data. In addition, through the analyzing of temporal images, it represents the occurrences and states of desertification. The ancillary data and remote sensing data will help determine desertification, concluding with a desertification map based on traditional criteria.

Chapter 6, Fuzzy Expert System for Desertification, discusses about the designing of a knowledge-base system. Within this Fuzzy Inference System (FIS), an analysis will be made of the relationships and correlations among indices; a rule-based system will be explained, which includes an expert and induction interface model to build a fuzzy expert system. Additionally, by analyzing the consistency of the rules and the simplification of a rule-based system, the total result is represented as a simple knowledge-based system for desertification by remote sensing and ancillary data.

Chapter 7, Conclusion and Recommendation, as the final part of the project, is a conclusion covering the present studies being undertaken in the field, as well as the limitations and recommendations for future study.

Chapter 2

Desertification Indices

Indicators are useful to simplify and determine the status and tendency (prediction) of complex processes such as desertification. Moreover, they are applied as synthetic information layer in GIS to determine the spatial distribution of the affected lands, which are impacted by human activity (causes) or environmental conditions (effects). Indicators for desertification are the various causal factor involved in soil and land degradation including erosion, sedimentation, land use changes, the abuse of pastureland, the destruction of renewable resources, and exploitation lands (Rubio and Bochet 1998).

In remote sensing, there are many approaches to explore and to examine land degradation problems quickly and accurately. Therefore, it will be helpful to define and clarify the meaning and property of the indices.

In this chapter, the goals are to introduce and define indexes of desertification related to remote sensing data and ancillary data. Regarding the objective of research, Vegetation Index (VI), Land Surface Temperature (LST), flooding (overflow), erosion and drought are explained. In other words, brief information of indicators and criteria for desertification risk assessment is described below.

2.1 Empirical Indices

In order to estimate land degradation and desertification, the “biological potential” of land has to be measured, for which various factors and methodologies are required (Eswaran et al. 2001). There are many indicators and criteria for desertification estimation, including erosion, vegetation, climate, and hydrology indexes (Figure 2.1). In the study area, the main desertification problems are numerous: vegetation deterioration, overgrazing, poor vegetation cover, invasive land cultivation; inappropriate use of groundwater, harsh climate, drought, erosion and salinity. All these problems influence vegetation, directly or indirectly.

An erosion index estimates soil loss, as well as its fertility; therefore, it is a decisive factor for land degradation. Hydrology (water) indexes have two aspects; one is low input as drought; the other is high input as the cause of erosion and flood (Farajzadeh and Egbal 2007; Sepehr et al. 2007). Application of indicators such as vegetation cover, surface run-off and soil erosions in monitoring land degradation in sub-Saharan Africa, shows that soil erosion is ultimately the effect of other factors (Symeonakis and Drake 2004).

Vegetation indexes are also imperative in land evaluation as vegetation is not only a protective and conservative factor against erosion, but it also is a supportive factor for all living organisms and primary production. Therefore, in remote sensing based studies of land quality, the vegetation status and thermal condition of land are considered; the former indicates vegetation deterioration and the latter exhibits the thermal condition in the environment. Indeed, vegetation condition and its trends are supportive for desertification studies. Nonetheless, in drylands low-vegetation coverage is a considerable impediment to achieving the interested goal (Okin et al. 2001).

Topographical indexes, such as aspect and slope indexes, are used as classification factors in land suitability as well as desertification evaluation. Therefore, besides remote sensing data, we also need ancillary GIS data, such as topography, geology, geomorphology, land cover, soil, hydrology, which are helpful in understanding the interpretation of remotely sensed data and index extraction - especially in determining soil erosion.

2.2 Vegetation Indices (VI)

In the late 1970s, it was found that net photosynthesis is directly associated with the amount of photosynthetic active radiation (PAR) that plants absorb, that means, the more a plant absorbs visible solar radiation (during the growing season); the more it photosynthesizes and the more it is productive. In other words, the healthier the leaves a plant have, the more reflection of these wavelengths becomes apparent. Therefore, a green leaf plant looks relatively dark in a PAR spectral region and relatively bright in the near infrared (Myneni et al. 1995).

Plants respond differently to the spectra in the range from ultraviolet to the thermal infrared; in the visible light regions, their reflectance is less than the near infrared regions. Having chlorophyll and pigment, the green leaves in plants absorb the visible light in the blue regions and the red regions at approximately 0.45 μm and 0.68 μm wavelengths, respectively. Green plants reflect the green wavelength at about 0.55 μm . In contrast to the visible light, green plants highly reflect the Near-Infrared (NIR) spectra, the wavelength in the range (0.75-1.4 μm). The high absorption in the range of middle infrared (at wavelengths longer than 1.4 μm) is also related to the water content in plants. Therefore, the high contrast between the absorption in the red light range and the reflectance in the near-infrared range is a useful index to detect the condition of vegetation (Morgan 2007).

In recent decades, the hyper-spectral and multi-spectral imagery sensors such as the Moderate-Resolution Imaging Spectroradiometer (MODIS) and Landsat provide up-to-date images in a wide range of wavelengths, from the visible light to the thermal regions, which are widely used in environment monitoring. The various products and indices derived from these images are useful in studying drought and desertification (Mather 2004).

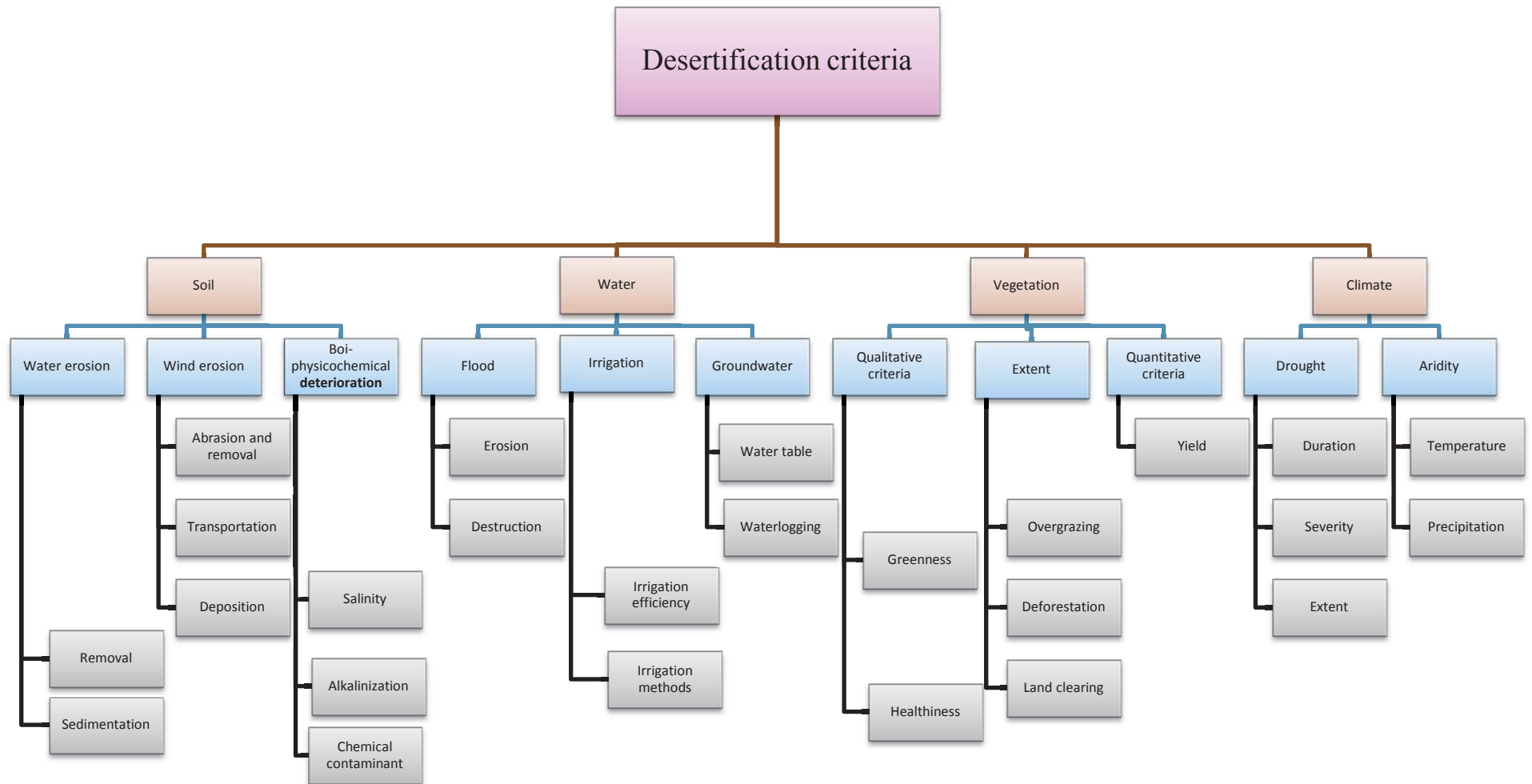


Figure 2.1: Desertification criteria

2.2.1 Normalized Difference Vegetation Index (NDVI)

NDVI stands for Normalized Difference Vegetation Index, which is the common measurement for the greenness of vegetation. In remote sensing, NDVI is used as an indicator for the greenness measurement in vegetation and shows the difference in the response of vegetation between red light and the near-infrared wavelengths.

Tucker (1979) proposed the NDVI index as an index for the diagnosis and detection of the healthiness and density of vegetation, which has since been used for the estimation of biomass, Leaf Area Index (LAR), plant production, the green cover identification, and land changes.

Chlorophyll, pigments and the intercellular structure of leaves in green vegetation absorb the red spectra and reflect highly the Near-Infrared (NIR) spectra. In fact, NDVI is the normalized difference between the red (R) band and the Near-Infrared (NIR) band. NDVI is well correlated with green leaf biomass; it is positively dependent upon green leaf biomass or Leaf Area Index (LAI). Water stresses such as drought decrease the contrast while the high quantity and quality of plants increases this ratio (Thenkabail et al. 2004). According to the different reflective properties of plants in the red and near-infrared bands, the ratio is defined by the following equation:

$$NDVI = \frac{\lambda_{NIR} - \lambda_{red}}{\lambda_{NIR} + \lambda_{red}} \quad (2.1)$$

where λ_{red} and λ_{NIR} are the reflective bands in red and the near-infrared ranges, respectively. The range of NDVI is between -1 and + 1. The two bands of MODIS are the red band (Band 1; 0.62-0.67 μ m) and the near-infrared band (Band 2; 0.841-0.876 μ m).

Because of the normalization of the ratio between two bands, NDVI has some advantages, such as the reduction of the atmosphere effects, the correction of topography effects, and the correction of the solar radiation variations (Guyot and Gu 1994). Nevertheless, in some areas like drylands, the interaction between soil and vegetation are not resolved, such as mixed pixels.

2.3 Land Surface Temperature (LST)

In drylands, land surface features have different temperature values, which originate from their internal characteristics, such as emissivity, thermal conductivity and specific heat, or from external factors such as radiation, temperature, humidity, wind and cloudiness. In other words, land surface temperature results from the interaction of climatic conditions, topographic patterns of surface, and received irradiance energy, as well as the physicochemical and thermal properties of land features (Alavipanah et al. 2007b).

Temperature is one of the fundamental factors to realize bio-physicochemical phenomena in the environment. Surface temperature is a basic criterion for the studying of thermal behaviour of features in the environment. Hence, thermal infrared remote sensing, in having utilities such as the estimation of land surface temperature (LST), will provide more information about the thermal properties of nature.

Land Surface Temperature (LST) is related to the reception of solar radiation and surface properties where latitude and height control the quantity of solar radiation and temperature. Therefore, in higher latitude, there is a positive relationship between vegetation growth and increasing temperature, especially at the beginning of the growth season. Even though drylands have high albedo, they are characterized by high temperature during daytime (due to low specific heat of surface material) leading to high evapotranspiration and drought, so surface temperature can show the behaviour of the environment to emit thermal energy.

Soil temperature also represents the latent heat of soil and its ability to evaporate moisture in the soil. Therefore, in areas such as drylands, which have a limited amount of water for vegetation growth, especially in midsummer, warmer soil is drier.

Although the difference in air temperature in open space and shade is low, the variance between air temperature and land surface temperature is high, occasionally with differences of more than 10 °C. Temperature of land surfaces differs due to the dissimilar properties such as different minerals (sand and clay), moisture content, and organic matter, or the different appearance and colouration of surfaces. For instance, in drylands, wet surfaces having high heat capacity are resistant to an alteration in temperature; they remain cold for a long time, while sand surface gain and loose temperature easily (Alavipanah et al. 2007b).

The relationship between land surface temperature and drought has shown the importance of thermal spectra. In this regard, many efforts have been made to develop the diagnostic techniques and criteria for the studying and exploring of the status of problems such as land degradation and soil erosion (Alavipanah et al. 2007a).

Land surface temperature (LST) is one of the most influential parameters for the development of vegetation. In remote sensing, to retrieve the surface temperature, the method split-window is used (Sobrino et al. 1993).

Because of the recent advances in remote sensing, land surface temperature can be easily monitored; especially by MODIS data, which can identify geothermal activities and determine pollutant heat sources as hot points.

2.4 Flooding (Overland Flow)

The worst desertification cases occur in semi-arid and arid areas, with average rainfall between 200 to 500 mm, where such areas are under the impact of water erosion, and the quantitative and qualitative deterioration of vegetation, overgrazing and land clearing. Especially in areas with 300 mm precipitation, degradation is intensified with the occurrence of droughts.

The recent flooding in Iran shows that land degradation impacts severely on the environment and natural resources. The high population rate, along with mismanagement in land use policies, has meant that forestland has been converted to pastureland or cropland. These activities have contributed to the most prominent reasons for increasing flooding and flood discharge in recent decades. Consequently, in upstream rivers, less water penetrates and permeates into the ground, and a high volume of water runs down into the plains. Therefore, floods often occur when rivers suddenly overflow with high intensity.

Although such disasters present a threat to human society, flooding also damages water supply infrastructures, wells, and Qanat systems, adding to the environmental crisis. Flooding, due to torrential rain and extreme rainfall in arid or semi-arid lands, also damages agriculture structures, leaving more serious desertification in its aftermath. The effects of flooding and water run-off transport high saline contamination and gypseous sediment from uplands, which accumulate and deposit in lowlands.

Although temporary and seasonal rivers are not initially contaminated with salts, passing through in saline lands causes salinity, so geological, climate and hydrological factors are influential in the salinization processes.

Studies have shown that in addition to a decrease in feeding aquifers in uplands, run-off causes the development of saline groundwater towards aquifers, especially in lowlands. Moreover, the residual gypsum and salt contaminated deposits, in a closed basin, induce soil degradation, eventually leading to complete loss of potential soil fertility, i.e. desertification. In drylands, wind also transports damaging salt particles and sand, which attack croplands nearby, resulting in less fertility, a drop in land value, and the eventual abandonment of barren terrain. Indeed, this process occurs in closed watersheds in central Iran, where there are two factors affecting floods: climate and watershed properties.

2.4.1 Climate Factor

Although rain is the main source of flooding, not all precipitation leads to flooding. Its condition is dependent on the extent, length, and intensity of precipitation; therefore, storms with extreme intensity, over a relatively long time and vast area, lead to higher flooding. In small watersheds with steep slopes in mountainous regions, short but vigorous showers might cause high intensive flooding. The spatial and temporal distribution of precipitation has considerable role in flooding. For instance, during precipitation, if the land surface is saturated, excess rainfall brings much stronger flooding. Rainfall, occurring nearer the outlet of the basin, is more likely to produce a high risk of flooding.

2.4.2 Watershed Properties

In semi-arid and arid regimes, despite low precipitation, sometimes storms occur with high intensity, which exceed infiltration capacity, cause high erosion and transport significant quantities of sediment (soil particles). Because vegetation distribution in drylands is scarce and the infiltration rate of land surface is low, it is more likely to flood after a storm.

Flooding in the watershed is mainly dependent upon the physiographical characteristics of the basin, namely land changes and developments in the watershed. The characteristics of the watershed that influence flooding are its size, slope, drainage network, land cover and land use.

- Shape and size

A great deal of research has been concentrated on the relationship between watershed size and run-off. Compared with small watersheds, large, vast basins produce a high volume of run-off, but their catchment-per-surface unit is low because precipitation intensity might be variant or uniform over space and time in large watersheds. Therefore, it is difficult to determine the correlation between the volume of run-off and precipitation intensity, whereas there is a specific association between them in small basins.

Regarding the temporal and spatial distribution of precipitation, the extent of catchment plays a pivotal role in flooding; the discharge-per-surface unit in smaller watersheds is greater than in larger basins. Furthermore, the shape and form of the watershed substantially affects the extent of the flooding. Longer or wider watersheds have a lower peak run-off. Round watersheds have higher peak run-off. In cases of short distances between the source and outlet, and low concentration time after a rainfall, it takes less time for the raindrops to run from the source to the basin outlet.

- Slope

Slope significantly affects surface run-off, relevant to factors such as depth, holding capacity, water infiltration in soil, and opportunities for soil permeability. The steeper the slope, the more influences are over these properties, when more run-off is generated. In particular, slope strongly affects water accumulation in reliefs. As slope increases, water accumulation decreases, and because flow velocity is faster in steeper slopes accumulated peak run-off is higher.

One of the main characteristics of a watershed, which is central to hydrology studies, is the channel's slope. Channel slope affects water velocity, and the volume of run-off. By increasing channel slope, water in the channel moves faster; consequently, much water is drained from the basin. In sloping areas, rivers have less discharge but have higher peak discharge.

- Drainage network

Drainage network status plays a key role in flood events. The flow in streams and channels is faster than run-off in ground surfaces. Therefore, in dense drainage network, the run-off accumulation rate is faster and the hydrograph curve peak is higher. Besides drainage density, hydrographic network patterns are influenced by geomorphic, lithologic, and soil characteristics.

- Land cover

Vegetation influences the hydrologic cycle in a watershed. Vegetation protects soil from rainfall droplets, and also reduces the velocity of run-off. Therefore, it increases the opportunity for water to permeate into the soil, whereby the organic matter in soil improves permeability. Many soil and hydrology experts believe that few, if any, floods occur in forestlands.

Land exploitation, or systematic land management, influences run-off in a variety of ways. For example, vegetation deterioration, overgrazing by livestock and land use changes are all factors in increasing run-off, because they increase soil compaction and decrease soil permeability. Repeated and frequent ploughing and poor practices can also cause hardpan in soil.

Soil and lithologic factors play an important role in the distribution of run-off. They control sensitivity and drainage density. Lithologic and soil characteristics directly affect infiltration rates and run-off, influencing river streams and flooding. The discharging of shallow groundwater into rivers is also influenced by lithologic characteristics.

The U.S. Soil Conservation Service (SCS) provides helpful data to estimate levels of flood discharge based on current land use status and capability. The Natural Resources Conservation Service (NRCS), formerly the Soil Conservation Service (SCS), measures run-off based on the Curve Number (CN) model which is a method for the estimation of maximum run-off in the event of rainfall. The interrelation between rainfall and retention in a watershed directly affects run-off; when the amount of rainfall exceeds the storage of land surface, run-off occurs. Nonetheless, the soil and land use properties influence the amount of run-off.

2.5 Soil Erosion

Soil degradation is the deterioration of bio-physicochemical properties, such as organic matter reduction, compaction, salinization, fertility loss and erosion.

There are many reasons for desertification in drylands; vegetation is reduced by drought and overgrazing by livestock, soil compaction and organic matter losses are induced by poor agriculture practice, and salinization increases with poor irrigation, which leads to the increase in soil erosion rates and, eventually, desertification. Therefore, the fact implies that the most imperative and leading indicator in the desertification processes is soil erosion.

Drylands are mostly susceptible to soil erosion (by wind and water), which is a natural geologic process associated with aeolian and the hydrologic cycle. Nevertheless, the process is more pronounced in drylands because there are less protective agents to save the soil from erosion.

The major factors in water erosion are climatic, soil erodibility, slope, vegetation and management (how to exploit the land) (Renard and Freimund 1994):

- Precipitation

Rainfall is the main reason for water erosion. The amount of rainfall and its intensity play a leading role in erosion. Rainfall intensity can, in two ways, hasten erosion: when the soil cannot absorb and hold water; therefore, producing run-off, and when the force of rain damages the soil surface.

- Soil erodibility

According to Wischmeier (1974), soil erodibility is soil resistance against the separation and transfer of particles. Soil erodibility is associated with soil texture, meaning that soils with silt content are subject to more erodibility. Additionally, the rate of infiltration, total water capacity, water holding capacity, soil structure and organic matter, all affect the capacity for soil erodibility.

- Slope

The primary characteristics of a slope, in relation to erosion, are gradient, length, shape and aspect. On sharp slopes, water moves more quickly, thus creating high kinetic energy, which is more erosive and destructive. Erosion on long slopes is higher than on short slopes.

- Vegetation

The density, growth rate, and vegetation cover directly affect water erosion; in forests, soil permeability is higher than non-forest areas.

- Management

Poor and exploitative land management increases erosion. Some of these methods include deforestation, overgrazing, and land extension in drylands.

Water can cause erosion in a number of ways: raindrop, sheet, rill, inter rill, gully and massive, stream bank, and badlands.

Over the years, many approaches have evolved to measure erosion and soil loss. The most widely used is the Revised Universal Soil Loss Equation (RUSLE), proposed by Renard. Its simplified version is used in GIS to estimate erosion. However, there are some limitations in RUSLE: it only estimates soil loss rather than absolute and real soil losses. RUSLE estimates only sheet and rill erosion (Toy and Foster 1998).

2.6 Drought

Drought is a long-term phenomenon that affects large regions, impacts adversely on human lives and economies. The cost of drought, collectively, is higher than any other form of natural disaster (Wilhite 2000).

Despite worldwide distribution, there is no clear, universal definition about drought. Generally, drought is the duration of low precipitation and soil moisture, which occurs through significant negative water balances. According to American Meteorological Society (1997), four types of drought are defined: meteorological, agricultural, hydrological, and socioeconomic droughts (Loukas and Vasiliades 2004), as shown in Figure 2.2. Three of these drought types are environmental disasters (Wilhite 2000). According to American Meteorological Society (AMS), their definitions are (Heim 2002; Shamsipour 2007):

- *Meteorological (climatological) drought* occurs when the rainfall over a region in some period of the year is less than normal precipitation, and atmospheric condition cause reduction in precipitation. This meteorological drought might happens quickly even for a short period. The deviation of rainfall from normal condition shows the intensity of the drought. Its definition is unique for each region, because weather conditions, which cause rainfall, vary for each region.

- *Agricultural or ecological drought* refers to drought during the developmental stages of plants in growing season, from emergence to maturity; any deficiency of moisture in soil layer (root zone) in this critical growing period might affect the plant growth; for instance, if the deficit of moisture delays germination or if it occurs during growing period, crop yield decreases. The onset of agricultural drought relates to soil

properties and its prior moisture condition.

- *Hydrological drought* is the period with a decline in precipitation (including snow) which affects run-off and groundwater. During this time, streamflow, river, reservoir, lake, and groundwater levels decrease.

- *Socioeconomic drought* is the combination of population demand for water, coinciding with meteorological, hydrological and agricultural droughts. In contrast to other droughts, the definition of socioeconomic drought depends on local and commercial conditions for demand, for goods, including water, forage, grain, fish and hydroelectricity.

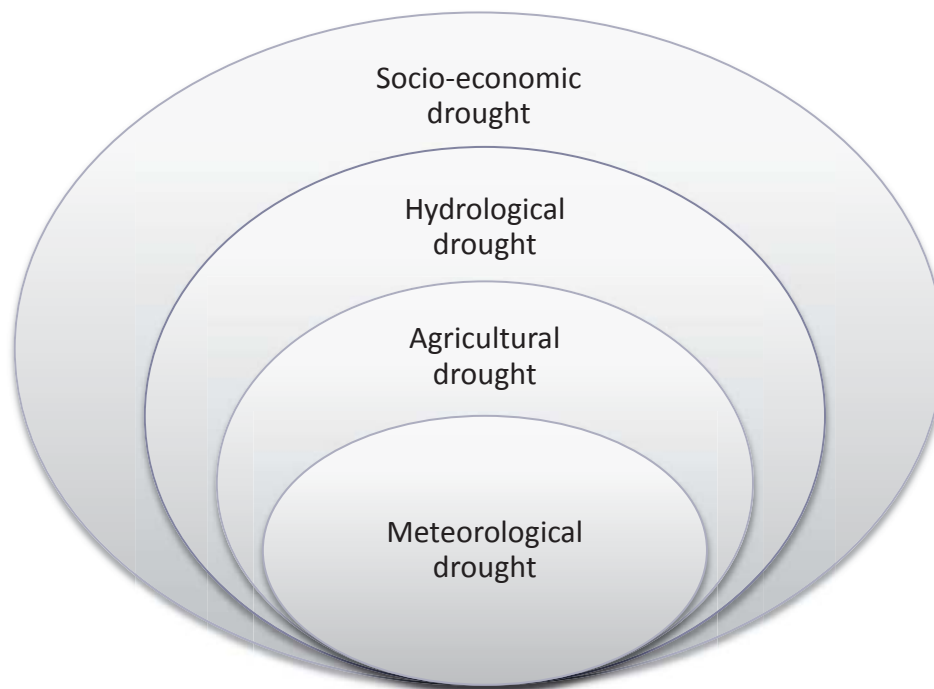


Figure 2.2: The intensity and severity of droughts

The frequency and severity of hydrological drought often can be expressed in the watershed or river basin scales. Nonetheless, hydrologists must pay more attention as to how water deficiency appears in the hydrological system. Usually hydrological drought refers to the longer period of drought that contains meteorological and agricultural drought. There are four parameters to evaluate and analyze drought (Shamsipour 2007):

- The beginning of drought

In early warning systems, the beginning, duration, and the end of drought are crucial stages. Sudden and unpredicted long droughts create chaos and have catastrophic consequences. It is evident that drought does not start after the last effective rain, but its onset is after the depletion time of soil moisture. Therefore, in general, drought starts whenever soil dries (agricultural drought) or water in reservoirs is depleted (hydrological drought).

- Drought severity

The less rain occurs than the average precipitation of a normal year, the greater the severity of drought. Equally, the duration of the drought relates to the severity of the drought. In the case of a short drought, soil moisture deficiency can be compensated by little water, whereas the adverse impact of a longer drought needs more time for the soil to recover its efficiency. The severity of drought is also associated with the extent of drought.

- Drought frequency

The frequency of drought in a specific period is one of the most noteworthy characteristics in drought analyses. This parameter is useful in the reassessment of the environment and can also be classified in the different intensities. The drought probability and return period (the interval occurrence) are used to forecast the occurrence of drought severity in the developing projects. According to meteorological statistics, the interval occurrence of severe drought for Kashan is approximately five years.

- Drought extent

Drought can occur at different spatial scales, from local to regional. It is also a fact that the spatial distribution and the severity of drought in a vast area are not uniformly consistent.

The Standardised Precipitation Index (SPI) is a statistical indicator to represent the measurement of drought and wet periods in a region. The SPI is the normalized index based on the bias of mean precipitation for the considered period, so that the positive values, above the mean precipitation, indicates wet periods, whereas negative values indicate drought periods (McKee et al. 1993). In addition to the flexibility and simplicity of calculations, SPI is a useful indicator for areas that have limited data, only requiring precipitation. SPI helps to determine the occurrences of drought in a given time scale.

SPI is also a helpful index to determine meteorological, hydrologic or agricultural drought. For instance, soil moisture content is sensitive to the short-term deficiency of water, whereas stream flow and groundwater respond to longer-term precipitation deficiency (Tsakiris and Vangelis 2004; Loukas and Vasiliades 2004; Quiring and Papakyriakou 2005). It can also be used to pinpoint the onset of a drought (Loukas and Vasiliades 2004). Additionally, although the distribution of rainfall is under effect of altitude, SPI is spatially invariant with low dependency to topography (Pashiardis and Michaelides 2008).

Chapter 3

Fuzzy Logic

3.1 Introduction

For many years, humans have challenged the acquisition of knowledge, explicitly without ambiguity. Since Aristotelian binary logic was introduced, this logic has helped mankind to achieve remarkable success in the development of modern technology. However, at the beginning of the 20th century, researchers and scientists realised that traditional logic could not answer some of the questions posed by natural phenomena. Therefore, some new approaches were invented in mathematics and logic, such as probability science and fuzzy logic; scientific theories that not only are proved in the abstract but also in industrial applications. In traditional knowledge, classical sets are used; even computer systems were at first based on them.

Fuzzy logic allows us to describe the course of actions through linguistic terms and rules. “IF-THEN” rule is the classic representation of knowledge. Therefore, fuzzy rule-based systems are used in problem solution and decision making (Cordón et al. 2001). Furthermore, adaptive fuzzy control is used in industrial automation as well as spatial decision-making solutions (Altman 1994). Fuzzy logic also helps us manipulate information to achieve the determined results even with imprecise and ambiguous information, especially in control systems. Its methods to control systems mimic how humans make decisions, but faster and

more accurately. Therefore, fuzzy logic is used in modern science to explain the robustness of conclusions and decision making, which agree with human thought (Garavelli et al. 1999).

Classic logic (so-called traditional, conventional, binary or crisp logic) has a significant place in the overall history of science, but fuzzy logic is more descriptive and applicable for some systems. Fuzzy logic is an extension of classic logic, that is, continuous logic. In fact, the creation of fuzzy logic was a response to continuous changes in the environment and physical variables, and proved an answer to the restrictions in environmental studies in conventional (binary) logic. Furthermore, fuzzy system simplifies processes in complex systems, even it works with incomplete data, which is not possible by conventional statistical methods; indeed, its application means there is no longer a need to solve complex equations in a control system.

As a real language, fuzzy control system allows us to incorporate the ambiguous and approximate nature of human logic into computers, which leads to the quick processing of development cycles as well as better and easier controlling of systems. The industrial application of fuzzy logic started after Mamdani (1974) used fuzzy rules in the control system of a simple dynamic plant, which was not possible with conventional techniques. Zimmermann also used fuzzy logic in decision support systems (fuzzyTECH 2001).

3.2 Uncertainty

Probability is central to any systems, so that phenomena in terms of probability strongly affect all branches of science, especially complex stochastic systems, which increases with the number of observations. However, the nature of uncertainty in such systems is different, where a phenomenon occurs randomly and by chance.

Mathematical disciplines, such as probability theory, information theory, and fuzzy set theory, deal with the description of uncertainty in knowledge, here, there are two types of uncertainty, stochastic and lexical uncertainty (Mian 1999). Consider these statements:

Statement 1 *“The probability of drought is 0.7.”*

Statement 2 *“In arid zones, this year will probably be a very dry year.”*

The first statement is about stochastic uncertainty, it says the probable occurrence of a certain event; its probability is 0.7. The second assertion is a lexical statement. Firstly, this event itself is not clearly defined; secondly it is a “subjective category” (Mian 1999). For some farmers, an unusually dry year means no water for land, whereas for others, it might mean that predicted rainfall will not exceed last year’s deposit. For one farmer, it might not be a fixed threshold to define whether this year is dry or not. In addition, in the second statement, there is no quantifying expression for probability within the environment. Hence, here the concept of a “drought year” is a subjective category.

Subjective categories in statements play key roles in decision-making processes. For example, in statement 2, even without quantity, the message is understandable and can be used successfully to evaluate a complex system. Sometimes, we add some flexibility in word definition, especially in decision-making such as the “appropriate” positions. For instance, in legal systems, there exist contradictory laws and regulations, such as in punishment and forgiveness, which are often judged on a situational basis.

In the natural environment, the boundaries of spatial features are not clearly defined (Jiang 1998), but are mixed, additionally, the variables are interactive. For instance, in the digital classification of soil types, the assigning of pixels for a certain class might have some uncertainties, particularly in the boundary of two classes. Any pixel might have the spectral mixture of inherent materials. Furthermore, some natural phenomena such as desertification inherently result from the contemporary various and different factors such as erosion (either wind or water), vegetation deterioration, flooding, and drought. Therefore, effects cannot be explicitly determined.

Sometimes uncertainty is due to the paucity of data, vague definition or internal variability. Without sufficient data, it is difficult to measure how various elements influence the spatial variation of concepts such as vulnerability and sensitivity. Consequently, there, methods will be needed to manage uncertainty (Agnew and Warren 1996; Bone et al. 2005). Relative to the heterogeneous and continuous nature of the desert environment, few researches have been performed, especially integrated vulnerability mapping with remote sensing, GIS, and fuzzy logic.

In land degradation mapping, a geologist or a geographer might provide different maps. Even for soil experts there are no identical maps. In fact, it is not possible to define rules for each possible case. For different cases, we define unique rules, which are discreet points in the

continuum of possible cases, which people respond to. Therefore, for a given situation, he or she combines rules and describes the analogical situation being observed. This approach is possible because of flexibility in the definition of words in rule forms (Mian 1999).

3.3 Linguistic Variables

Zadeh (1975) proposed linguistic variables in the concept of fuzzy logic, because for humans, imagining variables as terms or linguistic issues is better than to imagine them as numbers. Fuzzy set terms as adjectives describe linguistic variables; variables such as temperature, flow, pressure, and speed can be described by the term set {low, moderate, high}. A variable such as “error” might have the fuzzy set {large positive, small positive, zero, small negative, big negative}. For the variable “drought”, there might be the fuzzy set {dry, wet}, so that any of them will be projected by the appropriate membership function. Fuzzy logic describes ambiguous terms such as “high”, and “very low” as well as “average”; it fills the vacancy in crisp sets (Mahler 1995; Hodges et al. 1996).

3.4 Fuzzy Set

Fuzzy set theory at first was introduced by Zadeh (1965) and followed by fuzzy logic to process information. Instead of dealing with only truth and falseness as in the Aristotelian binary logic, fuzzy set theory handles the membership number between zero to one. In other words, in traditional binary logic, set has two memberships (zero, one) while in fuzzy set theory, set has the infinite memberships that have the values from zero to one. Therefore, this fact makes fuzzy logic closer to human thinking. So those members in set, besides the mode of being a member or not, can be defined between two modes.

In the classical (conventional) set theory, the elements of a set A considering the universe set X can be represented by specifying characteristic function $\chi_A(x)$ of elements:

$$\chi_A(x) = \begin{cases} 1, & \text{if } x \in A \\ 0, & \text{if } x \notin A \end{cases} \quad (3.1)$$

Therefore, $\chi_A(x)$ has only null (“False”) and one (“True”) to express truth degree. Therefore, classical sets are called binary set, or crisp set. Non-crisp set, which is known as fuzzy set, is an extension of classical set. In that, the characteristic function called membership function $\mu_A(x)$ to

indicate the degree of membership, which shows the membership value for any element, in the range of a closed interval $[0, 1]$. In other words, fuzzy set is the superset of conventional (Boolean) set that manipulates the degree of memberships by fractional true values between “fully true” and “completely false” (Glöckner 2006). The membership grade for an element in fuzzy set is calculated by mapping elements in the range of zero and one by using membership function.

In man-made maps like cadastres, we can find sharp and distinct boundaries among land use types such as croplands and residential areas. In drylands, land covers such as forestlands, pasturelands, lowlands, pediments and plateaus have no sharp and exact boundaries. In fact, their boundaries are vague and imprecise. Even though they share the spatial similarities of some land types, desert terrains are highly inhomogeneous; there are few homogeneous classes, and boundaries among them can be extremely vague (Erwig et al. 1997).

In drylands, except uniform land types such as sand dunes and permanent water bodies, all other features are so small or complex that they cannot be easily identified by coarser resolution satellite images. Therefore, there are many mixed pixels in the acquired images. Furthermore, in arid zones, changes over space and time will not occur drastically, as they evolve more slowly.

Considering an answer for the term “hot month in a year” in the northern hemisphere, they are the months of the warm season. To find an appropriate answer, a person would compare the status of months by two “prototypes”: firstly, “perfect” hot months of the year with sunny and scorching days, and another is “imperfect” hot months without these characteristics. Now it is possible to evaluate between two ranks.

In classical (crisp) logic, to make a model, first we should define the set of all hot months. Then, by using mathematical function, we decide about each month whether it is a member of set and is included or not. Therefore, the set may include {May, June, July, August, September}.

In order to clarify the concept of fuzzy set and crisp set, Figure 3.1 illustrates the set of “the hot months of a year” (the red line) including months with temperature $22.5\text{ }^{\circ}\text{C}$ or higher, the universe discourse is total months of a year. Figure 3.2 represents the concept of crisp, multi-valued and fuzzy membership; considering the prototype for “hot months”, for each month, a certain value of membership is allocated. This degree corresponds with “degree of membership”, $\mu(x)$ for the element $x \in X$, the set “hot months”. The temperature of the month

is also called “base variable” (Mian 1999) with $\mu_{(x)}$ varies from zero to one, representing the threshold for complete non-membership and full membership to “hot month” set, respectively.

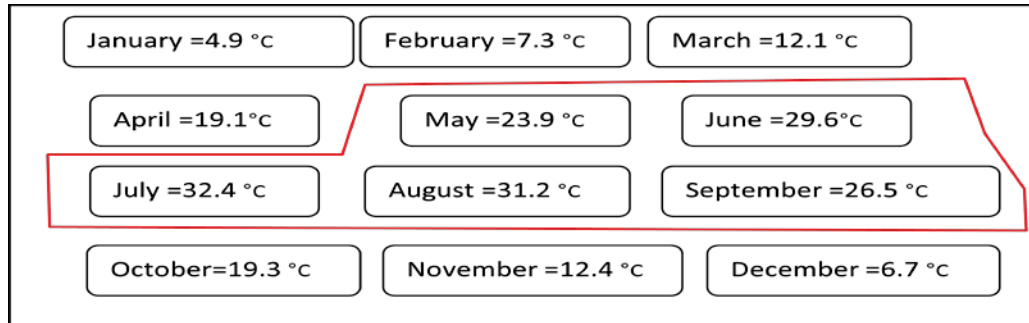


Figure 3.1: Set of “hot months” in crisp set theory; the data are the monthly average temperature of synoptic, meteorological station at Kashan, Iran, 1967-2008.

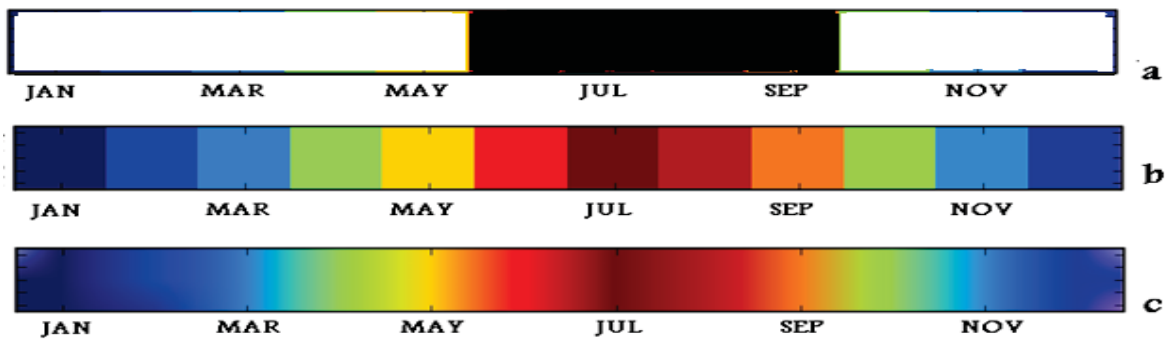


Figure 3.2: Crisp and fuzzy membership representation for “hot months”

In Figure 3.2 (a), according to classical (crisp) logic, the “hot months” are represented by filled black colour, with characteristic membership value of one. Figure 3.2 (b) is the multi-valued logic representation of “hot month” that includes all months; the red-coloured ones are “hot months”, considering discrete values. Figure 3.2 (c) shows the truly “fuzzy” set of “hot months” in a year with the inclusive, continuous membership degree between one and zero. In Figure 3.2(c), the contiguous and graduated changing of colours grades from red to blue, this indicates the degree to which the month temperature belongs to the set of “hot months”. A gradation of colour that makes the area in Figure 3.2 (c) looks as if it is fuzzy.

In Table 3.1, the monthly mean temperature values are brought from the meteorological station of Kashan, Iran. The membership degree for temperature is calculated for “hot” term in the range (25-30 Celsius degree); the months with temperature 30 °C or higher are designated as

full membership, and the month with temperature 25 °C and lower has no membership value. As temperature 25 °C or lower has no membership at all, a temperature of 30 °C or higher would have complete membership. Temperature values between the two ranges are members of the set, in considering temperature 25 °C as the crossover point.

As Figure 3.2 (a) shows that as crisp set, a temperature of 24 °C and a temperature of 27 °C, are evaluated differently, the crisp threshold has selected the latter one.

Table 3.1: Fuzzy and crisp values of monthly mean temperature of synoptic, at the meteorological station Kashan, Iran, 1967-2008

	Jan	Feb	Mar	Apr	May	Jun	Jul	Aug	Sep	Oct	Nov	Dec
Temperature	4.9	7.3	12	19	24	30	33	31	27	19	12	6.7
Crisp values	0	0	0	0	0	1	1	1	1	0	0	0
Fuzzy values	0	0	0	0	0.4	1	1	1	0.7	0	0	0

In converting crisp conventional logic to fuzzy set, we should consider the threshold for the selection boundary. Here, in the fuzzy set the temperature 25 °C has a membership degree of 0.5, which called the crossover point. In simple defuzzification, the crossover point will be used that the values higher than 0.5 get true value. For example, the expression, “the month has a temperature of 27 °C” would get “True” in crisp set in converting the fuzzy degree of 0.7. As fuzzy set is a generalized form of conventional crisp set, the membership degree in the set becomes the truth degree for each member of the set.

3.5 Fuzzy Inference System

A fuzzy inference system (FIS) has three main blocks: fuzzification, rule base, defuzzification. In fuzzification, the crisp input values are translated into linguistic concepts, fuzzy sets, by using the corresponding membership function. In fuzzy rule inference, or rule base, the defined fuzzy sets of different variables are connected to each other and the result is calculated; IF-THEN rules, which define the relationship between the linguistic variables, are defined as antecedent (IF-part) and conclusion (Then-part). Defuzzification, meaning the converse of fuzzification, the fuzzy linguistic concept of result from the rule base is converted to a crisp output value.

In fuzzy system, as with the modes of human cognition, reasoning plays a major rule. The reasoning in a fuzzy system is approximate rather than exact. The essential characteristics of fuzzy logic are as follows (Fullér 1995):

- In fuzzy logic, the results are derived by approximation reasoning like human nature.
- In fuzzy logic, everything belongs to its certain set from a universe of discourse by a graded degree of membership.
- Any conventional system can be converted to a fuzzy system
- In fuzzy system, knowledge is interpreted through rules and variables.
- A fuzzy model can control nonlinear system easily and simply, but in mathematical models, they might be too difficult or complex.

3.5.1 Fuzzification

Fuzzification is a stage that is applied to convert crisp values to the given fuzzy set by the function known as membership function (MF). Fuzzification is the mapping of inputs into the degree of membership by proper membership functions for the partitions of linguistic variables as linguistic term sets or linguistic values. The fuzzy term sets are most commonly used for converting objects or phenomena in the continuous values, where the classes have shared boundaries (Burrough 1989).

There are several forms of membership functions. Generally, the shapes of membership functions are triangular, trapezoidal, bell-like, or Gaussian forms that might be drawn linearly or non-linearly (Figure 3.3). The crisp quantities, as support, are on the horizontal axis. The results of the membership function $\mu(x)$ are projected on the vertical axis (y). The quantity on the horizontal axis is the "base variable" and represents the universe of discourse; while the quantity on the vertical axis is the membership degree to the fuzzy set.

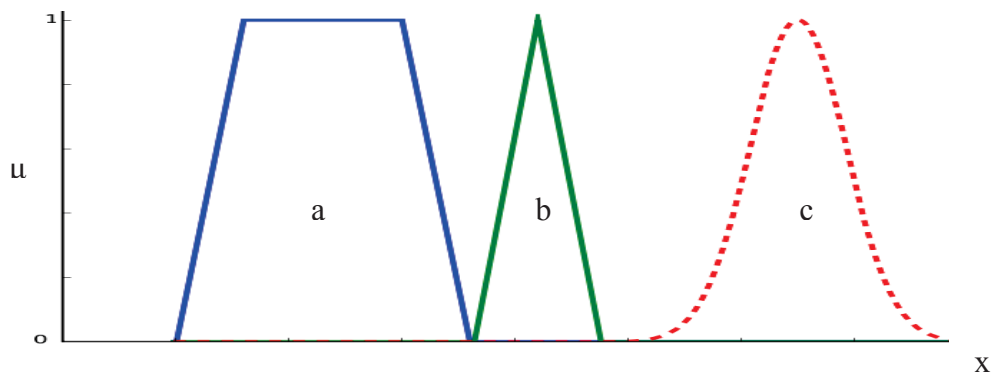


Figure 3.3: Membership functions; trapezoidal (a), triangular (b), and bell-shaped (c) forms

3.5.2 Operators

For building a rule-based system, experts designate some linguistic variables and applies operators such as union (OR), and intersection (AND) to connect variables and interpret elements of rule, which might constitute simple or composite terms.

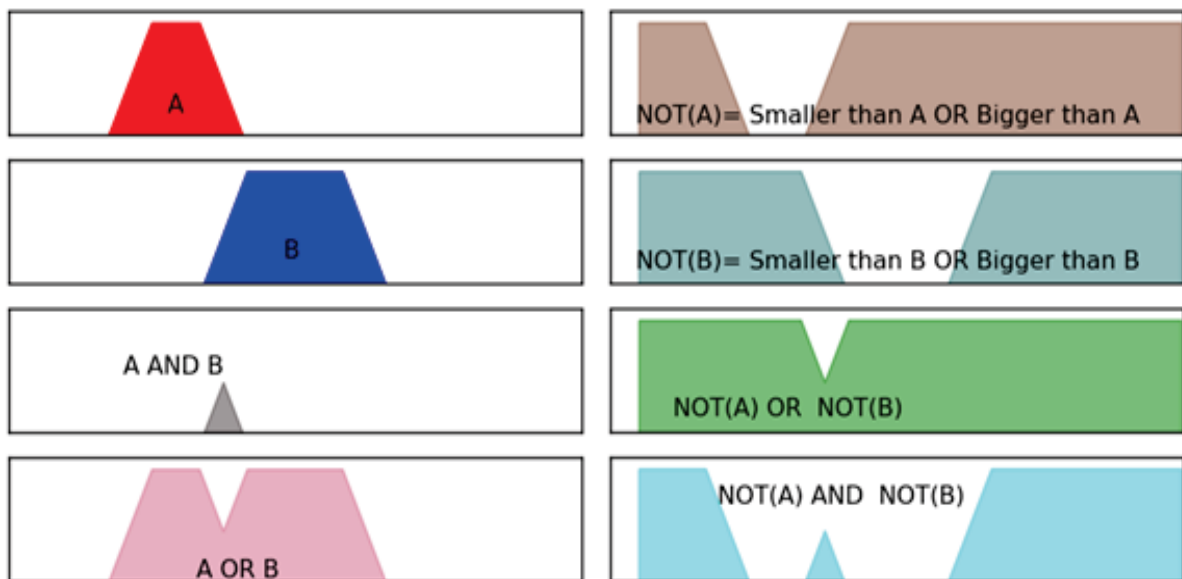


Figure 3.4: Possible linguistic terms and operators (AND, OR, and NOT) for a fuzzy partition with two linguistic terms (A, B).

For composite rules, experts use the combination of the binary operators; in practice, Minimum operator and Maximum operator are used for intersection (And) operator and union (OR) operator, respectively. The possible combinations of operators are illustrated in Figure 3.4 for possible forms with two fuzzy set terms (A, B); the two diagrams (top left) form strong fuzzy

sets. The others are derived from the combination of elementary terms and operators (Alonso Moral 2007).

Negation (NOT) as a unary operator is the complement membership degree of a variable, which is a subtraction from one. In practice, negation simply means values smaller or bigger than the relevant fuzzy set (Alonso Moral 2007), as shown in Figure 3.4 (top right).

3.5.3 Fuzzy Rule Inference

One utility of fuzzy models is the application of rules. In fact, humans often use rules in any situation, but these rules are not exactly fixed; however bi-valued systems could not operate based on such fuzzy concepts (fuzzyTECH 2001).

Fuzzy rule-based system is the extension of classical rule-based systems, which is incorporated in fuzzy set theory, by using fuzzy rules and linguistic variables. A typical fuzzy rule-based system has comprises of two parts: Knowledge Base (KB) and Inference System (IS). A Knowledge Base (KB) stores the knowledge about a system in forms of “IF-THEN” rules, as rule base while inference system uses the stored information in inference processing (Casillas et al. 2000).

A rule has two parts including premise (antecedent) and consequence (conclusion). Premises or antecedents are arguments as the facts that support the conclusion. In a fuzzy inference system, premises (P), which are partially true, reaches conclusions (Q), which are also partially true. As conclusions are proved by reasoning, the conclusion of a rule is a type of inference (Castillo and Melin 2008).

In general, fuzzy rule definitions are proven by the generalized modus ponens and the fuzzy implication principles. Cause-effect relations are defined as rules, which consist of two parts (IF-part and THEN-part), which are brought as following form (Bouchon-Meunier et al. 1995):

Rule: IF premise (antecedent), THEN consequence (conclusion)

$$P \Rightarrow Q$$

The IF-part (premise, P) comprises inputs which are aggregated by binary operators: Minimum (And) and Maximum (Or) operator. IF-part is used to fire the agent of rule, while Then-part is consequence (Q).

The inference consists of three sub-stages: aggregation, activation and accumulation (composition). Aggregation determines the degree of accomplishment of the consequence (Q) from the degree of membership of the sub-antecedent (Figure 3.5). However, if the antecedent (IF-part) consists of the combination of several sub-conditions, the degree of accomplishment must be determined by the aggregation of the individual values. If conjunction (intersection form) or disjunction (union form) combines with a sub-conditions of rules, the degree of accomplishment is calculated by means of And operator and OR operator, respectively.

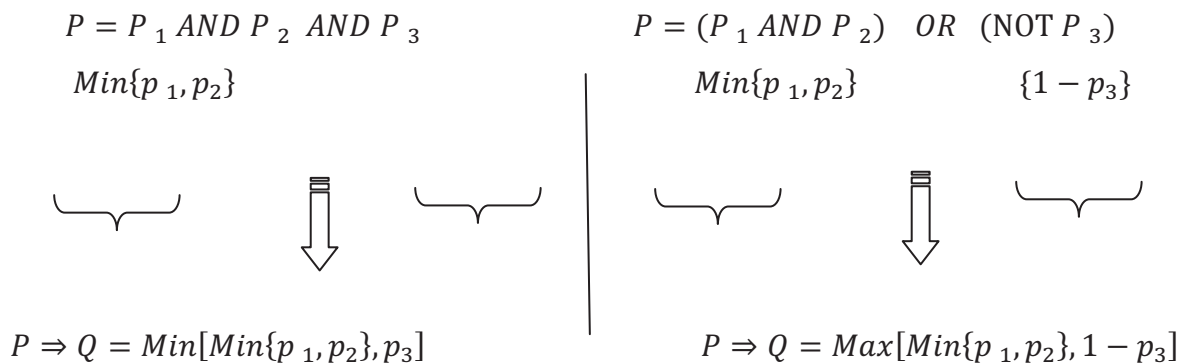


Figure 3.5: The principles of aggregation (National Electrical Manufacturers Association, NEMA 2005).

To compute the conclusion of the condition of rules, the activation method is used for the implication for each rule; that is, the conversion of IF-THEN-Conclusion. There are three kinds of implications: T-implication (triangular-norm or t-norm), S-implication (triangular co-norm or t-conorm), and R-implication. Triangular t-norm is applied for logical relations of AND forms while triangular co-norm (shortly t-conorm) is used for logical connection of “OR”. T-implication, which is practically implemented in systems, uses minimum operator in Mamdani model ($x \rightarrow y = \text{MIN}\{x, y\}$) or multiplication ($x \rightarrow y = xy$) in Larsen model. S-implication uses t-conorm and negation, which is based on the formulation ($p \rightarrow q = \neg p \vee q$), for instance, it can be shown with Max-operator as ($x \rightarrow y = \text{MAX}\{1 - x, y\}$) in Kleene-Dienes implication (Fullér 1995, p. 47).

Before accumulating all the rules, sometimes a weight factor is applied for each rule, which represents the participation of the rule in the inference system by giving weight for each rule (weight \times rule). If the weight factor as certainty is null, it means that the rule is not included in the

inference system (National Electrical Manufacturers Association, NEMA 2005). The accumulation stage is the combination of all activated rules to calculate the overall result. Generally, the maximum operator is used.

3.5.4 Defuzzification

In practical process and classification, the fuzzy set of output linguistic variable needs to be converted to a crisp result. Defuzzification converts the overall output of fuzzy system to a crisp value. There are many methods to defuzzify the overall accumulation output of rules such as Centre of Gravity (CoG), Mean of Maxima (MoM), the Left most Maximum (LM), and the Right most Maximum (RM). Centre of Area (CoA) or Centre of Gravity (CoG, centroid) is the most popular defuzzifying method (National Electrical Manufacturers Association (NEMA) 2005).

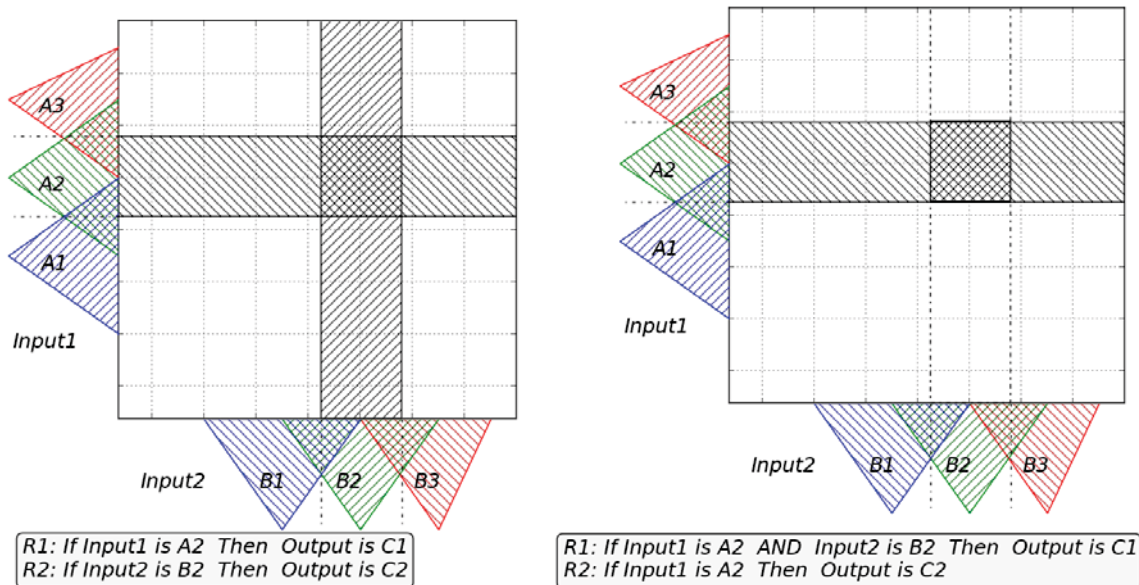
3.6 Rule-Based System Improvement

There are two methods to define the robust rule-based system: the definition by the expert or induction from data. Nonetheless, in rule building, some problems such as consistency, circularity, completeness, and redundancy should be evaluated. Since inconsistency and redundancy may appear during the rule integration stage, this section introduces all the possible conflicts with their solution, according to Alonso Moral (2007).

Consistency is the quality of the knowledge base to conduct true conclusions for all premises simultaneously; that is each observation or evidence should have a true consequence. Circularity or identical rules refer to duplicated rules. The completeness of rules means that any rule has to include all premises (input space) to conduct a conclusion. Redundancy is the existence of the same results and the contribution of the rule in output (Gerrits and Spreeuwenberg 2000).

In the rule-based system, the first rule base is defined by integrating expert knowledge and data, after the definition and designation of partitions and rules. The next step is the analysis of consistency to find conflicts among the rules. According to Alonso Moral's solution (2007), the consistency analyses are grouped into inconsistency and redundancy, based on the quality or inequality of output space.

Consistency between rules means having no contradiction and conflict among the rules. It is necessary to evaluate relationships such as equality, inclusion, and not empty intersection, or inequality of consequences, among rules and their space coverage. If the output spaces are different in the two rules, that is, if they have different conclusions, and the inputs' space is included (i.e. two inputs' spaces are identical), there is an inconsistency between the rules. In this case, one of the rules must be deleted. If two input spaces have only shared coverage in the intersection, one rule conclusion is not entirely contained in the other rule. In this case, the conflict is called “not empty intersection” or partial inconsistency (Figure 3.6, left).



Not Empty Intersection

Rule R2 is covered with rule R1

Figure 3.6: Linguistic conflicts (Alonso Moral 2007)

In order to avoid this conflict, the rules need to be split. For the common domain, a suitable conclusion might be chosen. In this case, the input space covered with one rule is fully included in other rule - this problem is called specialization. The first rule is the specialized form of the second rule (Figure 3.6, right). When a conflict arises in rules, one of rules should be deleted. The expert rule takes priority (Alonso Moral 2007).

To avoid the aforementioned conflicts, the suggestion is that rules have a canonical form, i.e. they must use the AND operator. Considering Figure 3.5, the operator OR might involve k adjacent terms of a given variable, while NOT operator with M terms will be extended into $M-1$ rules.

3.6.1 Simplification

Simplification aims to reduce the size of rules, premises and the number of labels (fuzzy set) in a rule base (rule block). The simplification of a rule block helps to improve interpretability, and ultimately to construct one simple, compact knowledge base without losing accuracy. Simplification is possible in rule base and data base stages; in the first stage, fuzzy partitions (fuzzy set) are not altered but some new composite labels appear. Data base simplification is involved in the updating of the partitions (Alonso Moral 2007; Alonso Moral et al. 2008).

3.6.1.1 Rule Base Reduction

According to Alonso Moral (2005), simplification in rule base stages includes following four steps:

- Elimination of redundant rules

In order to build interpretable and compact rule bases, it is necessary to resolve the redundant rules issues. For this reason, a more specific rule is deleted. Expert rules are more general, so they are not deleted. In the partial redundancy, the redundant part of the rules is removed. In circularity and identical problems, one of the identical rules is deleted.

- Merging of rules

If two rules with neighbouring linguistic terms in a fuzzy set are also linguistically compatible, and have the same consequence, they are likely to be merged. However, given the existence of data, the accuracy of the rule base system and the consistency of rules are factors to determine the merging of rules.

- Forced elimination of rules

If the space coverage of the rules is small and restricted only to few data, it is possible to remove this rule, by considering the acceptance threshold for accuracy. Alonso Moral (2005) used the weighting of the rules and the difference in the sum of the matching degree of the positive and negative examples.

- Forced elimination of premises

In this stage, according to Alonso Moral (2005), the less used premises are eliminated; in this regard, the number of premises and the rule base complexity are determined. According to the input frequency in a rule base block, the rules are first ordered, then input variables are ranked according to the user-defined threshold, and the premise is deleted.

3.6.2 Data Base Reduction

Data base reduction, which is similar to rule reduction, includes four steps: the removal of unused variables and labels, the merging of the adjacent labels, and, finally, the forced elimination of variables. At first, by searching, the variables and labels that are not used in any rules are found; then these variables or labels are candidates for elimination.

According to Alonso Moral (2005), in order to keep the strong fuzzy partition form, it is necessary to expand the adjacent side of the remained fuzzy sets in the neighbourhood of the deleted fuzzy set (partition). Its name is also changed, to correspond with the final new fuzzy set, with the term “more or less”. For this purpose, the left corner of the deleted fuzzy set should be the centre for the right side of the remaining fuzzy set on the left of removed fuzzy set. This procedure is necessary for the remaining fuzzy set on the right-hand side of removed fuzzy set, by the moving of the left side towards the left, until its centre locates on the right corner of the deleted fuzzy set.

Linguistic analysis helps to find out, and to merge, the adjacent labels which are always used together, and then by modifying the fuzzy partition definition, a new fuzzy label is built by using the term “OR”.

Finally, when a variable is removed in forced elimination, and in order to build a compact knowledge base, the effective variables are kept. In this way, variables are ordered according to their frequency, and the lowest ranked ones are deleted, based on a user-defined threshold.

3.7 Decision-making Principle in Rule-based systems

There are two main approaches in a rule-based system: expert or data-based learning. For building rules, expert learning can use basic knowledge and experience to determine rules. This type of system, which is of human orientation, is simple, general and interpretable. In contrast, data-

based learning is more complicated, and the created systems are also less interpretable; the system is dependent on the availability of input and output data.

3.7.1 Expert Rules

In environment, vegetation needs some essential resources, which are defined by Law Of Minimum (LOM) and Law Of Tolerance (LOT); therefore, these laws help in decision-making in preparing the susceptibility map.

In environment, the basic need of green plant is changeable, which depends on circumstances and species of plant. In this regard, the scarcity of an agent or a resource as a constraint controls the growth of plant. In other words, the minimum amount of element is a limiting factor of vegetation growth.

Vegetation demands sufficient nutrients to grow and develop properly. Any extreme reduction in a required nutrient restrains the growth of a plant. In other words, in natural resource management, the most limiting resource of growth controls the yield and production of plants, whichever the needed element is scarce or an environmental factor restricts the availability of this element. Under the circumstances, only the scarcest factor with the extreme minimum amount controls the growth of vegetation, although there are plenty of the other resources. In other words, deficiency in a resource is a constraint to develop despite high availability of other resource. It is known as Law of Minimum (Liebig's Law), which is also validated for moisture and non-nutrient factors such as temperature or temporal factors. Law Of Minimum (LOM) only describes the limiting factors, while Law Of Tolerance (LOT, Shelford's Law) explains extreme maximum amount of a resource.

According to Law Of Tolerance (LOT), any organism has a minimum and maximum tolerance threshold, which the organ survives. In other words, in environment, the success or failure of an organism depends on suitable conditions, which a deficiency or overplus of an agent control the living. In other words, the existence of an organism in environment is associated with a set of conditions; therefore, LOT deals with the maximum and minimum condition, which an organism in ecosystem tolerates. The deficiency of a needed element or an unfavourable environmental condition might affect life, which depend on the tolerance of organism. Therefore,

regarding the environmental factors such as light, temperature, and physiochemical elements, organisms have a "maximum limit", which can be tolerated.

3.7.2 Data-based Rule Learning

One of the most important stages in fuzzy system modelling is the designing of rules, which is conducted in two ways: human expert knowledge and data-based learning. The former uses linguistic information and human experience gained through heuristic approaches, while data-based learning gains its information from numerical data by matching paired input and output. The human experiences, in the expression of relation between input and output, are shown as "IF-THEN" rules which determine an action depending on a certain situation (Wang and Mendel 1992).

In order to generate fuzzy rules from numerical data, using paired input-output, Wang and Mendel (1992) proposed the following five steps (Casillas et al. 2000; Wang and Mendel 1992):

- Fuzzy partitioning of inputs: The first step is to partition the spaces of input and output into a fuzzy set. In this stage the space of input variables are divided into equal or unequal partitions; for each of these partitions is also defined a membership function. In the event of availability of expert knowledge, these partitions are selected by the expert. In our case, an overlapped symmetrical triangular of membership function is chosen for fuzzy partition.
- The determining of candidate rules: By examining input-output data pairs, and setting their coverage with the defined rule, (should a rule cover best space of input-output data), a nominated rule is determined and entered into a set of rules.
- The allocation of importance for each rule: The third step is the determination of the degree of importance for the contribution of each rule in the determined model, especially for the solution of possible conflicts among rules in the following step.
- The final rule base: The fourth step creates the final integrated expert-and-data rule base; the importance degree is given to select final rules by grouping rules based on different antecedents, and giving an importance degree for each group.
- Defuzzification: The fifth step is mapping the input space through rule base to output space to obtain a final result.

3.8 Fuzzy Control Language (FCL)

The theory of fuzzy logic in the application of a control system is known as "fuzzy control", which is a technology for the improvement of automatic industrial control, especially by using knowledge so-called linguistic rules base. Fuzzy control is widely used in various control systems, such as classification, pattern recognition, decision making. Therefore, the language used in the implementation of the fuzzy logic in control system is called Fuzzy Control Language (FCL), which is published by the International Electro-technical Commission (IEC), in which all steps and terms are clearly defined (National Electrical Manufacturers Association (NEMA) 2005). The formal structure and same styles are helpful to understand and write in programming language such as Pyfuzzy based on Python programming, which can parse the Fuzzy Control Language (FCL) format.

In Fuzzy Control Language (FCL), all components of the fuzzy system are defined by the specific name (Figure 3.7). "TERM" refers fuzzy sets, so that points are declared in pairs (x, y) for membership function, which x refers to the real values of variable and y is fuzzy membership value ranging from 0 to 1.

A simple example of fuzzy rule inference and the result is illustrated in Figure 3.9, by the following rules:

Rule 1: If vegetation is low and slope is high, then erosion is high.

Rule 2: If vegetation is high and slope is moderate, then erosion is low.

Figure 3.8 shows fuzzy control by FCL to calculate the erosion RULEBLOCK, in which "Vegetation" and "Slope" are linguistic variables as inputs.

```

FUNCTION_BLOCK <function block name>           *Function block
VAR_INPUT                                       *Input parameter declaration
  <Linguistic variable name> <variable type>; (*<range>*)
END_VAR
VAR_OUTPUT                                       *Output parameter declaration
  <Linguistic variable name> <variable type>; (*<range>*)
END_VAR
FUZZIFY <variable name>                          *Fuzzification
  TERM <fuzzy set name> := <points define the membership function>;
END_FUZZIFY
DEFUZZIFY value                                  *Defuzzification
  METHOD: <defuzzification method>;
  ACCU:<accumulation method>;
END_DEFUZZIFY
RULEBLOCK <rule block name>                      *Rule base or block
  <operator>:<algorithm>;
  RULE <rule number>: IF <condition> THEN <conclusion>;
END_RULEBLOCK
END_FUNCTION_BLOCK

```

Figure 3.7: Fuzzy control elements in FCL (after <http://ffll.sourceforge.net/fcl.htm>, 2010)

```

FUNCTION_BLOCK Erosion_Model
  VAR_INPUT
    Vegetation REAL; (* RANGE(0... 100) *)
    Slope REAL; (* RANGE(0... 100) *)
  END_VAR
  VAR_OUTPUT
    Erosion REAL; (* RANGE(0... 4) *)
  END_VAR
  FUZZIFY Vegetation
    TERM low := (0,1) (1, 5) (50, 0) ;
    TERM high := (5, 0) (50, 1) (100, 0) ;
  END_FUZZIFY
  FUZZIFY Slope
    TERM moderate:= (0, 0) (10, 1) (15, 0) ;
    TERM high:= (10, 0) (15, 1) (30, 1) ;
  END_FUZZIFY
  DEFUZZIFY Erosion
    TERM high := 1 ;
    TERM low := 2 ;
    METHOD: CoA;
    ACCU : MAX
  END_DEFUZZIFY
  RULEBLOCK first
    AND:MIN;
    OR:MAX;
    RULE 0: IF (Vegetation IS low) AND (Slope IS high) THEN (Erosion IS high);
    RULE 1: IF (Vegetation IS high) AND (Slope IS moderate) THEN (Erosion IS low);
  END_RULEBLOCK
END_FUNCTION_BLOCK

```

Figure 3.8: Fuzzy control elements in FCL for Erosion

Figure 3.9 represents the schismatic form of fuzzy model to calculate fuzzy system in the previous example of the erosion rule base with two rules.

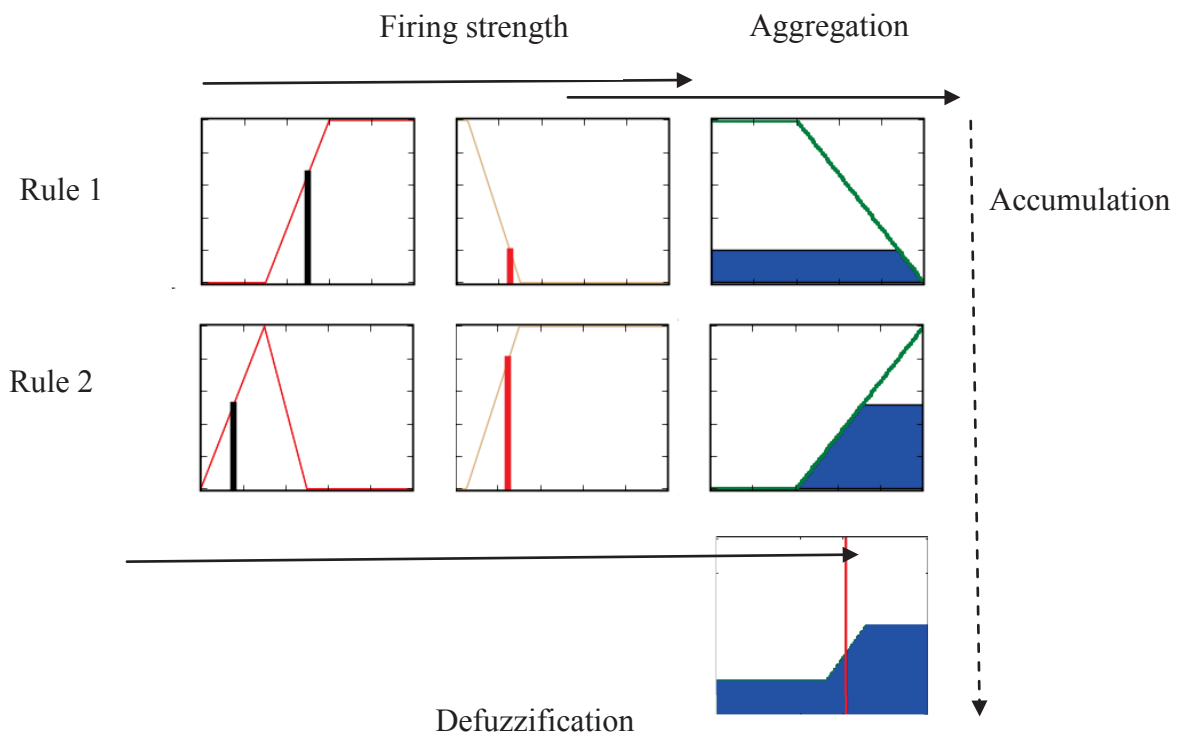


Figure 3.9: An example of fuzzy rule inference with two rules

Chapter 4

Description of Study Area

4.1 Introduction

This chapter presents general information about the study area, which includes the description of the main characteristics of watershed, land cover, and climate. The specific objectives here are first the identifying of main geomorphology units and land covers by PhotoMorphic Units method (PMU) and the visual interpretation of remotely sensed data; secondly the describing of climatic and bio-geophysical characteristics of the study area. For this reason, in order to create the false colour composite RGB (742) image of the study area, the seventh, fourth and second bands (channels) of Landsat (ETM+) satellite are used as Red (R), Green (G), and Blue (B), respectively (Figure 4.1); then the morphological and lithological land units are visually interpreted and the map of land units are prepared (Alavipanah et al. 2004), and the land cover map for the study area is illustrated in Figure 4.2.

The study area at Qom Watershed is located between latitudes 33°N and 34° 30' N and between longitudes 51°E to 52° 30' E in the westernmost region of Central Iran, politically in Esfahan and Qom Province. The main cities in the study area are Qom, Kashan, and Aran.

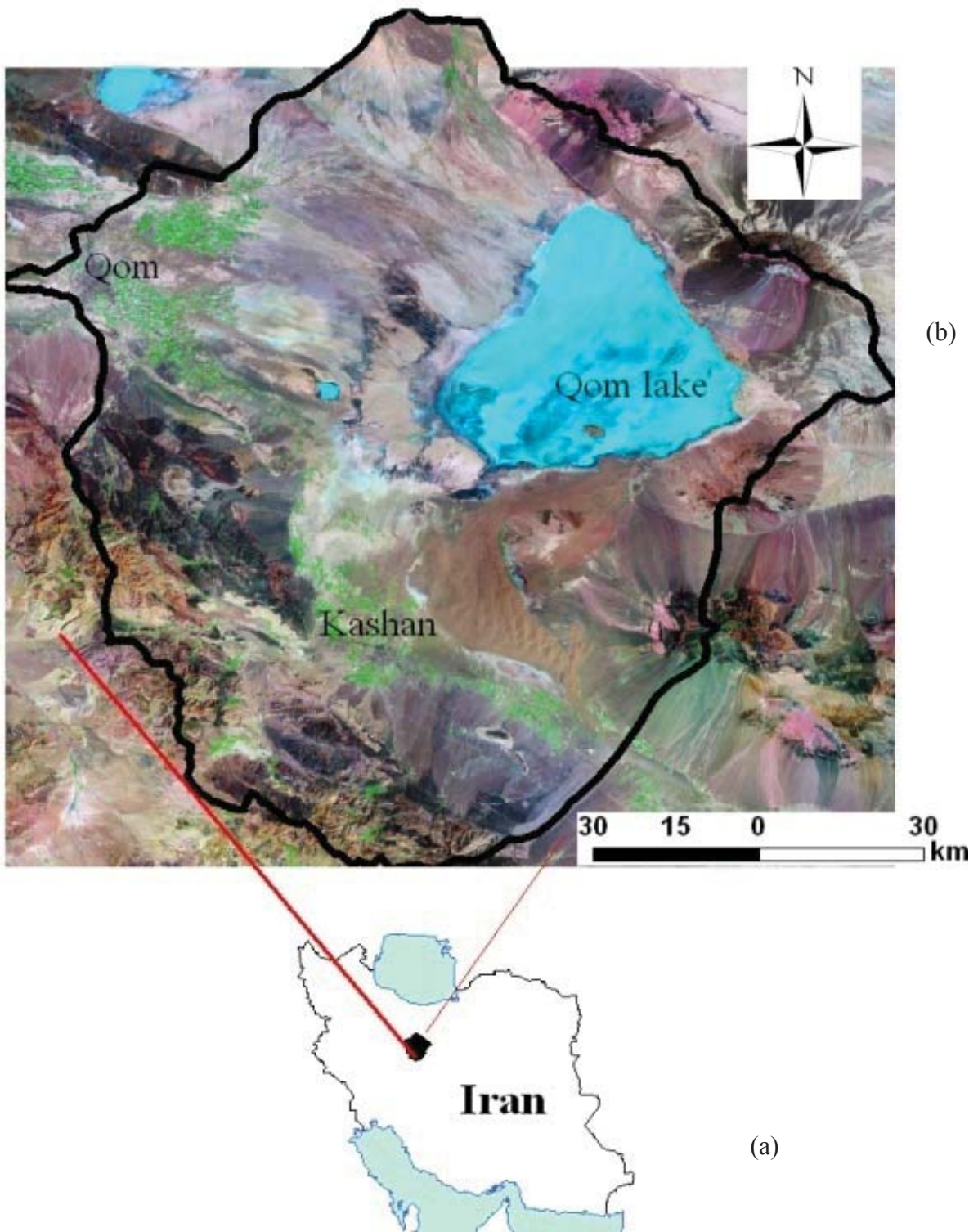


Figure 4.1: The study area located in Qom catchment and Esfahan Province, Iran (a); the darker grey rectangle in the map of Iran and (b); satellite image derived from False Colour Composite (FCC) image of Landsat satellite

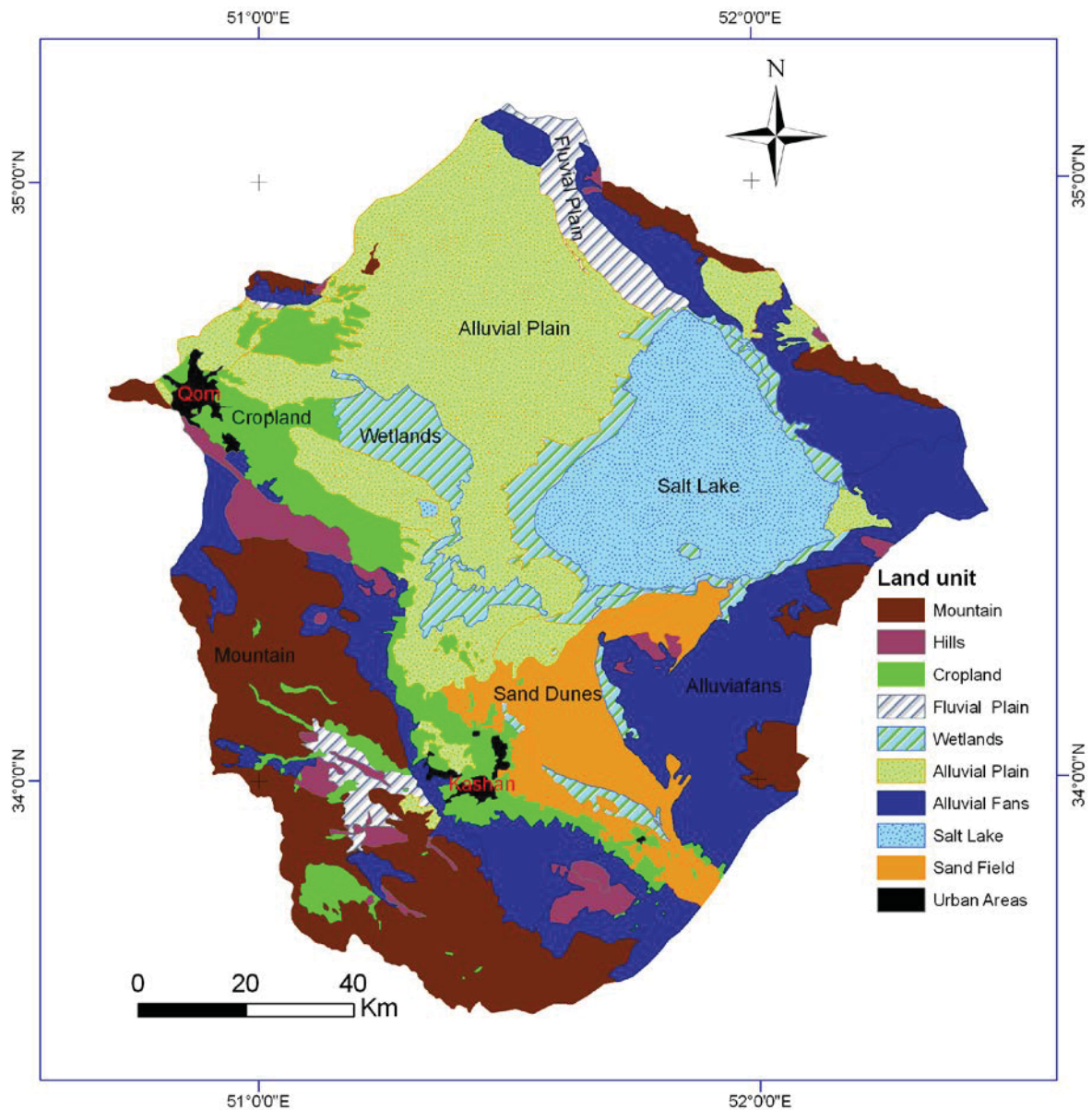


Figure 4.2: Land cover map of the study area

According to the Iranian Forest and Rangeland Department, this eco-region is characterized as man-induced land degradation and desertification phenomena with high erosion. Qom Playa is in the east part of the study area and the Zagros Mountains in the west part of the study area. Between these two parts, plains (pediments) and alluvial fans are located. There, croplands are also located, especially around Kashan and Qom, where soil and water are accessible and suitable; croplands are mostly irrigated by groundwater or Qanat system (Figure 4.1). These agricultural and croplands are located at the foot of the western mountain of the central

Iranian highlands. Alluvial fans are mostly covered with gravel; hence, desert pavements are major types.

4.2 Qom (Namak Lake) Watershed

Despite the vast hydrologic area, Qom Watershed, being the enclosed basin in central Iran, is the driest watershed in Iran. The most notable characteristic of the watershed is the dominance of the low-level plains, which is about 80 percent of the study area. Only about 20 percent of the study area is covered with the mountainous regions.

Another fascinating fact is Markezy Watershed located in the west of the study area, which is one of the main rainy watersheds in Iran. According to the Water Resource Organization (WRI) classification, based on a 16-year study between 1988 and 2003, it shows that the discharge rate in surface water volume in the Markezy watershed is about 33.74 million cubic meters and near to the country average (33.88 million cubic meters).

The area of the Qom watershed is about 15,939 square kilometres and with 35 pediments. According to the Water Plan of Iran (JAMAB), it is classified into six sub-watersheds; Shour, Karj-Jajroud, Kashan, Qomroud, Arak, and Gharechai. There is no main permanent river in Kashan and the Arak sub-watershed.

4.3 Geomorphology Characteristics

The study area with the various reliefs and landscapes is located in the northern half of the central plateau of Iran, and divided into two halves; the combination of highlands and fluvial plains in the western part, and the salt crust, alluvial plains and sand fields in the eastern half.

The study area is also a part of the Great Kavir, Iran, which was formed in the Tertiary (Cenozoic era) by the subsidence of southern Elburs. These geological formations are affected by the interaction of tectonic and interior (structural) forces, and they are also affected by exterior forces such as surface water and wind. The natural forces of wind and water are mainly responsible for erosion and morphogenesis. Despite the permanent aridity in the region, water erosion is a leading force in landform changes, which affected the alluvial plains and alluvial fans in the past and the fluvial plain in recent times.

The general direction of the mountain ranges are from the northwest to the southeast, as a result, the interior plain and pediments formed into a west- east trend. The tectonic forces which created the highlands in the north-east of the Zagros Mountains and the south-easterly reliefs, together with the perpendicular interior forces, have led to faults, syncline anticline, and the massive Karkas Mountain in the south-west.

In the study area, wind is an active force in landform change and erosion; due to wind erosion and sand movement, the massive sand field is located in the eastern part of Kashan and Aran. The study area comprises of three main types of geomorphology units: highland, plains, and lowlands (interior dispersion), whose coverage are brought in Table 4.1. These are various flat surfaces such as salt crust (salt lake), the predominant wetlands in the eastern part of the area; the salt crust area (the salt lake), in the Kashan watershed, is the lowest point.

Table 4.1: Land cover in the study area

Land cover	Area (sq km)	Percentage
Mountain	2,707	17.0
Hill	506	3.2
Croplands	1,191	7.5
Fluvial Plain	463	2.9
Wetlands	1,075	6.7
Alluvial Plain	3,785	23.7
Alluvial Fans	3,342	21.0
Salt Lake	1,720	10.8
Urban	139	0.9
Sand field	1,012	6.3
Total	15,939	-

Table 4.2: The properties of landform

Land types	Altitude (m)	Slope (percent)	Classification properties
Mountain	500 >	25<	Geological structure, lithology, vegetation cover, soil type, erosion and landforms
Hill	50-500	25>	Relief forms, soil type, erosion, vegetation and lithology
Plain	<50	<5	Land type, erosion, vegetation cover, and soil formation
Alluvial fan	<5	<1	Soil, gravel percentage, desert pavement
Lowlands	<2	<1	Sediment, soils, salinity, salt crust, or seasonal lakes

4.3.1 Highlands

The study area is surrounded by one of the highland areas of central Iran. The Gharoud heights, which form part of the Zagros Mountain range, start in the north-west and end in the south-east. At the eastern section of the study area, some parts of Yakhhab and Latif Mountains develop towards the vicinity of Qom Lake. These highlands are formed of igneous rocks, which make up most of the positive relief in the watershed (Figure 4.3 and 4.4). The landforms that are classified in the study area are based on their properties in Table 4.2, and then subtypes are determined.



Figure 4.3: A view of the mountain region near Kashan



Figure 4.4: The eroded hills near Kashan

According to topographic maps of the study area, the highest point in the relief is Mount Karkas (3,588 meters in height) is located in the south-west of Kashan (the border of water distribution with Qomroud watershed), near to the national wildlife park.

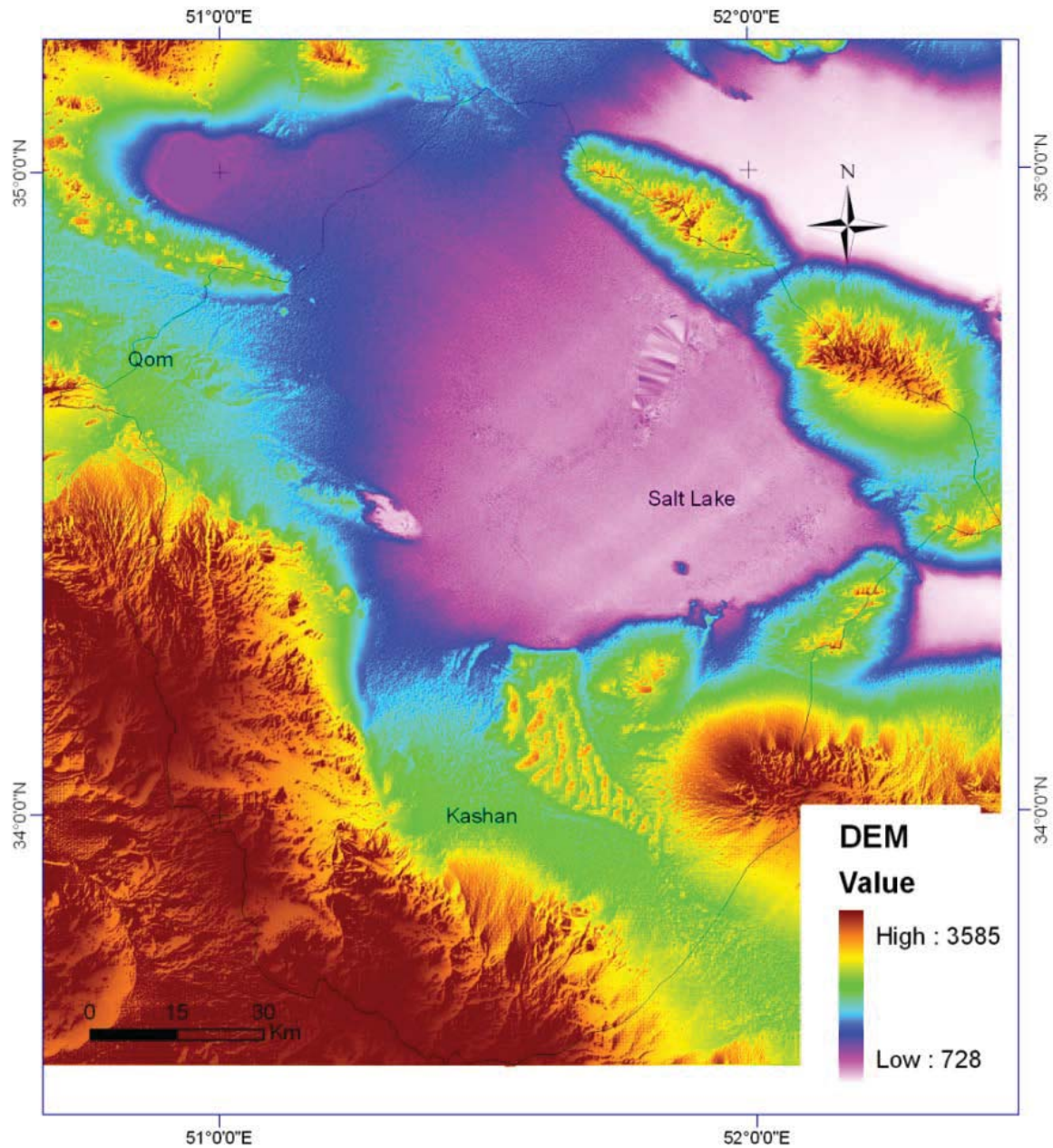


Figure 4.5. Relief map of the study area from the U.S. Geological Survey (USGS)

The lowest part of the study area is at an altitude of 750 meters above sea level, in the northern part of Salt Lake. Finally, the average altitude of the study area is approximately 2,200 meters above sea level.

The general slope trend is towards the north-east. The dominant slope in the study area is between zero and three percent in the plains; which cover all the areas in the neighbourhoods of Kashan and Aran except the mountain regions (Figure 4.5). Nonetheless, in hill and mountain region, the slopes are more than 25 percent.

4.3.2 Plains

Plains are the flat eroded surfaces at the foot of mountains and hills. In the study area, plains are divided into fluvial plains, alluvial plains, and alluvial fans.

Alluvial plains are the broad and relatively flat eroded surfaces with low reliefs, covered with alluviums, which were formed in the past by the run-off in arid or semiarid regions. Bajada is typically formed by alluvial fans joints. The associated alluvial fans create the areas of coalesced pediments (pediplains) in stretches around mountain fronts, where drainage channels are shallow.

Most of the alluvial materials are covered with a veneer of gravel, which is formed by the moving of the tinier materials and the remains of larger particles of surface gravel, especially during intermittent storms or through wind erosion, that form the bare gravelled surfaces called desert pavements (Dohrenwend and Parsons 2009). In the satellite images, these areas appear in darker tone. The highly gravelled areas or desert pavements are mainly bare lands, while alluvial plains with fine sediment have fertile soils, which make up the agricultural lands.

In the north-west of the study area around Salt Lake, the fluvial plain is observed, especially in the Qomroud and Gharechay rivers.

4.3.2.1 Qom Playa (Salt Lake of Qom)

Playa, or seasonally dry lake, is a geomorphology unit in the lowest flat part of a watershed, which is mostly covered with salt crust, fine-grained sediments and evaporite in dry flat lake beds. Playa is also referred to as a salt lake, because of the existence of a highly saline surface, known as Kavir (in Farsi), inland Sabkha (in Arabic), and Takeir (in Russian, and Turkish).

In certain studies, Qom Lake is also called Aran Lake, Namak Lake, Kashan Lake, Masileh Lake, Masileh Watershed, and Namak (salt) Sea (Ahmadi 1998; Shamsipour 2007). The Sefid-ab Mountain and Maranjab Kavir and Band-e-rig (sand field) encompass Qom Lake in the south, and the Siah-koh Mountain in the east, and the national wild park of Kavir in the north. The total area of Qom Lake is approximately 1,720 square kilometres, the border of which is variable, as in the wet season when water spreads into the muddy wetlands, taking the lake's dimensions to more than 1,900 square kilometres.

Qom Playa, a remnant of a Pleistocene lake (Krinsley 1970), occupies the easternmost and lowest part of Qom watershed (714 meters above sea level). Igneous and evaporite deposits comprise most of its adjacent north-east and south-east ridges, and a large part of its southern margin. Presently, Qom Lake has shallow water only for a few months, following the seasonal floods in wet years, when water levels reach some few meters in depth.

In the drier seasons, the surface of Qom Playa is dry, hard and covered with a thick crust of salt, which causes the bright colour and soft tone in satellite images. This surface is also devoid of vegetation, due to the presence of the salt crust; however, the regions in the margins of the playa, especially in the wetlands, some salt-tolerant plants exist, which provide winter fodder for livestock and other herbivores.

In wet seasons, this area becomes a dark, muddy surface (Figure 4.6). In salt crusts, highly evaporite sediments exist. The force of evaporation and changes in volume of the mixed clay and salt materials cause the formation of cracked-mud polygons, differing from 2 to 10 meters in diameter and 6 to 20 cm high in ridges.

The north-west margin of Qom Playa adjoins extensive alluvial plains whose streams mostly originate in the Zagros Mountains (Figure 4.5). The playa has the general form of an equilateral triangle with sides, approximately 60 km long.



Figure 4.6: Salt polygons and "cracked-mud" clay and salt materials in Salt Lake (Matinfar 2005)

4.3.2.2 Dune Field

Two primary factors are needed to create sand dunes – first is the sensitive material (sand), and the other the forceful and erosive power of wind (Mangimeli 2010). Both these conditions exist in central Iran as evidenced in the large sand dune fields (erg), generated in the east of Kashan and in the southern part of Salt Lake. The existence of the massive sand fields confirms that strong winds have actively eroded the region, whose pan-like shape is influenced by the interaction of the saturated lands and wind.

The ridges of the sand dunes in the south-western parts are relatively higher, more than 100 meters high, triangular in the form, with a 40 km long hypotenuse. Near Qom Lake

these ridges are linear and short, reaching about 70 km long in places, with a height exceeding 100 meters (Figure 4.7).



Figure 4.7: Sand field in the study area: nebkha (a), sand dune near Aran (b)

4.4 Climate

Climate is a primary factor in an environment; it is an independent variable and influences other agents. Temperature and precipitation are climate agents that determine the vegetation growth and soil formation in a place. Arid lands are not only bare surface areas with rare vegetation, but are also susceptible to climatic extremes such as drought and flooding.

These two factors play different functions dependent upon conditions. For instance, high temperature and low moisture equates to drought. Inversely, low temperature and high moisture leads to freezing; each of the cases prevents vegetation growth (Matinfar 2005). In drylands, because of low precipitation and high temperature, the development of vegetation and soil is poor.

The effective climatic agents in the study area are classified into local and continental agents. The altitudes, low latitude, the distance from the free sea, land cover are internal agents that control the local climate. The continental agents are the tropical winds, the Mediterranean wind currents, and the Arctic winds. In autumn, Siberian high pressure brings dry Arctic currents; in summer, the Arabian Peninsula hot winds cause hot conditions and sandstorms. The western and the Mediterranean wind currents mainly bring the effective rainfall (Shamsipour 2007).

4.4.1 Temperature

Temperature varies temporally and spatially in the study area. Throughout the day, temperature oscillates dramatically in the drylands such as Kashan and Qom regions.

According to the Kashan meteorological station (1967-2008), the warmest month in a normal year occurs in July, and the coldest month is also January, about 33.9 °C and 4.7 °C, respectively (Table 4.3). According to mean monthly statistics, in Kashan station from 1967 to 2008, the warmest month occurred in July 1975 with temperature 37.1 °C. The coldest month in this period was in January, 2008, which reached -4 °C, which is considered exceptional. Despite this month, a notable fact in Kashan station is the lack of months with a mean temperature below zero.

Shamsipour (2005) studied the drought variations in the period during March to May in Kashan region from 1994 to 2004 that affirmed the month of April as having the hottest daytime hours during the spring months in 2000 and 2001. It was noted that temperature at 3am was 15.8 °C, sharply increasing to 22.7 °C at 6am. Peak temperature was recorded at noon (28.3 °C), dropping slowly to 22 °C by 6pm. The highest temperature in the study region occurs between March and June. The difference in temperature in winter and summer exceeds 14 °C in the Kashan station.

4.4.2 Precipitation

Precipitation is the most changeable and stochastic component of climate; its temporal and spatial distribution is unique for each place, which has its own precipitation system. Nonetheless, precipitation in any form is a pivotal event in the improvement or degradation of an area.

There is low precipitation in the study area, due to the high distance from the sea and the effect of mountain shadow. The Albers-Zagros highlands prevent humid clouds coming in from north and west, making central Iran exposed to dry winds.

The most precipitation in the study area is rainfall (about 80 percent); the rainy season starts from December and ends in May. The western moist winds bring approximately 50 percent of total precipitation. February is the rainiest month in winter, with only 2 percent of total precipitation occurring in summer (Table 4.3). In the study area, in addition to local variations, the temporal fluctuation is high (Figure 4.8).

The minimum annual rainfall recorded at the Kashan Station was about 45 mm in 1973, while the maximum amount was 259 mm in 1972. Precipitation in the Kashan region follows the Mediterranean regime of long hot summers and mild winters with normal annual precipitation of 137 mm.

Table 4.3: Monthly mean precipitation and temperature of a normal year (1967 to 2008); P and T represent precipitation (mm) and mean temperature (°C, Celsius), respectively.

Parameter	Jan	Feb	Mar	Apr	May	Jun	Jul	Aug	Sep	Oct	Nov	Dec
P (mm)	26	19	25.4	17.5	12.9	1.3	0.5	0.4	0.2	4	11.9	18
T (°C)	4.7	7.7	13.2	20	25.4	31.3	33.9	32.5	27.7	20.6	12.8	6.8

The time series analysis of annual precipitation presents the onset, scale and development of drought (Figure 4.8 and 4.9). The rainfall time series for the meteorological station at Kashan (Figure 4.8) shows the period between 1985 and 1995 as being the driest 9-year period. The more recent years are dry years, especially the 3-year drought. Except December, all months were under normal conditions, especially the months of March and January, meaning the point for the emergence of seed and the production of vegetation, respectively.

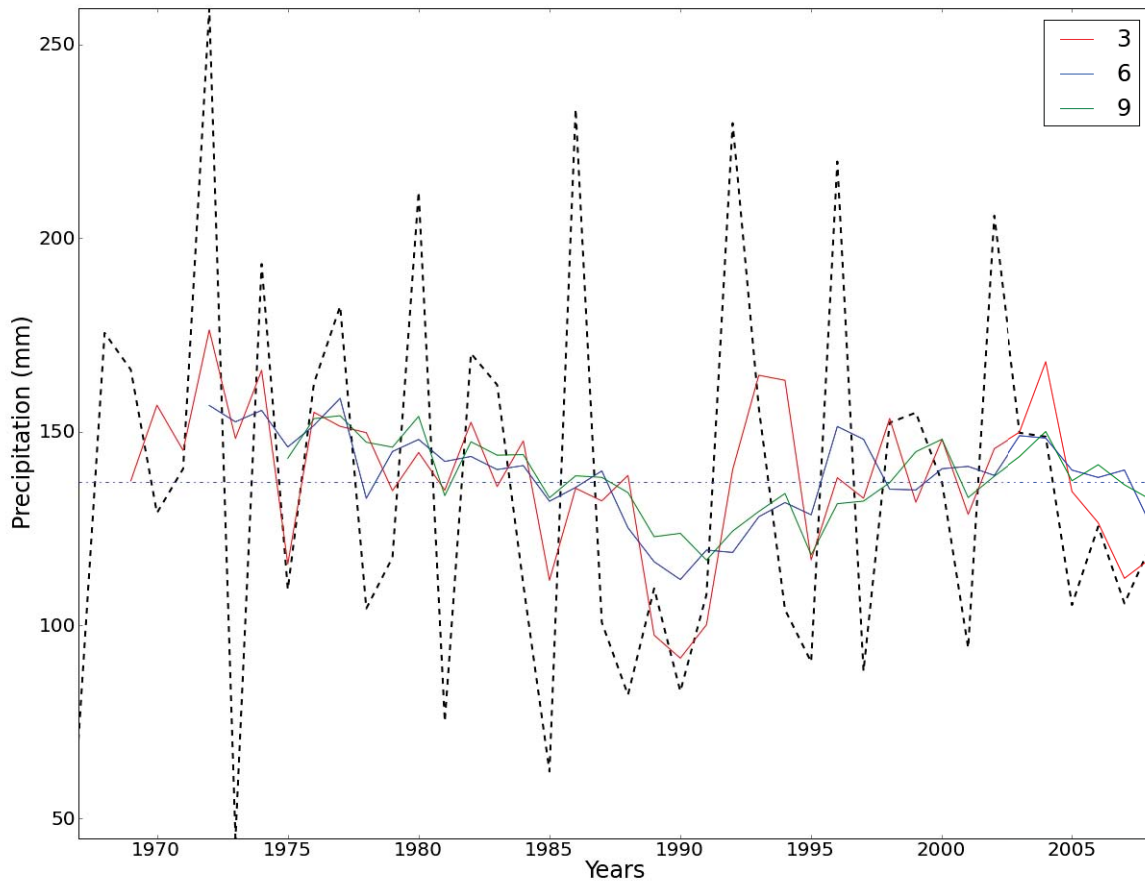


Figure 4.8: Time series of precipitation (1967-2008) in Kashan meteorological station; dash points shows annual rainfall (mm), the moving average of 3, 6, and 9 yearly scale in red, blue, and green, respectively.

In order to analyze the spatial distribution of rainfall over the study area, the rainfall records from 11 meteorological stations are interpolated for every year; the spatial average for each raster layer of rainfall is calculated. The time series trend of rainfall in the recent 9-year period (2000-2008) is plotted in Figure 4.9, which shows that the lowest yearly average rainfall in the study area is recorded in 2008 (108 mm) and the highest in 2002 (187 mm). Meanwhile, the actual and effective rainfall is lower than the optimum requirement for vegetation growth.

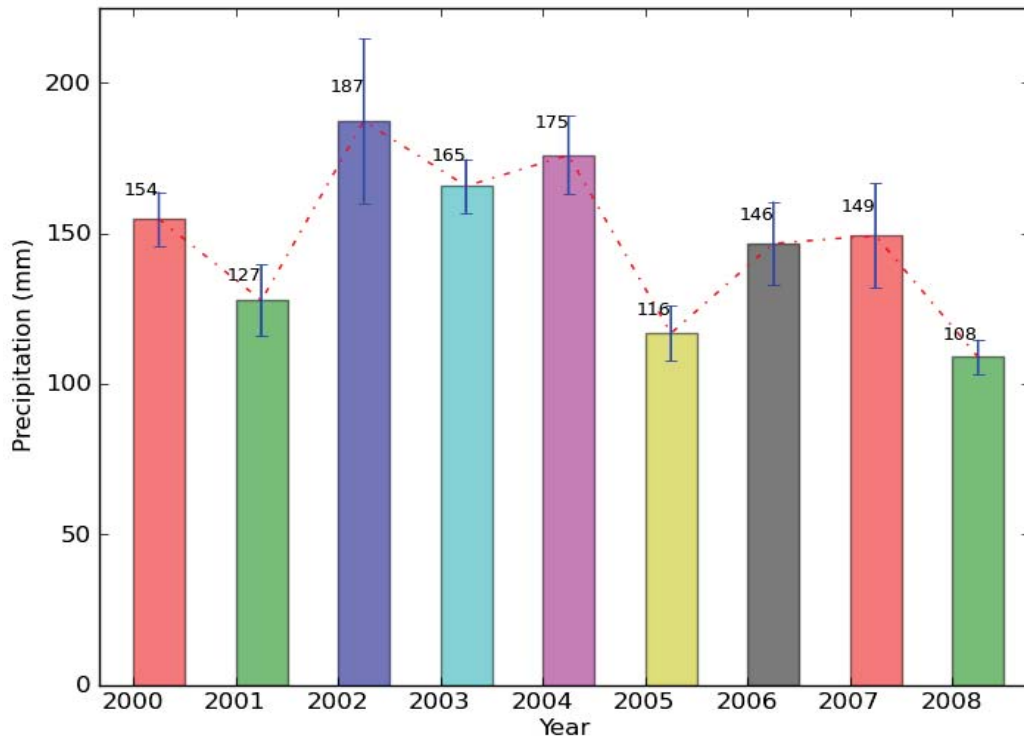


Figure 4.9: The spatial mean of precipitation trend in the study area (2000-2008)

In arid regions like the study area, rainfall is a rare and stochastic event in time and space. Despite low rainfall in the study area, sometimes a torrent of rain occurs and generates high erosion; for instance, the storm in May 2002, which brought 124 mm of rainfall, occurred in only two days.

The distribution of precipitation in Figure 4.10 represents rainfall reduction from the west (near mountains) to the east (towards the inner Central Desert of Iran). According to the spatial mean calculation of rainfall, the recent driest year in the study area was 2008 with 108 mm precipitation. In 2005, the rainfall was about 116 mm, which was the second driest year in the recent decade over the study area. Therefore, the years between 2005 and 2008 are also drought period in the study area.

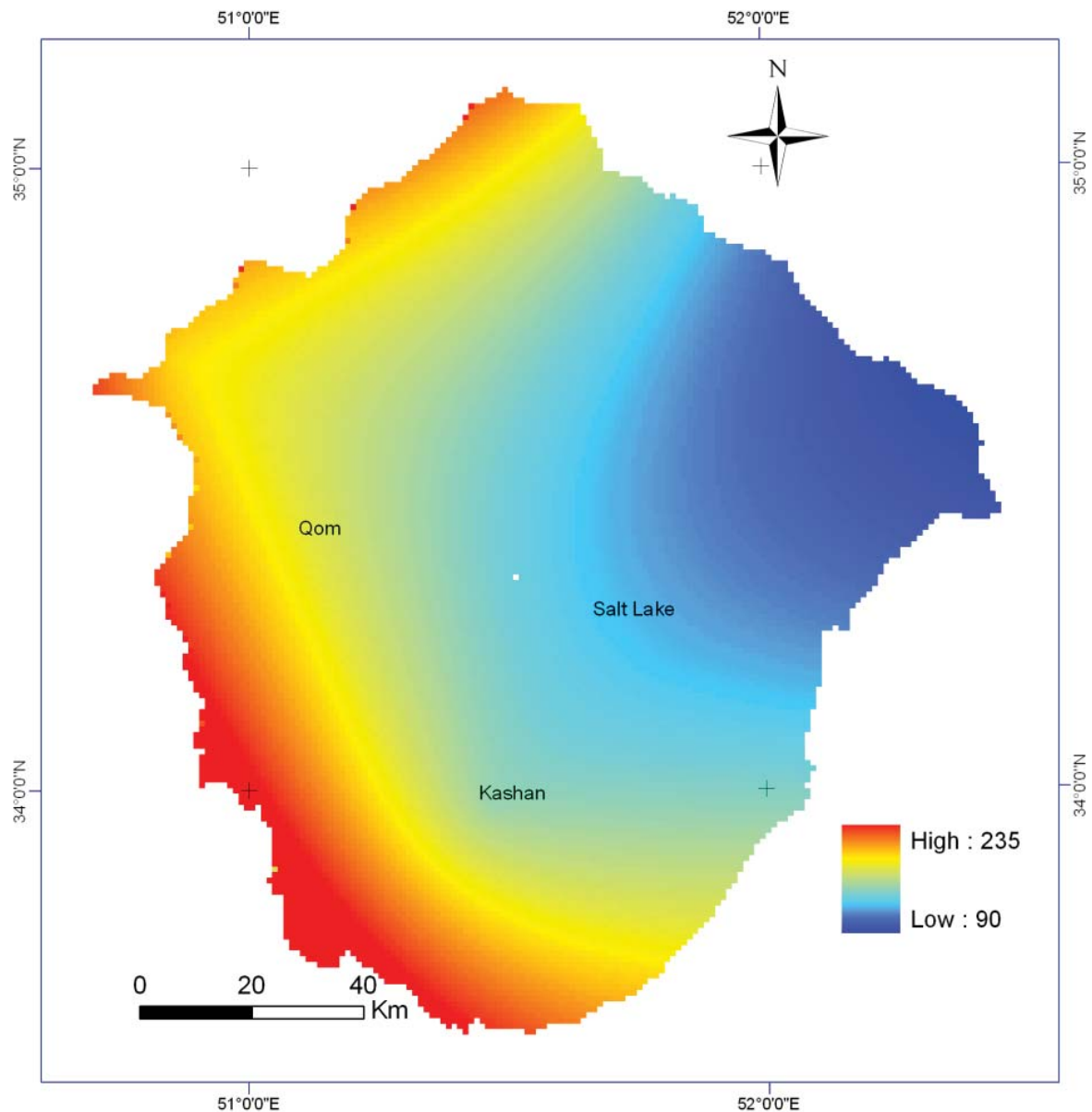


Figure 4.10: Precipitation spatial distribution (2006)

4.4.3 Climate classification

The empirical method of climate classification is a key index to identifying aridity conditions. Aridity is the permanent and continuous dryness of an area. Therefore, the aridity index represents the relationship between precipitation (input) and temperature, which is defined by the ratio of precipitation (P) and potential evapotranspiration (PET). Aridity is measured on an annual, seasonal or monthly basis.

In the 20th century, Köppen and Geiger proposed a climate classification to define an arid region, where rain mainly falls in the cold season, with yearly rainfall, P (in centimetres) less than twice of yearly temperature (2T, in Celsius).

$$P < 2T \quad (4.1)$$

Accordingly, the aridity index ($\frac{P}{2T}$) in the study area is about 0.35.

Aridity index (A) by UNEP defined, as follows (Middleton and Thomas 1992):

$$A = \frac{P}{PET} \quad (4.2)$$

where PET is potential evapotranspiration, and P is mean annual precipitation, respectively. PET and P must be expressed in the same units, e.g., in millimetres. For the study area approximately 0.12 that is classified as arid.

To determine the months with unfavourable conditions for plant growth, we can use another technique - ombrothermic diagrams - which plots mean monthly temperature (°C) and monthly precipitation (mm) on the vertical axes but with different scales. Numerically the precipitation values are twice as much as the temperature values (Emberger 1963).

The temperature and precipitation data are plotted against the axis of time (on the axis of X) and mean precipitation (P) and mean temperature (T) of a normal year in two Y-axes; dry months correspond to a period where precipitation value is twice the temperature value, for example, 20 mm of rainfall corresponds to temperature 10 °C ($P < 2T$).

The ombrothermic diagram shows the weakness of weather conditions and aridity severity. In fact, the lowest moist air point corresponds to the highest temperature, as well as the highest evapotranspiration potential, which are the most unfavourable conditions for vegetation growth.

The ombrothermic diagram in the meteorological station of Kashan is drawn in Figure 4.11, where the rainy season is from December to March. At least, seven or eight months of the year in Kashan are climatically challenging with severe drought periods, especially from March to November.

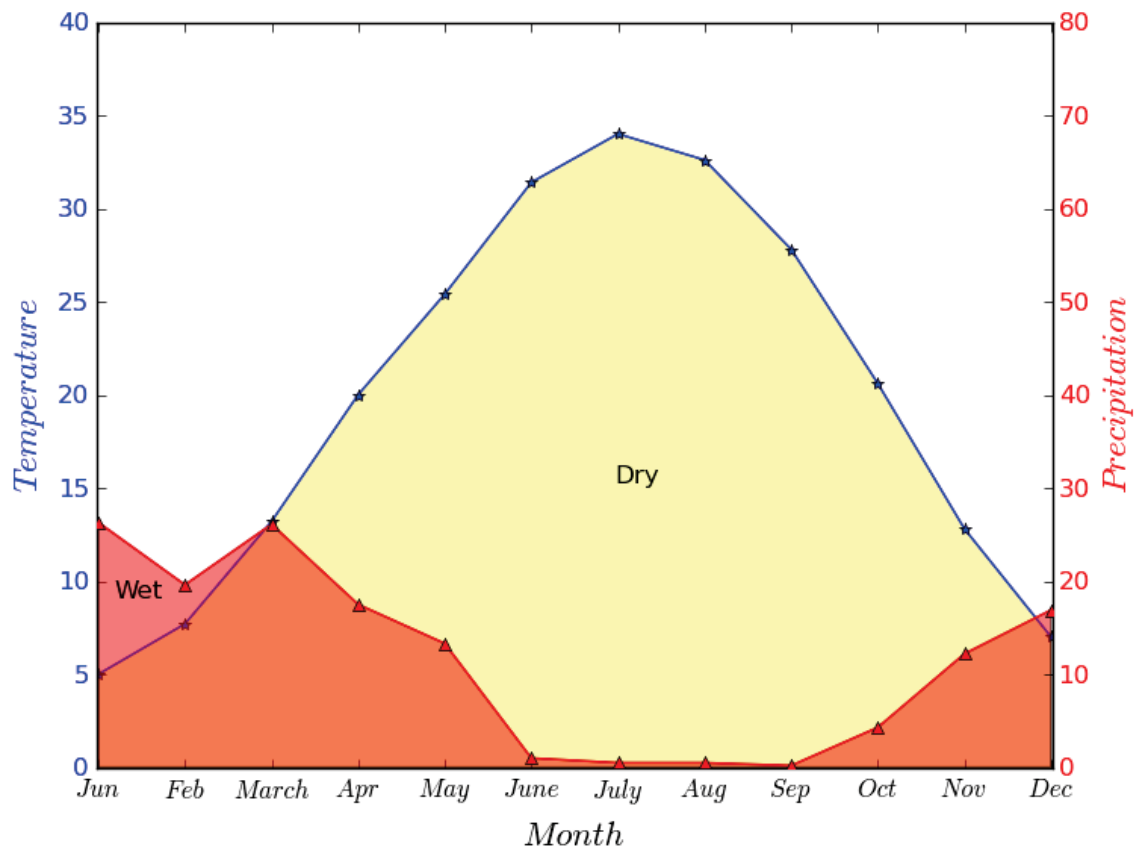


Figure 4.11: The ombrothermic diagram of a normal year, recorded at Kashan meteorological station.

The rarity of precipitation is severe, especially in summer, which corresponds to an increase in temperature and a decrease in moisture. For this reason, only three or four months in the year provide suitable opportunities to grow and develop vegetation. The main climatic properties of the study area are the following factors (Shamsipour 2007):

- Precipitation is an irregular and unforeseeable event. Its spatial and temporal distribution is also inconsistent. Nonetheless, sometimes the rainfall in drylands is so intensive and destructive that it causes massive flooding.
- Almost throughout the year in the study area, evapotranspiration is more than precipitation; therefore, water is mainly limited for agriculture and vegetation development.
- The changes in temperature and precipitation are high in spatio-temporal distributions. The north and north-eastern parts, devoid of vegetation, are called Kavir, where there is little precipitation and extensive saline soils.

4.5 Vegetation

In drylands, adapted plants can persist and survive in the harsh and adverse conditions with severe precipitation deficit and other water sources. The natural evolution of the dryland plants occurs because of morphological development, which gain moisture from the environment and withstand moisture loss. The morphological changes in dryland plants are in the roots, stems and leaves; some have deep root systems. The stem might change to thorny and spiky stems, the fleshy and juicy stems or water storage system. The leaves in the arid land plants are either small in size or ceriferous, greasy in surface texture. Some dryland plants secrete adjusting hormones against the dry climate, some store moisture, while other varieties reduce transpiration. The plants resistant to aridity are known as “xerophytes”, and the plants, which tolerate salinity, are called “halophyte”.

Regarding the climate in the study area with low precipitation and high evapotranspiration, this region is devoid of plants or has sparse vegetation cover. Rangelands also lose their quality animal-edible grasses due to overgrazing and drought.

Table 4.4: Main species of vegetation in the study area (Matinfar 2005)

Plain and Pediments	Alluvial fans	Mountains
Petrophyron sp.	Heltemia sp.	Aremisia herbaalba
Hultemia sp	Scariola orientalis	Astragalus spp
Launaed sp.	Stachys inflota	Amygdalus scoparia
Alhagi comelorum	Petrophyron sp.	Tuclrium polium
Euphorubia sp		
Launea spinosa		
Salsola tomentosa		

The main and dominant species in pediments, terrace lands, and gravel alluvial fans are given in Table 4.4. The variant species of halophyte species grow in the drylands, from bushes to trees, such as tamarisk. Except for the high-salty lands and the barren lands, the variant ephemeral plants or steppe rangelands cover other lands in drylands (Matinfar 2005).

Since 1962, many efforts and investments have been carried out in the study area, and forest farming strategies and national plans have been established. National plans have recognised land suitability, identifying the needs of the ecosystem, the potentiality of natural resources, and the

effective factors behind land changes. The plans also determine environmental capabilities and the sensitivity of natural resources.

At present, Aran-Bidgol Township occupies more than 120 hectares of the conserved tamarisk forest, which protects industrial and residential areas and farmlands from aggressive sand movement. Deep rooted tamarisk not only tolerates the harsh climate, but can also prevent wind erosion and sand movement, by acting as windbreakers (Figure 4.12).



Figure 4.12: Vegetation type in the study area

4.6 Water Resources

In the drylands of Qom and Kashan regions, water is a significant factor; therefore, the development in the natural ecosystem or the man-made element is dependent on the availability of water and its quality. The growth of ephemeral plants is also reliant on rainfall. In croplands, groundwater supports agricultural farming, especially during the deficiency of precipitation.

A typical Qanat irrigation system or Kariz (Figure 4.13) is a subterranean channel, which connects an aquifer on uplands to croplands in lower parts. The Qanat system in Kashan supplies approximately 80 percent of the water used in the agriculture lands. Nonetheless, the current Qanat systems are not as efficient as those in the past. Evidence shows that the level of groundwater drops in dry seasons, due to evapotranspiration and the depletion of groundwater, but is offset by runoffs in wet seasons (Jomehpour 2009).

The Qanat (or Ganat) irrigation system has developed over time against the harshness of hostile climatic conditions in the country. However, because of poor land management policies and poor irrigation practices the natural system has lost its efficiency.

The consumption of groundwater (in irrigation) has had an adverse effect on aquifers. Changes in irrigation systems (from the traditional Qanat system to recent deep well systems) have exhausted groundwater and aquifers. Because of this deficiency in the natural balance, salty groundwater shifts from playas towards fresh groundwater. Since, in playa, groundwater has high salinity, this process changes farmlands to salty lands (Emam et al. 2003). Therefore, the groundwater table and its quality are significant keys in the detection and recognition of desertification (Emam et al. 2003).



Figure 4.13: Abandoned Qanat, the underground irrigation system between an aquifer and cropland in lowland, near the city of Aran

4.7 Soil Characteristics

In the study area, the vast alluvial plains of the southern basin of Qom Lake are extended, and their general slope inclines south to north. In the eastern and northern parts of the plains, sand dunes have been shaped as a stripe from south-eastern towards north-western, 120 km long, and average 25 km wide, and between 800-1,000 meters high, which are locally called “Band-e-rig” (Figure 4.14).

Sandy soils and barren soils have high oscillation in temperature during the day and night. Furthermore, saline groundwater and the evaporite minerals affect soils in wetlands. For this reason, it has become necessary to acquire information about climatic and environmental conditions in the investigating of albedo, surface temperature, other vegetation and environmental regions (Shamsipour 2007).



Figure 4.14: Sandy soil in Band-e-rig



Figure 4.15: A sample of the soil profile near Aran town

Chapter 5

Data Acquisition and Processing

5.1 Introduction

In the Qom and Kashan regions, being amongst the most arid zones in Iran, desertification has become a serious problem for environmental, industrial and economical development. In order to detect and to determine the risks and crises of desertification in time, it necessitates novel approaches and innovative methods such as the methods in remote sensing.

Desertification is caused by the interaction of climate, environment and human activity in a recognised period of time. Besides ancillary data, desertification studies require appropriate temporal and spatial resolution satellite images; therefore, for the analysis of desertification, we used MODIS (the Moderate Resolution Imaging Spectroradiometer) data, since this data gives appropriate temporal resolution and is easily available.

In dryland studies, remote sensing methods play a leading role in the detection of land features as well as land changes – using spectral and thermal properties of land features. Furthermore, the prevalent characteristics, such as bare land and clear sky with low atmospheric haze, provide an excellent opportunity to use remotely sensed data in the identification of geomorphologic features in drylands. Although the use of thermal data in geology studies is acceptable, the dominance of soil reflectance makes vegetation detection difficult in thermal and reflective bands. In other words, in drylands which have sparse vegetation, the strong reflection of the soil dominates the

radiance, which is measured by sensors; therefore, almost all pixels in satellite images are mixed, thereby making the identification of pure spectral vegetation difficult.

This chapter is divided into three sections: the first section describes the sources and acquisition of data such as meteorology, satellite, and soil data. It also introduces some methods to calculate the indexes of desertification and their previous temporal properties. The second section provides a map of desertification by using the main conventional criteria in desertification. The final section introduces the evaluation of errors in the prepared maps.

5.2 Data Sources

This section incorporates overviews of the data used in the scientific investigation, such as MODIS satellite products, meteorological data and the other ancillary indexes which are derived from the digital elevation model, land use, and soil maps (Table 5.1).

The Digital Elevation Model (DEM) was downloaded from the online database of the U.S. Geological Survey's Earth Resources Observation and Science (EROS) Centre and NASA's Land Processes Distributed Active Archive Center (LP DAAC), and used to prepare the slope map. The meteorological statistics were obtained from Iran Meteorological Organisation (IRMO), for the period 1960-2008 in nine synoptic meteorology stations, including Tehran, Khorbiabanak, Garmsar, Kashan, Qom, Natanz, Golpaigan, Ardestan, and Saveh. According to the meteorological data, in different timescales, SPI is calculated from monthly rainfall precipitation for each station. The spatial distribution of SPI, as a drought map, is interpolated based on the Radial Basis Function (RBF) interpolation method, which is implemented in Python programming – using Scientific Tools for Python (SciPy) and Geospatial Data Abstraction Library (GDAL).

In this study, the base map of land cover was prepared by utilising Landsat (ETM+). By using False Colour Composites (FCC) of three bands, from Landsat image (TM₇=red, TM₄=green, TM₂=blue) and preparing the photomorphic units map method (PMU), the main types of land cover in the study area were visually classified, and their polygons were digitized in an ArcGIS environment. In the preparation and updating of the land cover map, available previous maps were also considered. The land cover units were classified into mountain, hill, plain, cropland, alluvial fan, wetland, salt crust, and sand dune (Figure 4.1 and 4.2).

MODIS/Terra images were downloaded from the NASA website; NDVI data were obtained from The Vegetation Index product (MOD13A3); Land Surface Temperature (LST)/Emissivity was also selected from the product (MOD11A2) of the MODIS/Terra online database.

Table 5.1: Database sources

<i>Data</i>	<i>Sources/ database</i>	<i>Date</i>
LST	MODIS / Terra online (NASA), h22v05	2000-2009
NDVI	MODIS/ Terra online (NASA)	2000-2009
Meteorological data	Iran Meteorological Organization(IRMO)	1950-2008
Landsat (TM and ETM) data	U.S. Geological Survey	September 9, 2001
Soil map and Land cover	Iran Soil Research Organisation	2000
Geology map	Iran Geology Organisation	1970

5.2.1 Satellite Data Acquisition

The satellite images of MODIS are available twice daily: from the Terra satellite, which orbits the earth in the morning, and from the Aqua, which orbits in the afternoon. The MODIS images, with 36 spectral bands, are provided in different spectral resolutions (from 0.4 μm to 14.4 μm), spatial resolutions (250 m, 500 m and 1 km), and temporal resolutions (in 1 to 2 days). All images captured by MODIS are in the sinusoidal projection. The MODIS data are provided in the HDF-EOS format (Hierarchical Data Format-Earth Observing System (EOS) format) developed by the National Center for Supercomputing Applications (NSCA) (Huete et al. 1999). According to NASA policies, the processed MODIS data are freely available without cost.

The Surface Reflectance products of MODIS include Vegetation Indices, Land Cover, Snow Cover, and Thermal Anomalies. Vegetation Index products provide data about the spatial

and temporal measurement of the condition of vegetation as well as the evaluation of the photosynthetic activity in plants. The Vegetation Index (VI), which represents the biophysical properties of vegetation, plant greenness, is useful to indicate the greenness and healthiness status of vegetation in the ecosystem in time and space. MODIS Surface Reflectance product (MOD09) is calibrated from the surface spectral reflectance bands, between two or seven of the corresponding full 36-band scenes in MODIS. These provide the estimated "at surface" spectral reflectance (Vermote and Kotchenova 2008).

5.2.2 Vegetation Index

One of the advantages of remote sensing methods in the assessment of the natural resources is the analysis of vegetation changes. In this regard, there are several indices to detect vegetation conditions which are derived from the spectral characteristics of plant. Vegetation distinctively interacts with energy; healthy plants reflect infrared spectra which are not used in photosynthesis, but they absorb visible light. In remote sensing, this differential spectral characteristic is defined as NDVI, the quantitative index of vegetation. Geothermal remote sensing has also practical benefits to distinguish and discriminate green cover types (Eastman and Worcester 2001).

In MODIS products, there are several composite vegetation products. Sixteen-day composites are available in different spatial resolutions, including 250-metre, 500-metre, 1-kilometer, and 0.05-degree, but monthly composites are provided in 1-kilometer and 0.05-degree resolutions. The monthly Vegetation Index products have a label prefix of MOD13A3 for the Terra sensor and MYD13A3 for the Aqua sensor (Huete et al. 1999) – an example NDVI image of the study area is shown in Figure 5.1.

In order to calculate minimum and maximum values of NDVI in the period between 2000 and 2009, the equations 5.1 and 5.2 are used by maximum and minimum functions, respectively:

$$\max\text{NDVI} = \max(\text{NDVI}_1, \text{NDVI}_2, \dots, \text{NDVI}_n) \quad (5.1)$$

$$\min\text{NDVI} = \min(\text{NDVI}_1, \text{NDVI}_2, \dots, \text{NDVI}_n) \quad (5.2)$$

where $\max\text{NDVI}$ and $\min\text{NDVI}$ are maximum and minimum values of NDVI in i^{th} year in n years, respectively.

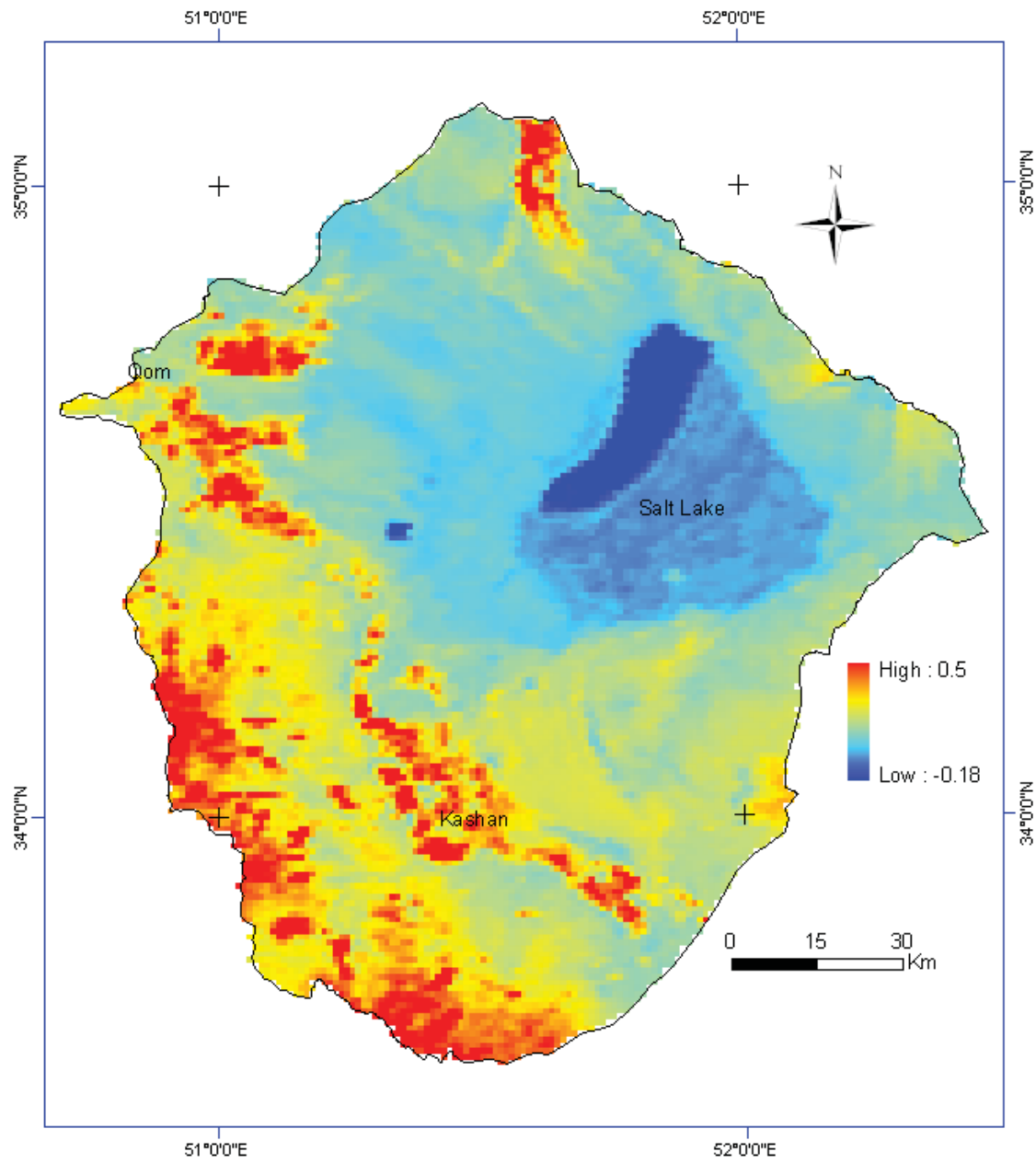


Figure 5.1: The MOD13A3 image from MODIS/Terra Vegetation Indices Monthly L3 Global 1 km resolution; the pseudo-coloured NDVI as the biomass health in Kashan region (July, 2002).

5.2.2.1 Vegetation Condition Index (VCI)

Vegetation Condition Index (VCI) is the normalization of NDVI between the greatest and least values, which was proposed for the monitoring of drought in vegetation (Kogan 1995):

$$VCI_j = 100 \times \frac{NDVI_j - NDVI_{min}}{NDVI_{max} - NDVI_{min}} \quad (5.3)$$

where $NDVI_{max}$ and $NDVI_{min}$ are maximum and minimum values of NDVI for the considered month or year during the study period, respectively. The current month or year is indicated by j.

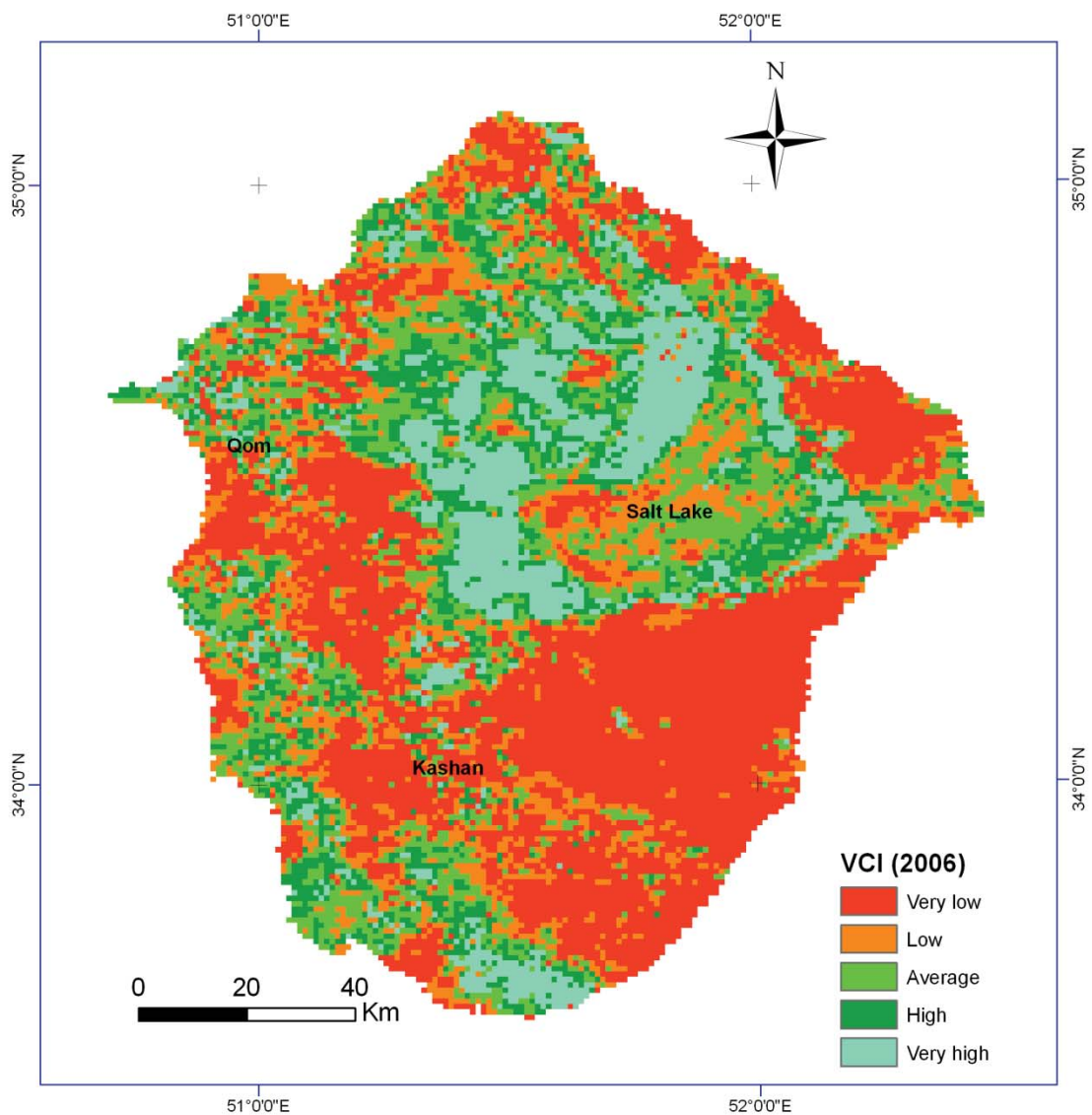


Figure 5.2: VCI distribution in the study area (2006)

The optimal condition of vegetation is more than 50. The values lower than 50 represent the stressed conditions of plant - i.e. dry periods. In other words, if the VCI value reaches zero, it equals the minimum value of NDVI in the recorded period, whereas the VCI values equal to 100 indicates the best condition for NDVI in the recorded period. The threshold for severe drought is approximately 35 (Kogan 1995). Therefore, in Figure 5.2, the spatial VCI values in the study area are classified into 5 classes as “very low” (0-20), “low” (20-40), “average” (40-60), “high” (60-80), and “very high” (80-100).

5.2.3 Thermal Index

In order to calculate a thermal condition index (TCI), Land Surface Temperature (LST) is selected from the product MOD11A2 in MODIS/Terra data. This product, LST, is based on an average of eight-daily data with 1-km spatial resolution; regarding the quality of daily data, two or eight images are used (Parida 2006).

However, there are pixels with no data values in the eight-day product, due to cloud coverage and noise, meaning that their digital number (DN) in raster is an undefined pixel. Undefined data create problems in the algebraic calculation in the raster-based statistics, such as the calculating of the average value. In GIS environments of ARCGIS, the undefined data are called “NoData”.

In order to solve this problem, firstly the NoData values are replaced by zero values, so that they do not affect summation, while keeping track of the number of replacements, so that the average can be correctly computed. Supposing that there were four raster layers ([B1]... [B4]) of an eight-day product of MODIS in the map algebra calculation, in ARCGIS, “IsNull” function is to find the NoData value. The output raster has integer value, either 1 or 0 ([N1]... [N4]). The corresponding pixels with NoData in the input are given a value of one on the output.

$$N_i = \text{IsNull}([B_i]) \quad (5.4)$$

Secondly, “Con” function is used to replace the NoData value with zero value:

$$A_i = \text{Con}([N_i], 0, [B_i]) \quad (5.5)$$

The average values are calculated as follows;

$$\text{Average} = \frac{\sum_{i=1}^4 A_i}{4 - \sum_{i=1}^4 N_i} \quad (5.6)$$

The calculation relies on the convention of using 1 to represent “True” value and 0 to represent “False” value in the Boolean grids (i) from N1 to N4, whence the denominator ($4 - \sum_{i=1}^4 N_i$) counts the number of non-null values in the corresponding pixel. Furthermore, all pixels in the corresponding raster with NoData values will result in computing zero/zero, again yielding NoData.

For the study area, the averaged MODIS LST datasets between 2000 and 2009 are used. In order to calculate minimum and maximum values of LST, the following equations are used.

For maximum function:

$$\text{maxLST} = \max(\text{LST}_1, \text{LST}_2, \dots, \text{LST}_N) \quad (5.7)$$

For minimum function:

$$\text{minLST} = \min(\text{LST}_1, \text{LST}_2, \dots, \text{LST}_N) \quad (5.8)$$

where maxLST and minLST are maximum and minimum values of LST in i^{th} year, respectively. N is the number of year in the study period.

Kogan (1990) proposed Temperature Condition Index (TCI) developed with AVHRR data to separate the short-term weather signal from the ecological signal (Seiler et al. 1998).

$$\text{TCI}_i = 100 \times \frac{\text{maxLST} - \text{LST}_{\text{cur}}}{\text{maxLST} - \text{minLST}} \quad (5.9)$$

where LST_{cur} is the brightness temperature or Land Surface Temperature (LST) under the considered period, and maxLST and minLST are the maximum and minimum values of LST on the recorded historical data, respectively.

Kogan (1995, 1997) suggested Thermal Condition Index (TCI) and its algorithm calculated similarly to VCI. In order to show the negative impact of higher temperature on vegetation growth, the deviation of current Land Surface Temperature (LST) from the highest points of LST is calculated; the higher the temperature, the more extreme the drought is.

Equation 5.9 shows the response of land surface and vegetation to temperature; the high values of TCI represent ideal conditions; TCI values more than 50 are considered as fair or normal conditions of temperature. Lower values of TCI show periods closer to the hottest land surface temperature (Kogan 1997). TCI has also shown convincing results in drought detection tracking; however, the application of this index requires long-term thermal data processing (Unganai and Kogan 1998). Figure 5.3 shows the classified TCI in five classes such as “very low” (0-20), “low” (20-40), “average” (40-60), “high” (60-80), and “very high” (80-100).

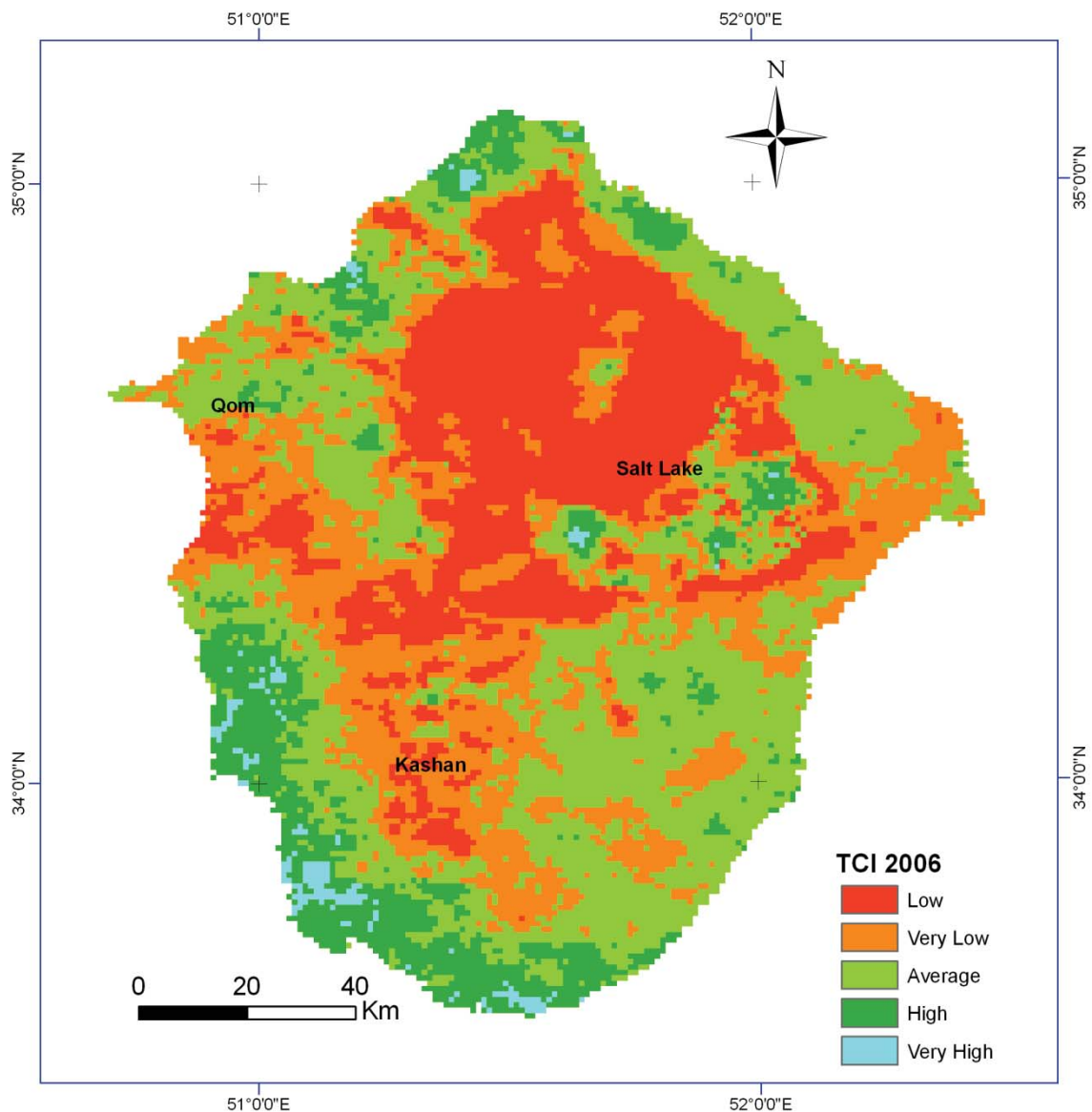


Figure 5.3: Spatial distribution of TCI in the study area (2006)

5.2.4 Standardised Precipitation Index (SPI)

According to the classification of severity of drought into wet and dry classes, McKee et al. (1993) proposed the Standardised Precipitation Index (SPI) to determine the severity of drought. SPI is computed in different temporal scales, which helps to determine the drought severity and frequency, as well as the duration of drought. In other words, SPI estimates the rainfall deficit in the different time scales which show the impact of drought. Therefore, SPI can determine meteorological, agricultural, and hydrological drought. Agricultural drought occurs when soil loses its moisture due to relatively short-term periods of low rainfall, while hydrological drought (water shortages in groundwater and river) happens in the period of long rainfall deficiency. Therefore, McKee et al. (1993) designed SPI in 3, 6, 12, 24-month timescales and then classified the drought classes into the categories that are shown in Table 5.2. As a result, drought occurs if SPI values reach below zero or less.

Table 5.2: Classification of SPI and its probability (McKee et al. 1993).

SPI Values	Category	Probability percent
2 and more	Extremely wet	2.3
1.5 to 1.99	Very wet	4.4
1 to 1.49	Moderately wet	9.2
-0.99 to 0	Mildly wet	34.1
0 to - 0.99	Mildly dry	34.1
-1. to -1.49	Moderately dry	9.2
-1.5 to -1.99	Severely dry	4.4
-2 and less	Extremely dry	2.3

As SPI uses only precipitation, it is less complex than other indices like Palmer Drought Severity Index (PDSI), which needs data of temperature beside precipitation. The SPI calculation is principally modelled on the standard deviation of normalized data. In SPI computation throughout each period, firstly precipitation data are summed over a timescale, and the data are then fitted to gamma probability density function (PDF). After that, each probability density function is transformed to normal distribution (McKee et al. 1993). The

nominal SPI is categorized in Table 5.2, which also contains the corresponding probability of each class of severity (Lloyd-Hughes 2002).

SPI, however, cannot be used to predict drought (Chopra 2006). Additionally, it might give misleading interpretations about permanent dry months in hyper-arid regions with long-term drought.

SPI is calculated by the fitting of precipitation frequency to gamma Probability Distribution Function (PDF) in a meteorological station. The gamma function is defined by a definite integral, which is an extension of the factorial function to real and complex numbers (Soto et al. 2009; Chortaria et al. 2010):

$$\Gamma(z) = \int_0^{\infty} e^{-t} t^{z-1} dt \quad (5.10)$$

The gamma distribution is defined by its probability density function (PDF):

$$f(x; \alpha, \beta) = \frac{1}{\beta^{\alpha} \Gamma(\alpha)} x^{\alpha-1} e^{-\frac{x}{\beta}} \quad \text{for } x \geq 0 \text{ and } \alpha, \beta > 0 \quad (5.11)$$

where α and β are shape and scale (dispersion) for the gamma probability density function. There are two methods to measure these parameters: the method of moments and Maximum Likelihood Estimation (MLE). In the latter, the optimal estimates of parameters are calculated as follow:

$$\alpha = \frac{1}{4A} \left(1 + \sqrt{1 + \frac{4A}{3}} \right) \quad (5.12)$$

$$\beta = \frac{\mu}{\alpha} \quad (5.13)$$

where;

$$A = \ln(\mu) - \frac{\sum \ln(x)}{N} \quad (5.14)$$

where N and μ are the number of input data and the average values of precipitation observations (x), respectively. Moreover, “ln” is the natural logarithm. These calculated parameters are used for the cumulative probability of observed precipitation for the given month or timescale for the specific meteorology station. The cumulative probability is given by:

$$F(x) = \int_0^x f(x) dx = \frac{1}{\beta^\alpha \Gamma(\alpha)} \int_0^x x^{\alpha-1} e^{-\frac{x}{\beta}} dx \quad (5.15)$$

After substituting “t” for x/β, Equation 5.15 is converted into the incomplete gamma function:

$$F(x; \alpha, t) = \int_0^x f(x) dx = \frac{1}{\Gamma(\alpha)} \int_0^x x^{\alpha-1} e^{-t} dt \quad (5.16)$$

Because the gamma distribution function is only valid for numbers greater than zero and rainfall data contain zero values, the cumulative probability becomes the following equation:

$$H(x) = q + (1 - q)F(x) \quad (5.17)$$

where q is the probability of zero values in rainfall data. The cumulative probability H (x) is converted to the standard normal distribution (Z), which is the value of the SPI (Abramowitz and Stegun 1965).

$$Z \cong \text{SPI} = -\left(t - \frac{c_0 + c_1 t + c_2 t^2}{1 + d_1 + d_2 t + d_3 t^3}\right) \text{ for } 0 < H(x) \leq 0.5 \quad (5.18)$$

$$Z \cong \text{SPI} = +\left(t - \frac{c_0 + c_1 t + c_2 t^2}{1 + d_1 + d_2 t + d_3 t^3}\right) \text{ for } 0.5 < H(x) \leq 1 \quad (5.19)$$

where c_0 , c_1 , c_2 , d_1 , d_2 , and d_3 are 2.515517, 0.802853, 0.010328, 1.432788, 0.189269, and 0.001308, respectively. These are constants, which are used to calculate the Percent Point Function (PPF), which is the inverse of Cumulative Distribution Function (CDF). In addition, t is an intermediate variable as follows:

$$t = \sqrt{\ln\left(\frac{1}{(H(x))^2}\right)} \quad \text{for } 0 < H(x) \leq 0.5 \quad (5.20)$$

$$t = \sqrt{\ln\left(\frac{1}{(1-H(x))^2}\right)} \quad \text{for } 0.5 < H(x) \leq 1 \quad (5.21)$$

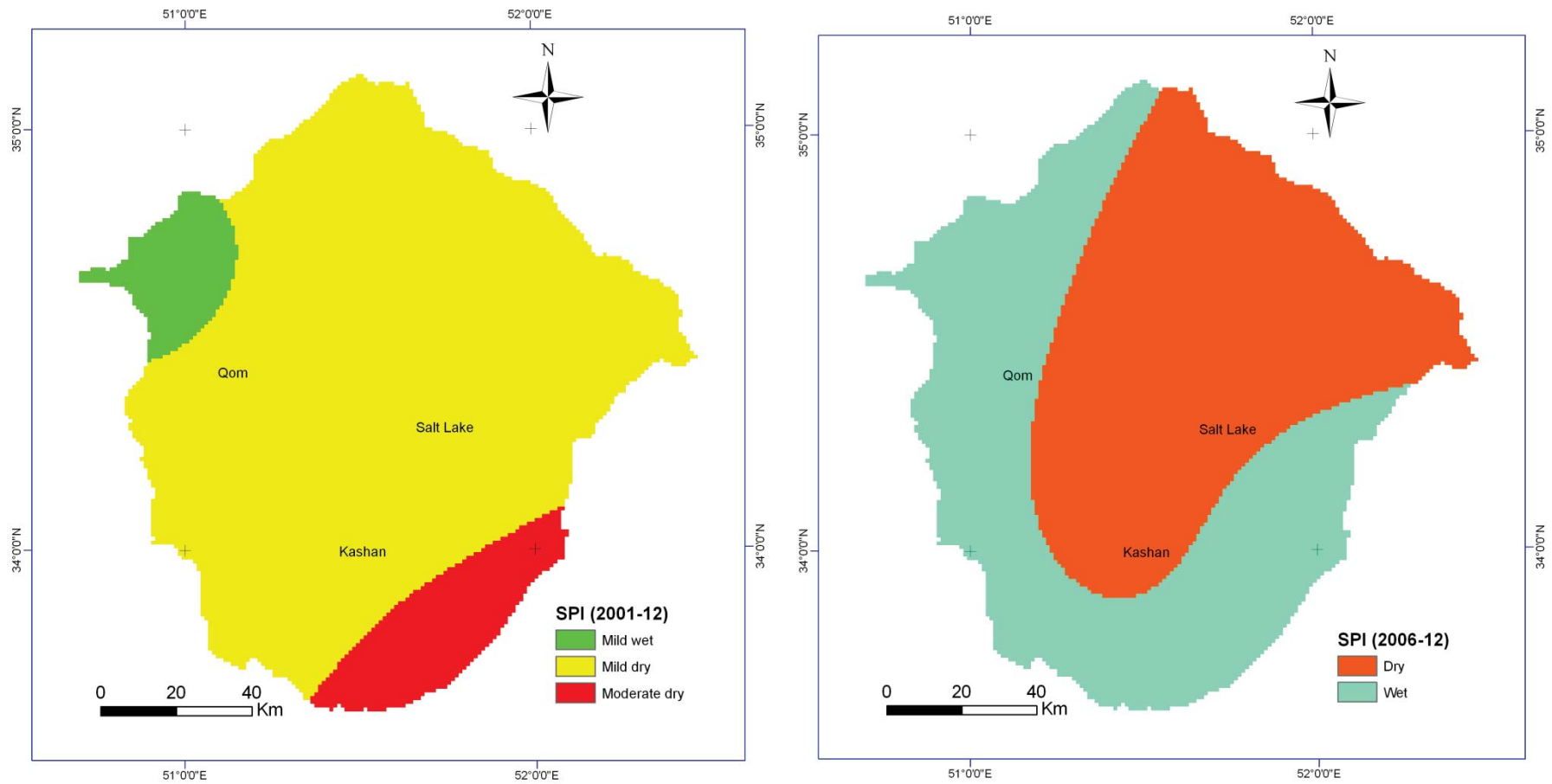


Figure 5.4: SPI maps for December 2001 (left), and December 2006 (right)

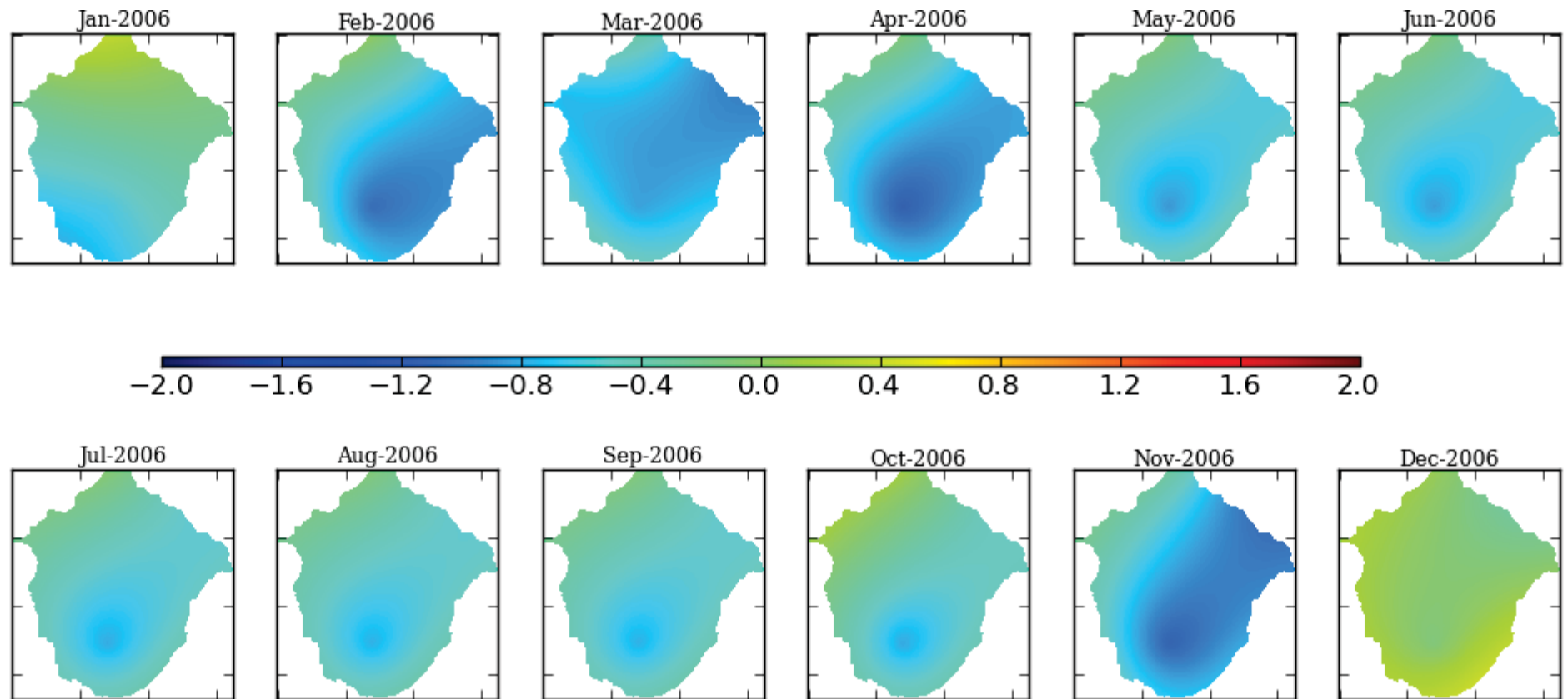


Figure 5.5: Interpolated SPI map for 12-month timescale SPI from January 2005 to December 2006

In the study area, June is considered the onset for drought, marking the beginning of drought season. In order to produce the spatial distribution of climatology data for SPI in the stations located in the study area between 2000 and 2008, the data in the stations were interpolated according to the Radial Basis Function (RBF) method. The result is shown in Figure 5.4.

SPI data are used to compare the precipitation of two consecutive 12-month periods. The SPI 12-month timescale data for the end of January 2000 includes the cumulative precipitation data from February 1999 to January 2000 (Figure 5.5).

5.2.5 Flooding (Overflow Method)

In the estimation of run-off, there are two main factors: precipitation as input and land surface properties as effect. Therefore, there are various methods to calculate flooding and run-off. One of the most practical methods in hydrology studies is the ratio of flood (overland flow and run-off, Q) to effective storm rainfall, proposed by the Natural Resources Conservation Service, formerly US SCS, or US Soil Conservation Service (Werner et al. 2004).

In this method, the physical characteristics of land, such as size, shape, topography, soils, and vegetation are considered. Engineers and hydrologists have widely used direct run-off estimation because it is simple and flexible. The SCS run-off equation can be expressed as follows (Mishra and Singh 2003):

$$Q = \frac{(P-I_a)^2}{(P-I_a)+S} \quad (5.22)$$

where Q is the amount of run-off (mm), P , is rainfall depth or direct run-off from a precipitation (mm), I_a is the initial abstraction ($I_a \approx 0.2S$) and S the potential maximum retention (or watershed storage). The initial abstraction (I_a) is composed of interception, infiltration and depression storage; all of which occur before run-off begins (Dervos et al. 2006; Hammouri and El-Naqa 2007). Its empirical relationship is as the following equation:

$$I_a = 0.2S \quad (5.23)$$

Substituting equation (5.23) for I_a in equation (5.22), it yields:

$$Q = \frac{(P-0.2S)^2}{P+0.8S} \quad (5.24)$$

The parameter S is calculated based on soil and land cover conditions of the watershed:

$$S = \frac{25400}{CN} - 254 \quad (5.25)$$

where CN is the value of Curve Number, which is a function that is derived from hydrologic soil group, land cover, land treatment and hydrologic conditions. In other words, CN is the combination of land surface properties such as soil hydrologic group and land cover. It is dimensionless and has values in the range from 30 to 100 (Table 5.3).

Table 5.3: CN values for land use and soil type in soil moisture condition II (Werner et al. 2004, 2007)

Land use	Cover condition	CN for soil type			
		A	B	C	D
Agriculture		31	77	86	91
Bare land	Bare exposed rock	98	98	98	98
Range land	Desert shrub – poor	63	77	85	88
Salty land	Dry salt Flats	74	84	90	92
Sand dune		63	77	85	88
Urban	65 percent impervious area	77	85	90	92

Table 5.4: Hydrologic soil group according to soils run-off, producing characteristics as used in the NRCS Curve Number Method (Werner et al. 2004).

Soil Group	Soil Texture	Infiltration rate	Impermeable layers(cm)	permeability (mm/h)
A	Sand, loamy sand or sandy loam	High	> 100	7.6 - 11.4
B	Silt loam or loam	Moderate	50 - 100	3.8 - 7.6
C	Sandy clay loam	Low	water table 100 - 150	1.3 - 3.8
D	Clay loam, silty clay loam, sandy clay, silty clay or clay	Very Low	Hardpan	<1.3

There are four Hydrologic Soil Groups (HSG) such as A, B, C, and D (Table 5.4). The “A” soil group has high infiltration rate and low run-off potential, which includes sandy texture soils. Soil group “B” means moderately well-drained soils and have also a moderate infiltration rate, such as soils with loam texture. Soil group “C” have slow infiltration rates and may contain a

layer of fine texture. Soil group “D” is attributed to soils with poor drainage and a high clayey texture - it includes some saline soils and those soils with permanently high groundwater levels. In this study, Residential areas were allocated to hydrologic soil group B, and the places such as salt lakes are attributed to D group (Werner et al. 2004). The soil map was developed from soil map of Kashan-Isfahan in 2000. Each soil type, according to its texture types, is assigned to its corresponding hydrologic soil group.

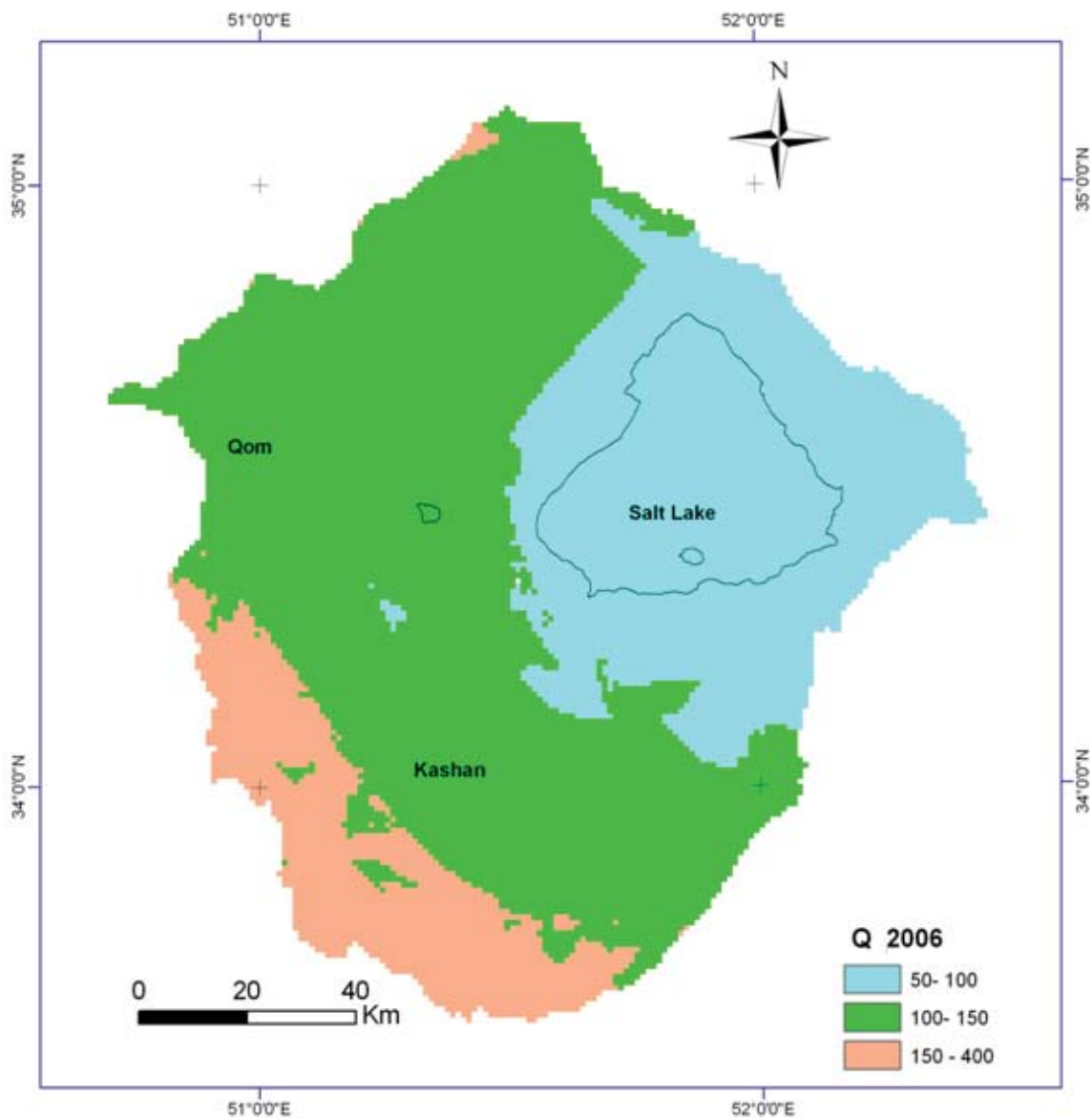


Figure 5.6: Flood map (Q) for 2006

The raster analysis was performed by combining hydrologic soil groups (A, B, C, and D) with the land use map in GIS. Then, the land cover map and the hydrologic soil groups were merged to develop the CN map (Zhan and Huang 2004).

The monthly precipitation has been created by IRMO, Iran, for the period 1960-2008 based on daily measurements. The data are converted to spatial surface data by using Radial Basis Function (RBF) interpolation method without consideration of the elevation effects, and then according to Equation 5.24, the flooding map of the study area is calculated in GIS (Figure 5.6).

5.2.6 Revised Universal Soil Loss Equation

Erosion is one of the most pertinent issues in watershed as the affected areas with erosion are almost irreversible. In this regard, the Revised Universal Soil Loss Equation (RUSLE) estimates the water erosion, which is the potential sediment from the field. The RUSLE is the updated version of the Universal Soil Loss Equation (USLE). In this model, to predict the long-term average annual soil loss caused by sheet and rill erosion, six main factors are calculated, such as rainfall intensity, landforms, soil sensitivity, conservation and management (Renard et al. 1996). In GIS, the generalized model of RUSLE is also used. The equation takes the simple product from the following six factors (Wischmeier 1974):

$$A = R \times K \times LS \times C \times P \quad (5.26)$$

where,

A = average annual soil loss [tonnes per hectare per year]

R = rainfall erosivity factor [megajoule-millimeter per hectare-hour-year]

K = soil erodibility factor [tonne-hour per megajoule-millimeter]

LS = slope length factor (dimensionless)

C = land cover and management factor (dimensionless, ranging from zero to one)

P = support practice factor (dimensionless, ranging from zero to one).

The precise calculation of RUSLE requires a great deal of effort and time, therefore, to study the estimated erosion in the affected areas with GIS, a simplified version is used.

5.2.6.1 Rainfall Erosivity Analysis

Rainfall is the main cause of soil erosion. In this regard, intensity and duration of rainfall are the most fundamental characteristics in rain erosivity. Wischmeier (1962) used the maximum 30-minute rainfall intensity by daily precipitation acquisition. Later he proposed the yearly-simplified equation using the annual precipitation as follows (Renard et al. 1996):

$$R = -0.334 P + 0.006661P^2 \quad (5.27)$$

where R and P are annual erosivity index and annual precipitation, respectively.

5.2.6.2 Topographic Factors; Length and Steepness (LS) of Slope

In RUSLE, length and steepness of slope (LS) is provided by modelling complex slope and slope-length relationships with erosion (Renard and Freimund 1994). Topographic factors influence predicted erosion rates; the longer slope is, and the steeper it is, the greater the erosion during rainfall. Slope length and steepness factors are combined and defined as the topographic factor, so that the longer the slope length, the greater the amount of cumulative run-off; the steeper the slope, the higher the velocity of the run-off (Wischmeier and Smith 1978).

Calculating length and steepness (LS) is an empirical equation provided in USDA Agriculture Handbook (Wischmeier and Smith 1978):

$$LS = \left(\frac{x}{22.13}\right)^n (65.41 \sin^2\theta + 4.56\sin\theta + 0.065) \quad (5.28)$$

where x is slope length in feet; θ is the degree of slope; and n equals to 0.5 if the slope percentage is 5 or more, 0.4 on slopes of 3.5 to 4.5 percent, 0.3 on slopes of 1 to 3 percent, and 0.2 on uniform gradients of less than 1 percent.

The calculating of LS is founded on flow accumulation and slope steepness, which is also derived in GIS. The equation is of the following form (Mitasova and Mitas 1999):

$$LS = \left(\frac{F.C}{22.13}\right)^a \left(\frac{\sin(S \times f)}{8.96 \times 10^{-2}}\right)^b \quad (5.29)$$

where LS is the length and steepness of slope (dimensionless), F is flow accumulation map, C, cell size in meter, S is slope in degree, f equals to $\frac{\pi}{180}$, and constants a and b are 0.6 and 1.3, respectively.

5.2.6.3 Soil Erodibility (K)

The soil erodibility or detachability factor (K) represents vulnerability of soil to erosion and the amount and rate of run-off. For example, fine textured high-clayey soils and coarse textured sandy soils have lower K values; the former resists detachment and the latter has high permeability. In contrast, soils with high silt are the most erodible of all soils. Organic matter also decreases the susceptibility and detachability of soil and increases infiltration; therefore, it reduces run-off and eventually soil erosion. Soil structure is also a factor in susceptibility, detachability and infiltration. An estimate for K-value from soil properties can be calculated (Renard et al. 1996):

$$K = \frac{1}{7.59} \times \frac{[2.1 \times 10^{-4} M^{1.14} (12 - OM) + 3.25(S - 2) + 2.5(P - 3)]}{100} \quad (5.30)$$

where OM stands for organic matter, and M is the particle size parameter, which is calculated:

$$M = \%silt \times (100 - \%clay) \quad (5.31)$$

Division of the right side of this equation, and subsequent K factor equations with the factor 7.59, will yield K values expressed in SI units of tonne-hour per megajoule-millimeter. S is soil structure code. P is the profile permeability class (Table 5.5)

Table 5.5: Profile permeability class (P) and soil structure code (S) (Renard et al. 1996)

S	P	Value
Very fine granular	Rapid	1
Fine granular	Moderate to rapid	2
Medium or coarse granular	Moderate	3
Blocky, platy, or massive	slow to moderate	4
	slow	5
	Very slow	6

5.2.6.4 Cover-Management Factor (C) and Support Practice Factor (P)

Cover-management factor is used to express the effect of crop and practice management on erosion rates. It is the most common factor used to describe the relative impact of management options for conservation plans.

Table 5.6: Land cover classification and C, P factors (Sepaskhah and Sarkhosh 2005).

Land cover types	C	P	Land cover types	C	P
Urban area	0.1	1	Paddy field	0.1	0.5
Bare land	0.35	1	Dense grassland	0.08	1
Dense forest	0.001	1	Sparse grassland	0.2	1
Sparse forest	0.01	1	Mixed grassland and cropland	0.25	0.8
Mixed forest and cropland	0.1	0.8	Wetland	0.05	1
Cropland	0.5	0.5	Water body	0.01	1

C-factor is an indicator for the conservation plan which affects the average annual soil loss and soil-loss potential during farming activities, such as crop rotation and other management systems. Based on the land cover map (1:250,000 scale), C factor indicator is shown in Table 5.6. The support practice factor (P) refers to any practices and management to control erosion, mainly by reducing surface run-off, e.g. terracing, buffer strips, and tillage methods (Sepaskhah and Sarkhosh 2005).

The classified map of potential erosion rate for 2006 is illustrated in Figure 5.7. In the numerical multiplication of factors for RUSLE calculation, slope and rainfall intensity play a key role which determine erosion occurrence. Therefore, only in the rainy highlands in the west of the study area is examined, where erosion is prevalent; whereas in the lowland areas and low sloping lands water erosion is estimated around zero. In these flat areas, other forms of water erosion, such as gully and wind erosion are active, which are ignored in the RUSLE model.

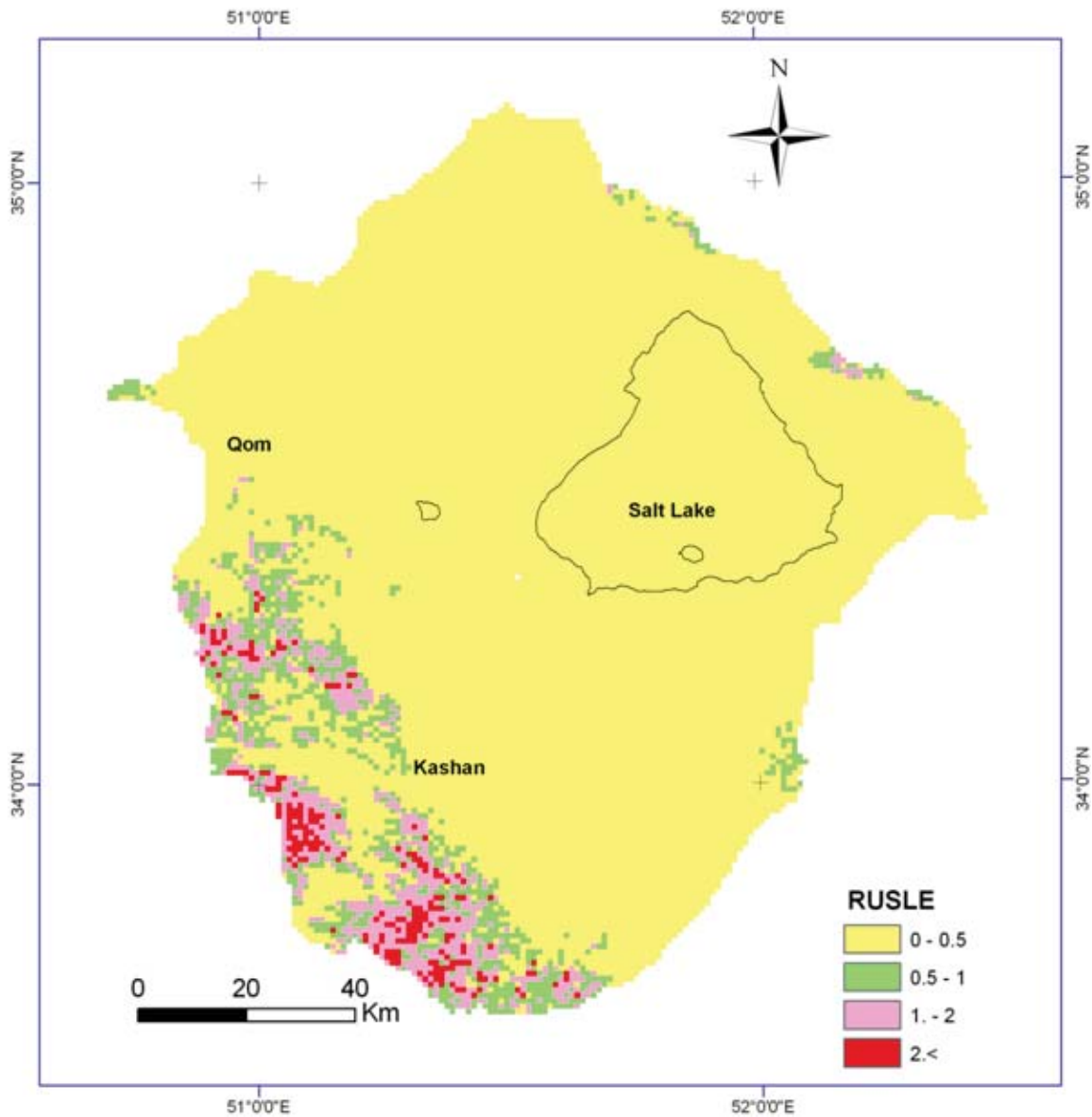


Figure 5.7: Areas affected by water erosion according to RUSLE (2006)

5.2.7 Vegetation Health Index (VHI)

Vegetation Health Index (VHI) is based on Temperature Condition Index (TCI) and Vegetation Condition Index (VCI), even though there is no significant correlation between TCI and VCI. However, each index provides additional information about land surface. In other words, Temperature Condition Index (TCI) provides information about the thermal properties of land surface, and Vegetation Condition Index (VCI) also indicates the status of vegetation. The integration of these two indices is defined as Vegetation Health Condition (VHI). Indeed, the

integration of these indexes is necessary to evaluate land surface temperature and the vegetation canopy status.

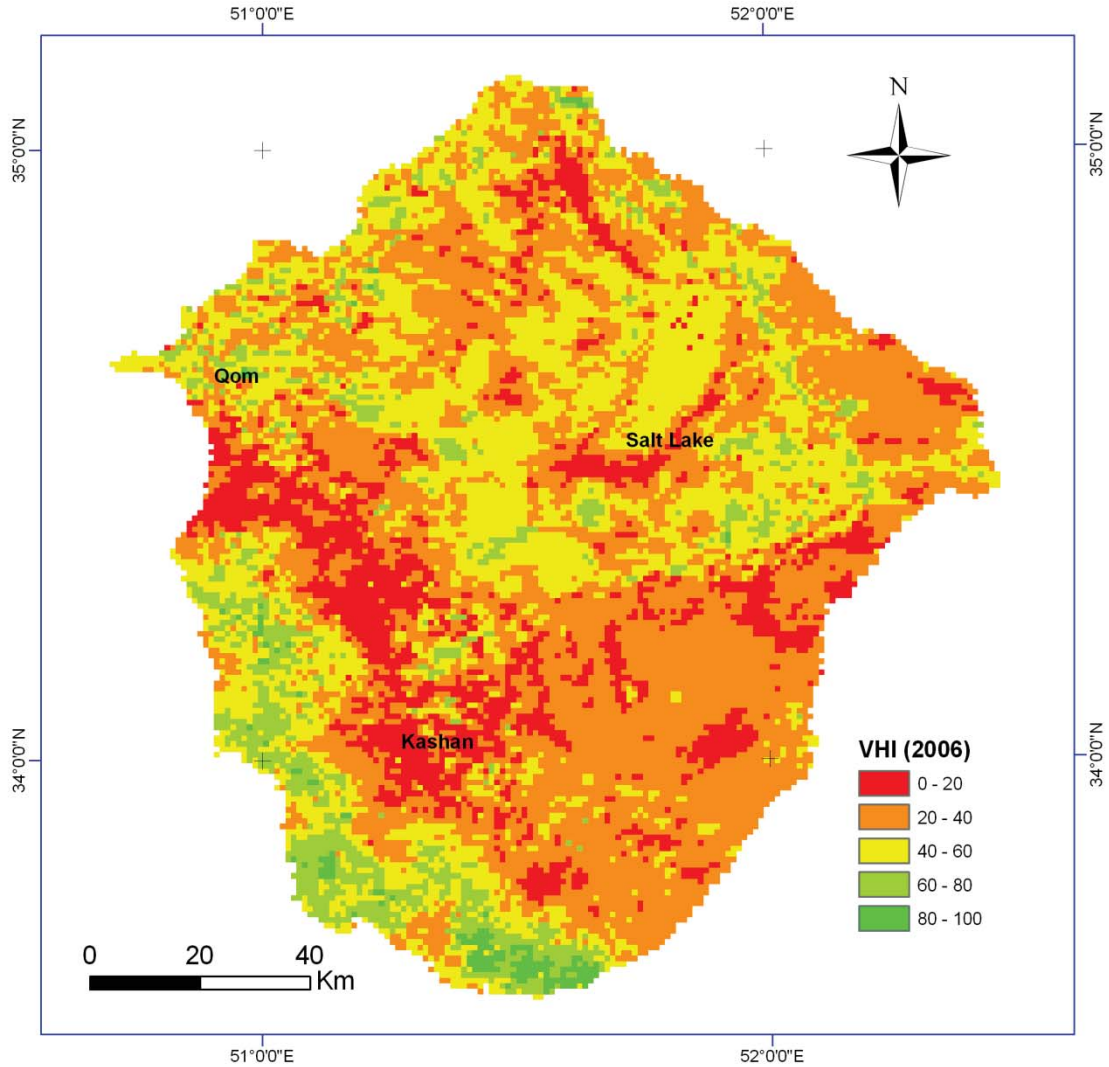


Figure 5.8: Vegetation Health Index in 2006

In the affected areas the quality of vegetation decreases due to erosion and drought. Therefore, the health of the vegetation is a practical indicator to detect land degradation. The index has many advantages such giving information about the reduction of climatic and temporal noise in time series data and the fluctuations of NDVI and LST independent to weather conditions. Kogan et al. (2004) suggests the following vegetation health index (VHI), based on TCI and VCI as a good measurement to gauge this factor.

$$VHI = aVCI + (1 - a)TCI \quad (5.32)$$

where VCI and TCI represent vegetation condition index and thermal condition index, respectively, where “a” is a coefficient showing the contribution of VCI and TCI in the VHI, and “a” equals 0.5 (Thenkabail et al. 2004). The result of Equation 5.32 is shown in Figure 5.8 that shows the classified VHI in five classes such as “very severe” (0-20), “severe” (20-40), “moderate” (40-60), “high” (60-80), and “very high” (80-100).

5.3 Desertification Map

In this section two approaches are used to prepare the desertification map: First, according to five indicators including VCI, TCI, SPI, Q and RUSLE, the map of potential desertification is created. Second, according to the main factors of desertification based on FAO method, the desertification map of the study area is prepared.

5.3.1 RS-GIS-based Crisp Method

According to desertification susceptibility of the study area, the user-defined thresholds are determined, which are shown in Table 5.7; the values lower than 35 in VCI and TCI images shows the affected areas (affected class) by drought and temperature, respectively. In the SPI map, negative values show drought condition, and in the erosion index, RUSLE, the values higher than 0.5 demonstrates the affected areas. The threshold for index Q is 150; any higher value than this represents the effect of flooding in the study area. The binary classifications of indicators are summed up to estimate the frequency of effects in the area, as shown in Figure 5.9 and 5.10.

Table 5.7: Thresholds for desertification indicators

Indicator	VCI	TCI	SPI	Q	RUSLE
Threshold	<35	<35	<0	>200	>0.5

Figure 5.9 illustrates the occurrence frequency of VCI or TCI in the study area. That is, Class No. 0 shows the values for both indexes of VCI and TCI are lower than the threshold, 35. Class No. 1 indicates that one value of either VCI or TCI is higher than the threshold, while Class No. 2 shows both VCI and TCI have values higher than the selected threshold. Concerning drought and desertification severity, the Class No. 1 and Class No. 2 are the severe and extremely severe

classes, respectively. These classes predominately cover most of the study area. In addition, Class No. 2 (the extremely severe class) is located around the populated areas, where the areas of farming and pasture, especially in Kashan areas, lie.

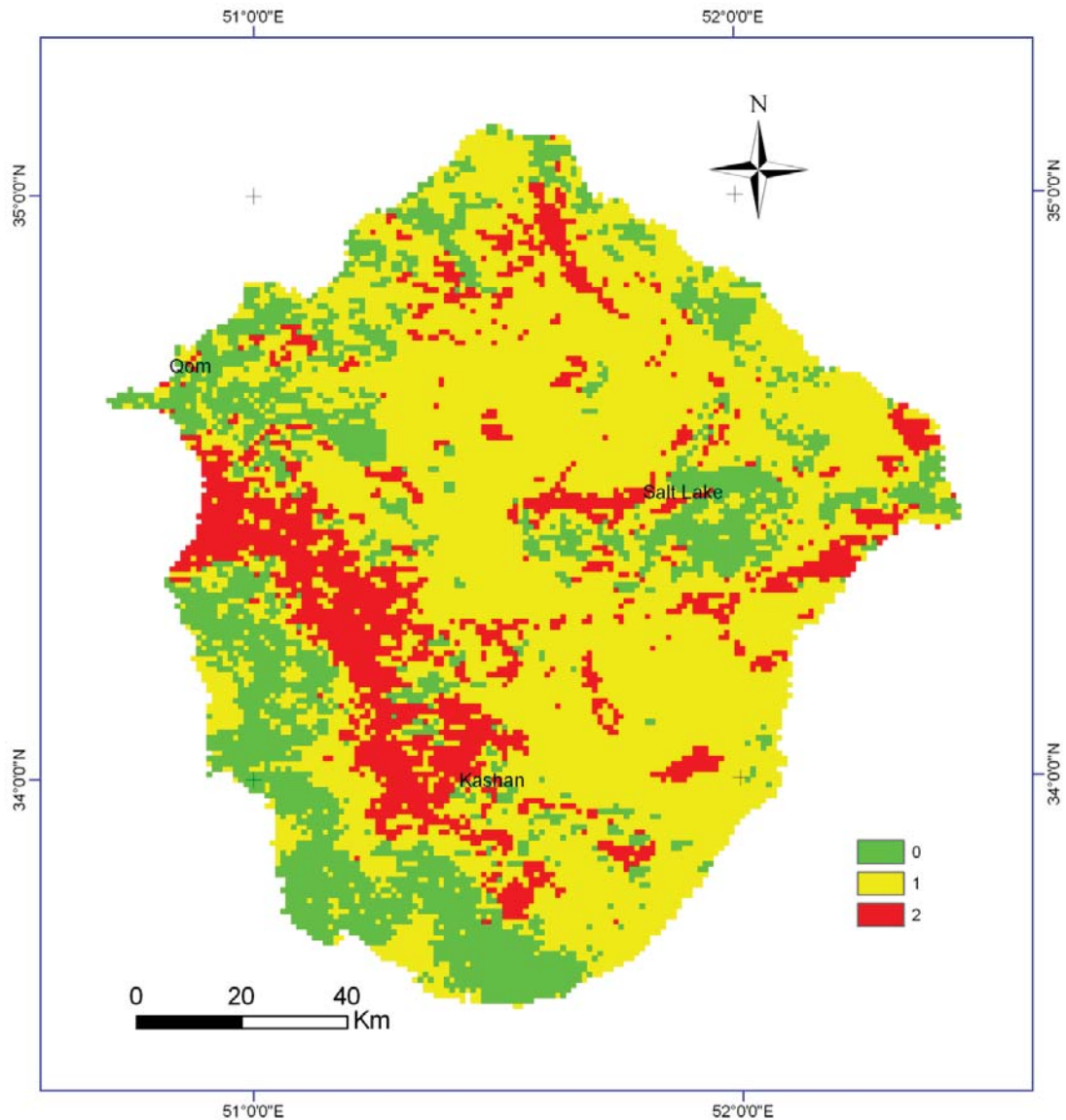


Figure 5.9: Desertification map according to the frequency of VCI and TCI

Class No. 0 is prevalent in high mountainous areas, according to Figure 5.9, which means that none of the considered indicators (VCI or TCI) are observed there. Furthermore, this class is also seen in the south-east of the salt crust of Lake Qom.

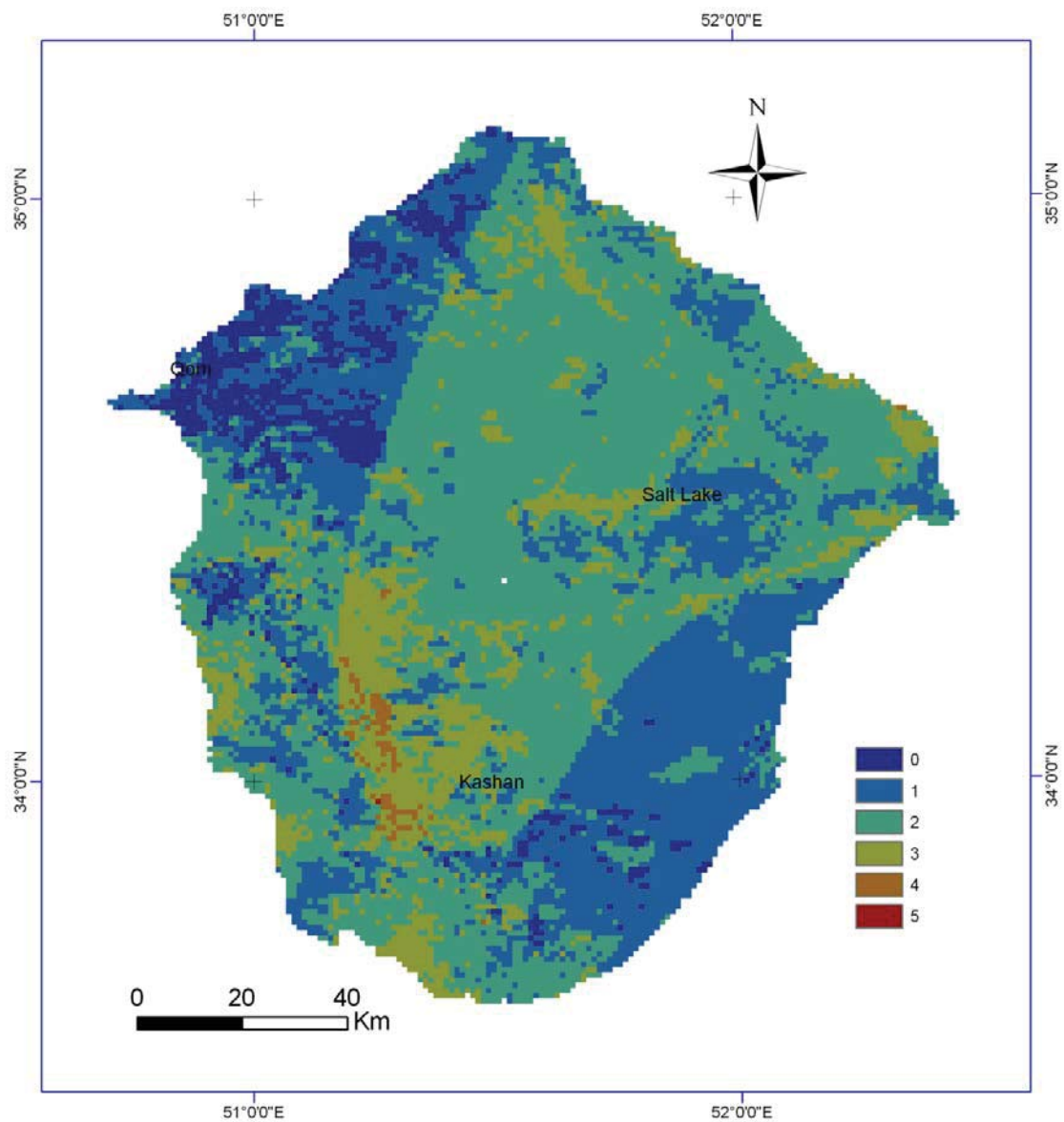


Figure 5.10: Desertification map according to the frequencies of five factors (VCI, TCI, Q, RUSLE, and SPI)

Figure 5.10, also represents the effect of the five indicators of desertification in the study areas, such as VCI, TCI, Q, RUSLE, and SPI. In this map, the frequency of desertification intensity is shown.

5.3.2 Conventional Multi-Criteria Method of FAO

Persistent, harsh climatic conditions throughout the study area make the region vulnerable to drought and desertification. Even though these problems are not entirely avoidable with current technology, the best-known methods for combating consequential damage are the recognition of causative criteria and the making of appropriate decisions. For this reason, the analysing of historical events will help researchers and decision-makers.

In the study area, overgrazing and land clearing are the main man-made causes of desertification, which affect vegetation and soil through the decrease of vegetation quality and organic matter, erosion (wind and water), sand encroachment, salinization, and contaminations.

Therefore, ancillary meteorological data, such as precipitation and temperature are useful in recognising previous drought events. Geomorphology, geology, and land use maps are valuable in highlighting vulnerable areas. Where quantitative maps for desertification are unavailable, it is possible to produce qualitative maps based on subjectively-defined factors, which are selected and categorized by field experts. In this regard, the remote sensing data are also practical in defining land and geomorphology units.

The main purpose of this section is to prepare desertification maps and to establish susceptibility classes based on FAO methods with GIS techniques and the visual interpretation of remote sensing images. In this study, the satellite data, Landsat (TM and ETM) data, on September 9, 2001, were used to interpret and classify geomorphology units and land cover features. In order to prepare the desertification maps, supporting maps such as soil map and geology, climatology, hydrology maps were used.

The use of desertification maps is to determine the susceptibility of lands and the overall image of desertification processes in the specified region. Desertification maps are also used in the planning of development projects and in the combating of desertification.

In preparing desertification maps, main and sub-factors are qualitatively graded according to desertification criteria and susceptible intensity. By determining the effectiveness of factor over susceptibility of land, desertification maps are prepared. There are three maps in this research, including the status of desertification, a map of potential desertification, and an overall desertification map. The latter map is the average values of the status map and the

potential map. In order to evaluate desertification factors, according to different aspects such as the current status conditions, the natural capability, the probability of risk, and the influence of criteria, and the severity of desertification are sectioned into four classes, including “low”, “moderate”, “severe” and “very severe” as shown in Table 5.8, as follows (Feiznia et al. 2001):

- Class 1 or “low”: degradation in soil and vegetation is scant, or where there is no land degradation.
- Class 2 or “moderate”: where from 25 to 50 percent of the area’s plant life is formed by high quality and valuable species, or where 25 to 75 percent of the primary soil surface is lost and soil salinity causes from 10 to 50 percent reduction in potential crop yields.
- Class 3 or “severe”: where high quality species comprise only 10 to 25 percent of the plant species or all surface soil layers are eroded, or where more than 50 percent of potential crop production is lost because of salinity.
- Class 4 or “very severe”: where high quality species comprise less than 10 percent of the plant community, or where land is covered with sand dunes or deep gullies, salt crusts and saline soils with low permeability. “Very severe” is a class considered as real desert. This land degradation class indicates an area where much human population suffers on account of the consequences of degradation. Here, the land is so degraded that reclamation is not possible, and economically impossible to rectify.

Table 5.8: Desertification severity classes

Status	Desertification severity classes			
Qualitative	Low	Moderate	Severe	Very Severe
Quantitative	< 35	35-55	55-75	75<

According to the criteria in Tables 5.9, 5.10, 5.11, and 5.12 (Feiznia et al. 2001), the desertification map of the study area is shown in Figure 5.11.

Table 5.9: Desertification status criteria (DC) (Feiznia et al. 2001)

Criteria		Class	Very low 0-2	Low 2-5	Moderate 5-10	Severe 10-15	Very severe 15-20
		Intensity					
Soil Erosion	Wind	Vegetation mounds	-	5-10 cm	20-100 cm	High sand dune, (nebkha,1-2 m)	Sand field, vegetation mounds (nebkha,3-5m)
		Gravel percentage	-	15<	15-30	30-50	>50
	Water erosion and its coverage in percent		Low < 5	Sheet and low rill erosion 5-15	Sheet and rill erosion 15-25	Sheet, rill and gully erosion 25-35	Sheet, rill gully, and badlands erosion 35-50
Vegetation	Coverage (in percent)		25-50	25-35	15-25	5-15	<5
	Quality (Dominancy)		High valuable species	Average dominant the high valuable species	Dominant with the average valuable species	Dominant with aggressive species	Bare lands
	Yield percent (ref. to ideal agriculture)		80-100	60-80	60-40	20-40	Bare lands
Soil salinization	Salt crust coverage (in percent)		-	0-5	5-25	25-50	50>
	EC		<4	4-8	8-16	16-32	32<
	SAR		<8	8-13	13-30	30-70	70<
Groundwater table (cm)			<1	1-10	10-20	20-30	30 <

Table 5.10: The effective criteria in land degradation (potential desertification map) (Feiznia et al. 2001)

Criteria	Class	Low	Average	Severe	Very Severe
	Intensity	0-2	2-4	4-7	7-10
Climate(C)	Drought duration (monthly)	2-3	4-6	7-9	9-10
	Aridity	Sub-humid	Dry sub-humid	Semi-arid	Arid
	Wind speed (m/s)	2	2-3.5	3.5-4.5	5
	Rainfall intensity, frequency	Low	Medium	High	Very high
	Drought duration (yearly)	1	2-3	3-5	5
Geomorphology	Wind erosion (landform and slope in percent)	Highlands	Hills	Plain, pediments, alluvial fans	Salt crust and clay flat
		Slope > 20	10 < Slope < 20	5 < Slope < 10	Slope < 5
	Water erosion (slope in percent)	Slope < 5	5 < Slope < 10	10 < Slope < 20	20 < Slope
Geology(L)	Lithology	Massive igneous, quartzite, gypsum, crystalline rock	Hard texture; hard conglomerates and metamorphic rock with average hardness	Sandy and soft texture; soft conglomerates, marl, shale	Evaporite and alluvial sediments; marl, clay, shale
Soil(S)	Wind erosion	Clay	Sandy clay	Loam	Sandy
	Water erosion	Sandy	Loam	Sandy clay	Clay

Table 5.11: Hydrology and desertification classes; Electrical Conductivity (EC) and the Sodium Absorption Ratio (SAR) (Feiznia et al. 2001)

Criteria	Class	Very low	Low	Average	Severe	Very Severe
	Intensity	0-1	1-3	3-5	5-7	7-10
Hydrology	Groundwater table (m)	5>	3-5	3-1.3	1.3-0.75	<0.75
	Salinity (EC)	<250	250-750	250-2250	2250-5000	5000<
	SAR	<10	10-18	18-6	26-30	30<

Table 5.12: Criteria in man-made desertification and the severity classes of desertification (Feiznia et al. 2001)

Criteria	Class	Low	Average	Severe	Very Severe
	Intensity	0-2	2-4	4-7	7-10
Pasture management	Overgrazing	Little	Average	High	Very high
	Shrub-cutting percent	<10	10-25	25-50	50<
Agriculture management	Plough	Good	Medium	Bad	Very bad
	Cultivation	Compatible with nature, no decrease in yield	Moderately compatible, little decrease in yield	Incompatible, high decrease in yield	Incompatible, very high decrease in yield
	Irrigation system	Good; acceptable	Moderate; acceptable	Poor; unacceptable	Very poor; unacceptable

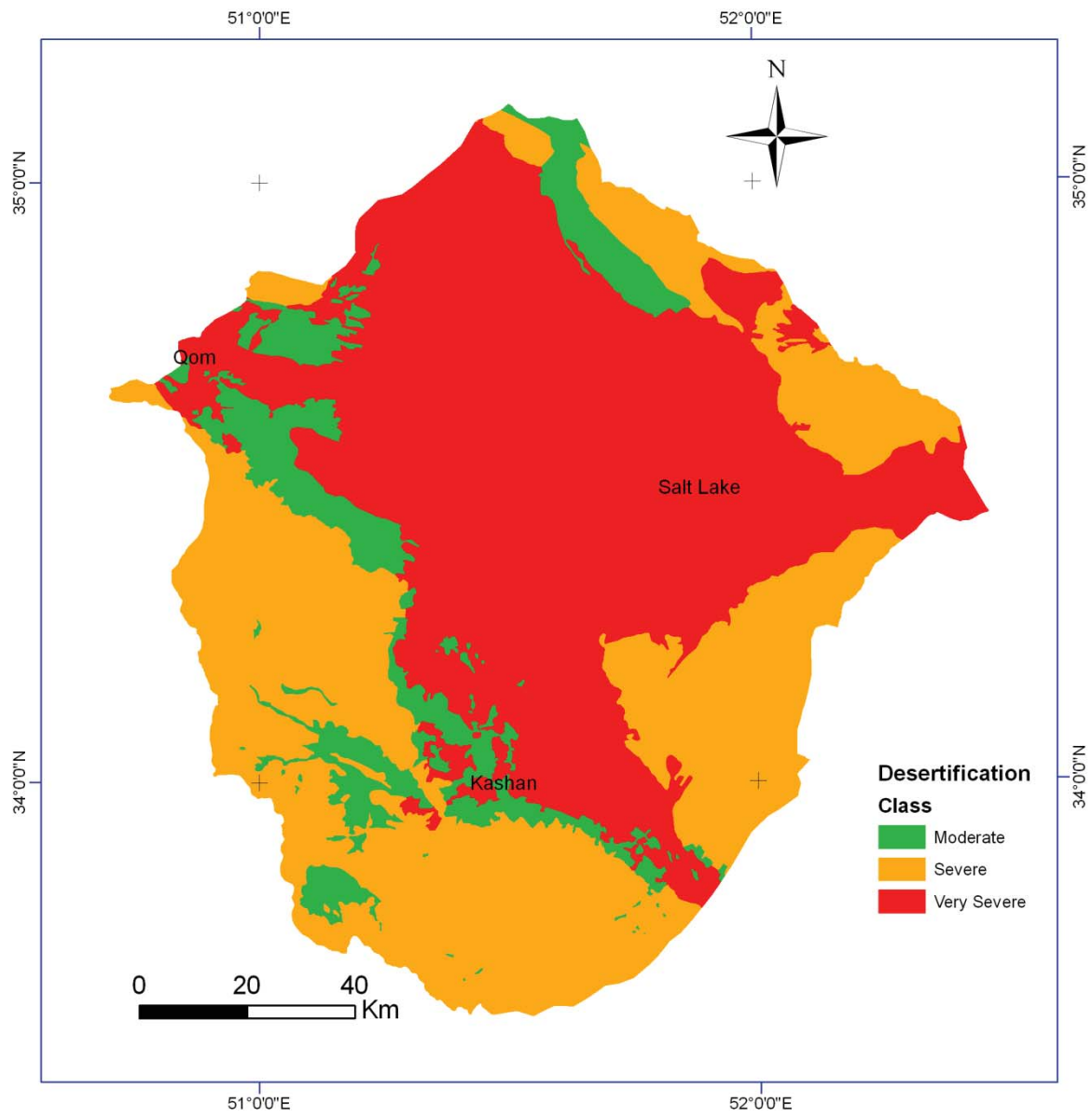


Figure 5.11: The overall desertification map (FAO Method)

5.4 Evaluation of the Accuracy of Results Using Error Matrix

For the evaluation of results in this research, a truth-ground map of desertification is prepared by sampling, based on fieldwork and satellite images, i.e. Landsat and Google maps. Considering the evidential criteria of signature sampling for these data, the sampling method is supervised by expert knowledge, so that the training sites are selected based on the spatial position of the sampling point and its visual spectral information. Even though some parts of the study area, such as sand dunes, wetlands and salt lakes are inaccessible, the specific characteristics of the sample points in these landforms are well-known through land cover maps and satellite images. The uniformity of land features, such as sand dunes and salt crust, helps us to recognise the characteristics of pixels; therefore, a colour composite of three bands of Landsat satellite images, including seventh, fourth and second band of ETM+, is applied as red, green, and blue (RGB) in the colour composite image (Figure 4.1) to recognise the severity of desertification, as well as land use.

In this report, the sample points are based on different surface cover types in the study area, and then the evaluated severity value of desertification for each point of samples is assigned. The following table represents the three selected severity classes of desertification as sample sets and their statistics (Table 5.13).

Table 5.13: The characteristics of severity classes

Desertification severity class (No.)	Desertification severity class	Land units	No. Samples	Percentage
3	Very severe	Eroded plains, sand dunes, salt crust.	23	5.8
4	Severe	Mountains, hills, plains	125	31.3
5	Average	Vegetation cover	252	63

Depending on the spatial location of the samples and their visual spectral characteristics related to desertification severity, samples are divided into five classes, from the best condition of land (no desertification, class 1) to the worst condition (extreme severe desertification, class 5). The other classes are listed as follows: slight desertification (class 2), moderate desertification (class 3), and severe desertification (class 4). Accordingly, the extremely affected areas, such as sand dunes, salt crust (salt lake), saline wetlands, are identified in class 5. The other affected

areas, i.e. the areas prone to salinization-alkalization and wind-and-water erosion, are indicated as severe desertification, in class 4. Areas with thriving vegetation are also classified as average class, (class 3) because of some limitations such as soil salinity level.

5.4.1 Sample Size

The sampling pixels are selected randomly, and the number of samples is also based on binomial probability theory, in which the acceptable error and the confidence level play a significant role in the sample size. According to Cochran's sample size formula, the following relationship indicates the number of experimental points according to the acceptable error:

$$n = Z_{\frac{\alpha}{2}}^2 \frac{(p)(q)}{E^2} \quad (5.33)$$

where n is sample size, and Z equals 1.96, which is a value for selected alpha level of 0.025 in each tail of a normal distribution histogram. Alpha level, here 0.05, is the accepted level of risk that also shows statistically the confidence level (95 percent) that is considered in this research; alpha level is also equal to 1- confidence level. The parameter (p) is the estimated proportion of a class to total population, and q is 1- p ; the product of p and q gives the estimate of variance. If p equals 50 percent, maximum variability is possible, whereas E is the acceptable error (5 percent). Furthermore, if the size of the population is small, the calculation of the final number of samples (m) is the equation below (Bartlett et al. 2001):

$$m = \frac{n}{1 - \frac{n}{N}} \quad (5.34)$$

where N is population size, and n is the result of Cochran's sample size formula. Therefore, in this research, m is calculated at about 395, but because of the error in sampling (0.02 percent) five more samples are added, bringing the total sampling point to 400.

5.4.2 Confusion Matrix

In remote sensing, to compare the agreement of two maps (truth-ground map and the classified map), both are matched and crossed pixel by pixel, and their corresponding values are stored in a pivot table, a so-called confusion matrix or error matrix.

A confusion matrix is a table to estimate errors between two categorical maps (truth-ground map and the classified map); it is also called error matrix for two maps in the research, which are the reference map and the result map. In other words, the confusion matrix is used to evaluate any misclassification between these two maps. The reference map is the test set/ground truth samples whose classes comprise the columns of the table, while the classes of the result map are also displayed in the table rows. Diagonal elements in the matrix correspond to correctly classified pixels for each class, whereas off-diagonal elements represent incorrectly classified pixels as errors occurred during the estimating of the result map. In this regard, there are defined sorts of accuracies and errors.

The proportion of correctly classified pixels along major diagonal elements, to total pixels in sampling, is defined as overall accuracy, which represents the agreement or disagreement between the two maps: reference data and the classified data. Non-diagonal columns contain the misclassified pixels of the reference map as omission error; these pixels are excluded from the nominated class. In other words, they are omitted from the lists of the true classes, and they are also inaccurately classified as another class. Regarding accuracy point, the producer's accuracy is the proportion of correctly classified pixels to total pixels in each column; from the viewpoint of the producer, these pixels belong to their correct classes, which are duly assigned to another class by the classifier. The producer is interested in how accurately it is possible to classify a certain class and to show correctly the real land features on the prepared map. Non-diagonal elements in rows represent the commission error, that is, the pixels of other classes are incorrectly included in a certain class, and are classified incorrectly. From the point view of accuracy in this regard, the user's accuracy is defined as the ratio of the correctly classified pixels in major diagonal element to the total pixels of each row. In fact, users are dependent upon the reliability of a classified map that indicates what is actually on the field (Congalton et al. 1991).

Additionally, the KAPPA Index of Agreement (KIA) or K_{hat} measures the difference induced by chance and "real" dis/agreement, that is, the proportion of the difference between actual observed accuracy and chance agreement to complement chance agreement, as follows (Eastman and Worchester 2001):

$$K_{\text{hat}} = \frac{P_o - P_c}{1 - P_c} \quad (5.35)$$

where P_o is the observed accuracy, which is the proportion of summed diagonal elements to the total number of pixels, while P_c is the expected agreements (by chance) for agreements in different categories (the proportion of combination total row i and total column i to grand total pixels). The alternative equation is (Jensen 1995):

$$K_{\text{hat}} = \frac{N \sum_{i=1}^r x_{ii} - \sum_{i=1}^r (x_{i+} \times x_{+i})}{N^2 - \sum_{i=1}^r (x_{i+} \times x_{+i})} \quad (5.36)$$

where

N = total number of pixels

r = number of row in the cross-classification table

x_{ii} = correctly classified pixels in each diagonal element (i.e. pixels for row i and column i along the diagonal)

x_{i+} = total observation in row i

x_{+i} = total observation in column i

The KAPPA Index is between zero (non-agreement) and one (complete agreement), and is arranged into five agreement classes, as follows: poor (≤ 0.2), fair (0.21 - 0.40), moderate (0.41 - 0.60), good (0.61 - 0.80), and very good (0.81 - 1) (Koutroumpas et al. 2010).

Chapter 6

Fuzzy Expert System for Desertification

6.1 Introduction

Recently, the application of intelligent and rule-based models for land evaluation has attracted the attention of environment researchers and experts. These models are designed to improve the applicability and efficiency of previous models, especially the categorical-based land evaluation system (Baja et al. 2005) and land cover changes (Tang 2004), and soil sciences (Burrough 1989; Burrough et al. 1992).

There are two different points of view in land suitability evaluation: First, the quantitative methods based on statistical criteria, which include quantitative results and qualitative maps; second, the qualitative methods based on subjective criteria. In this regard, various methods are widely used to evaluate land suitability evaluation and vulnerability assessment, such as Multi Criteria Analysis methods (MCA), Analytic Hierarchy Process (AHP), and fuzzy expert system (Baja et al. 2005).

In remote sensing (RS) and geographic information system (GIS), the theory of fuzzy logic is applied to study the objects or phenomena with some degree of uncertainty, or to use vague geospatial datasets - especially linguistic variables involved in the assigning of geographical data (Abbaspour et al. 2003; Robinson 2003; Bone et al. 2005).

There exists more practical challenges and endeavours to utilize fuzzy systems and to represent vulnerability issues in spatial phenomena (Bone et al. 2005): For example, land cover change (Tang 2004); land evaluation and soil survey (Burrough et al. 1992; Davidson et al. 1994), and the enhancing classification of remote sensing images (Wang 1990; Brandtberg 2002; Lee and Lee 2006).

In this regard, fuzzy systems deal with issues such as risk estimation of desertification, following forest fire (Sasikala and Petrou 2001); land evaluation (Burrough 1989; Davidson et al. 1994); modelling of saline and alkaline classification (Metternicht 2001); environmental suitability index (Baja et al. 2005); and soil mapping (Zhu et al. 2001).

The main goal in this research is to provide desertification mapping by using integrated remote sensing and a fuzzy expert system. Therefore, a model is designed which integrates the concept of fuzzy theory with remote sensing to define desertification and aridity in drylands.

6.2 Fuzzy Expert System

The project aims to present integration expert knowledge and data knowledge generation in remote sensing. For generation of the knowledge base system, Alonso Moral (2007), proposed the integrated model of expert-based method and data-based model. In this section, the desertification components are used to establish a fuzzy rule-based system for desertification problems, and to create the final map of desertification. From remote sensing data and ancillary data in GIS, a RS-integrated fuzzy system is used as shown in Figure 6.1.

A fuzzy system comprises three fundamental elements: fuzzification, fuzzy inference engine (rule base), and defuzzification (Klein 1999; Metternicht 2001). Nonetheless, for pre-processing, preparing, and final stages, sub-stages are shown in Figure 6.2 in which boxes describe processes over inputs and outputs.

The first main stage in a fuzzy system is fuzzy partition and fuzzification, where linguistic variables are divided into suitable fuzzy sets by partitioning of each variable. In other words, fuzzification is the partitioning of each variable into fuzzy sets (linguistic terms) as well as applying a membership function over each fuzzy set (partition). Therefore, in this stage, the partitions of variables are allocated their linguistic terms. In other words, fuzzy sets (linguistic

variables and its set terms, or fuzzy partition), and membership functions (MF) are the main stages of fuzzification.

The next step, rule base, is the generation and building of rules, where expert-based or data-based methods are involved in rule definition. In a data-based method (induction), the purpose is to scrutinise the relationship between inputs and outputs, which extracts knowledge from data by automatic learning rules. The generated rules are called data-based rules. In the expert-based method, expert defines rules, by using his experiences and considering principles such as “Law Of Minimum” (LOM), to make suitable decisions, these rules are known as expert rules.

After building a rule base, the consistency of the rules and possible conflicts among the rules are checked. Using a simplification method and linguistic analyses, a simplified model of a knowledge-based system is provided.

In a fuzzy expert system, the rule base (rule block) is the most salient part of the system, which performs the inference of the model; however, the selection of appropriate fuzzy sets as the fuzzy partition of the linguistic variable has a strong influence over the efficiency of the system.

The complexity of a rule-based system increases exponentially by the number of fuzzy sets and variables; therefore, the interpretability of the system gets low. For this reason, one possibility is to divide the variable and build more rule bases (Alonso Moral 2007). Therefore, in this model, we divided the involving factors in the studying of desertification into two rule bases (RB1 and RB2). The rule base RB1 is namely Vegetation Health Index (VHI), which is generated by using the remote sensing data such as VCI and TCI, and the integration of the induction method and expert knowledge instructions. In building of rule block RB1, in order to generate rules, two different methods are considered such as learning from data and guiding by experts. Particularly there is no precise desertification map; the method is only used for Rule Block (RB1), which is about the Vegetation Health Index (VHI) resulted by the simple arithmetic summation of TCI and VCI.

In the rule integration phase, the establishing of interpretable rules by an expert, or through the generation of rules based on data is a key goal. Therefore, the applying simplification and consistency over rule base is to build an interpretable rule-based system (Figure 6.1).

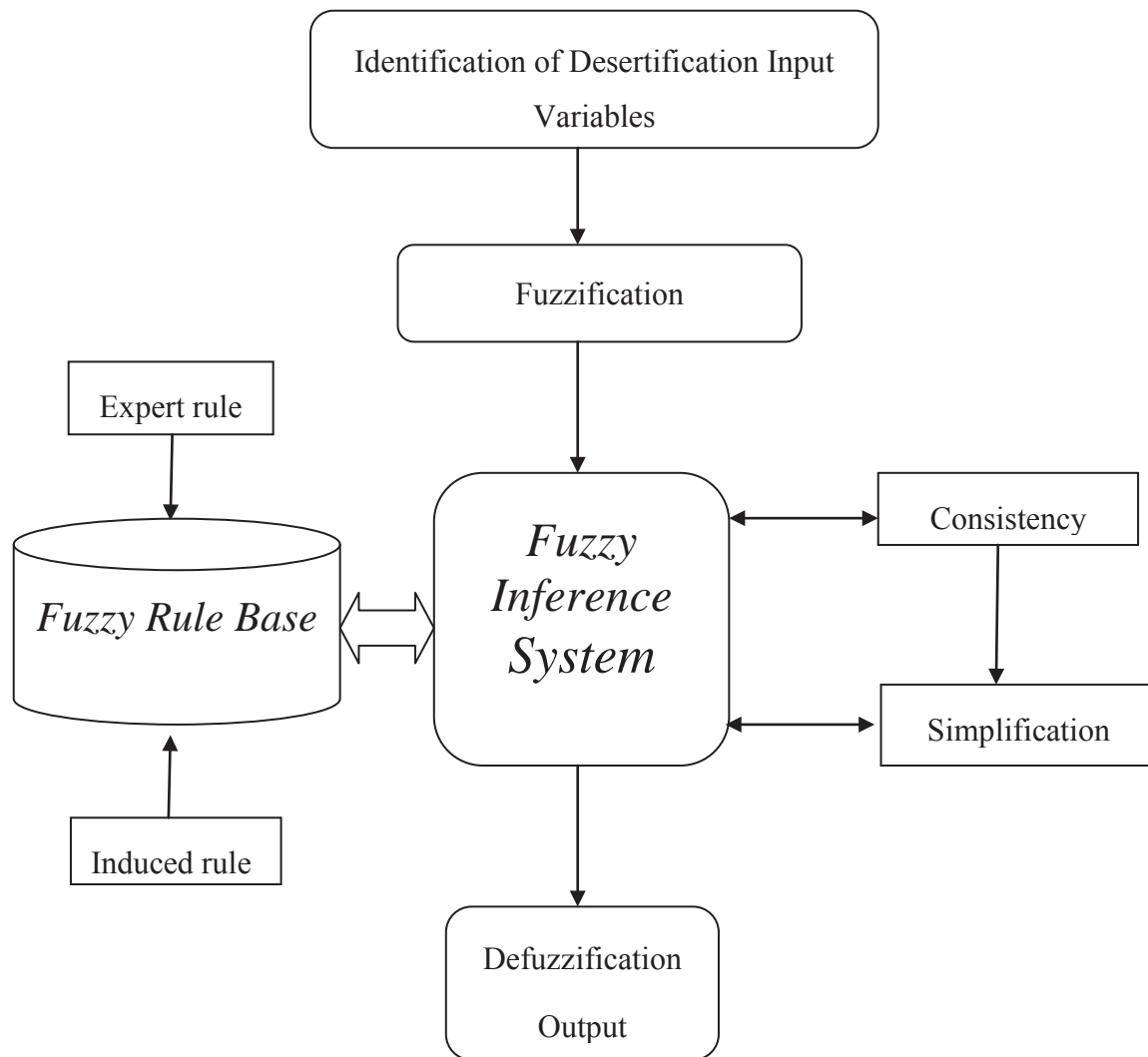


Figure 6.1: Fuzzy Expert System Model

The second rule base, RB2 is the soil-climate condition, developed by integrating the soil erosion index (RUSLE), the flood index (SCS model) and the climate index (SPI). RB2 represents the sensitivity and intensity of soil condition, and dryness as the major causes of desertification. Finally, these two knowledge bases or rule bases/blocks (RB1 and RB2) are integrated to estimate overall desertification index and the susceptibility of the study area. The general processes are illustrated in the diagram below (Figure 6.2).

As the study area is located in the dryland of central Iran, especially in the margins of the desert areas, desertification is one of the most serious problems, along with aridity, salinization, erosion, and vegetation degradation.

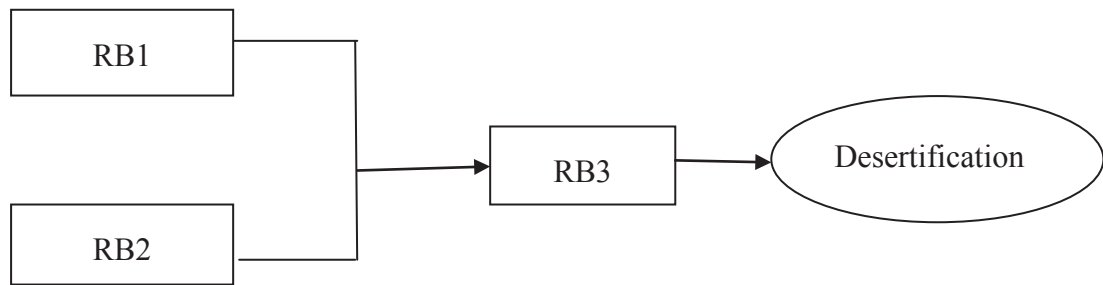


Figure 6.2: The knowledge base (Rule Base, RB) for the desertification process

An integrated remote sensing and fuzzy system helps in the building of an expert model for desertification evaluation. In order to study the affected area in the Qom watershed, an integrated vulnerability model can be simulated (Figure 6.1), which shows the main processes involved in developing a fuzzy expert system for desertification.

6.2.1 Step I-Identifying Variables and Indices

In a fuzzy system, the first step includes the identification and selection of linguistic variables and the responsible agents involved in desertification. The preparing of indexes from remote sensing images and ancillary GIS data were described in Chapter 5 including Vegetation Condition Index (VCI), Thermal Condition Index (TCI), Standardised Precipitation Index (SPI), flooding or over flow (Q), and erosion index (RUSLE), used in the modelling of land vulnerability (susceptibility) as the desertification map. As it is mentioned in the same chapter, in the first step, indices were calculated and the required information layers were prepared from remote sensing and ancillary data, which are calibrated in GIS.

In this step, calibrated layers are used in a fuzzy system to infer information on the variables; these variables are then integrated in raster-based GIS. This results in multiple layers of information that correspond to different variables.

According to Fuzzy Control Language (FCL), the selected inputs, as the desertification indexes for the evaluation of land degradation, are shown in Figure 6.3 as follows; the Function Block (FB) is declared in the Structured Text (ST) and Function Block Diagram (FBD). The input variables for the system have "REAL" type.

```

VAR_INPUT
    VCI    REAL; (* RANGE (0...100) *)
    TCI    REAL; (* RANGE (0...100) *)
    RUSLE  REAL; (* RANGE (0 ...1) *)
    Q      REAL; (* RANGE (0...350) *)
    SPI    REAL; (* RANGE (-1... 1) *)
END_VAR

```

Figure 6.3: Linguistic variables declared in FCL

6.2.2 Step II-Fuzzification or Fuzzy Partition

In the second stage, in addition to the definition of membership functions, fuzzy sets as linguistic terms or adjectives for each variable are introduced. Later these fuzzy sets or fuzzy partitions are incorporated in the rule block (rule base). A fuzzy set as an adjective for variable partition represents the degree of allocation as a membership degree for each set. In other words, this section explains how to choose fuzzy sets (partition) for the linguistic variables to determine their fuzzy sets (terms). The selection of suitable membership functions for fuzzy sets is one of the most important parts in a fuzzy system, which perfectly represents the fuzzy modelling.

For a given variable, the maximum information of expert in the definition of membership function is the determining of the universes of discourses as the domain of interest, and the number of linguistic terms (fuzzy sets), and the creation of the prototypes for some linguistic labels (names). The range of data as the domain of interest is easily determined from the extent of the data: i.e., maximum and minimum ranges; experts also can select these ranges. The expert determines the number of fuzzy sets and their names which are linguistic properties (Alonso Moral 2007).

The complexity of a fuzzy rule-based system relates positively to the number of variables and the number of sets in each variable, so that the number of rules increases exponentially as the number of variables and fuzzy sets increase. In other words, choosing more sets and variables

will increase rules exponentially as well as the complexity of the system. For instance, having five variables (m) and supposing three fuzzy sets (n) for each variable, the total number of rules is 243 rules (i.e. m^n yields 3^5); therefore, the interpretability of system decreases (Alonso Moral 2007; Ledeneva et al. 2008; Anarmariz et al. 2010).

The rule integration is mainly dependent on the quality of the partitioning of variables. The readability in the fuzzy partitioning of variables is necessary to construct the interpretable rule base, therefore, each linguistic variable in fuzzy systems should be defined by the certain and appropriate sets of partitions, i.e., fuzzy sets. Here, we aim at designing a well-interpretable partition by integrating expert knowledge and data (induction). Nonetheless, considering the expert knowledge, the expert should have at least some knowledge about the linguistic variables of the system. For partitioning properties and the determination of fuzzy sets, in the absence of more knowledge about term sets, experts can select odd numbers of sets and put the partitions around a central label (Alonso Moral 2007).

For clustering the variable by data distribution, there are several methods to cluster data such as k-means, Hierarchical Fuzzy Partitioning (HFP), and regular partitioning as implemented in Fispro (Guillaume et al. 2002), and KBCT (Alonso Moral 2007):

- **Regular Partition:** the uniform and standardised strong fuzzy partition, based on the range of the data and coverage of fuzzy sets.

By partitioning the linguistic variable into linguistic terms (fuzzy set), it is possible to allocate the proper fuzzy set as an adjective for a linguistic variable; this fact represents a vulnerability variable and the positional uncertainty of objects.

Vegetation Condition Index (VCI) is based on the standardization of NDVI, which is the indicator that shows the changes in vegetation cover, and ranges from zero to 100. The linguistic variable VCI can be described by linguistic terms (fuzzy sets) {"very low", "low", "medium", "high", "very high"} ranging from the worst condition to the best condition in respect to vegetation condition. The decrease in the quality of plant life is indicated by a "low" term, which corresponds to an increase in the vulnerability of desertification. In other words, according to the relation between severe drought and healthy vegetation (no drought), the threshold for drought is approximately 35. As the lowest value is more important in the allocation of the severe class, the values around 35 get a "low" rating. The VCI values above 50 indicate "optimal" or "above-

normal” conditions, so in regard to a healthy condition they will get a “high” fuzzy set rating. At a VCI value of 100, the NDVI values for the considered month are equal to the maximum values of NDVI (Kogan 1995, 1997; Kogan et al. 2004).

Regarding regular clustering, Figure 6.4 shows the elected fuzzy set and the corresponding membership function, defined by translating the variable VCI into five linguistic terms {“very low”, “low”, “medium”, “high”, “very high”}: as they shift towards the left the influence of vulnerability (bad condition) increases. This means that vulnerability does change as the condition of vegetation worsens. Conversely, a shift towards the right indicates the non-affected vegetation. This suggests a negative relationship between desertification and the existence of vegetation.

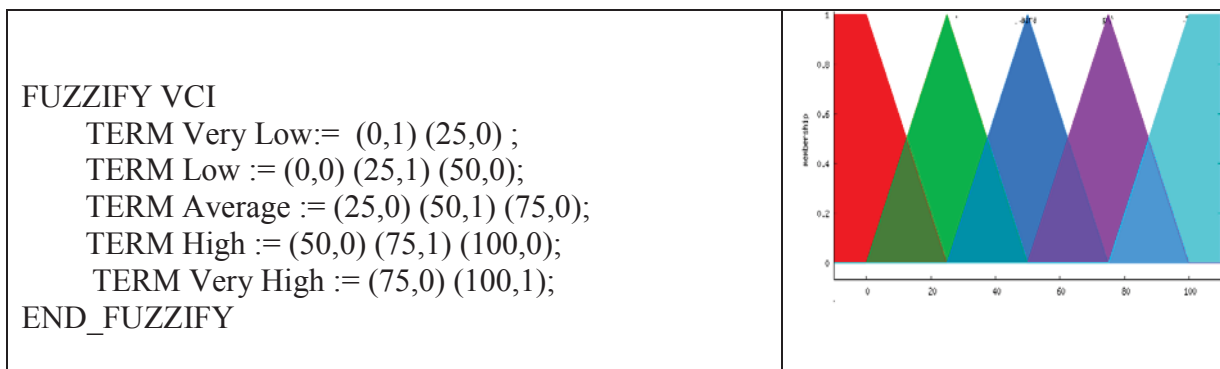


Figure 6.4: Membership function for VCI with three linguistic terms

The effectiveness of Thermal Condition Index (TCI) and Vegetation Condition Index (VCI) in Vegetation Health Index are equal, and their importance is identical (Kogan 1995, 1997; Kogan et al. 2004). In this research, we also assume the same functional characteristics for TCI and its membership function.

Standardised Precipitation Index (SPI) ranges from drought to wetness as negative and positive values, respectively (Table 5.2). The modified category for SPI in Fuzzy Control Language with only two fuzzy sets {dry, wet} is shown in the following Figure 6.5.

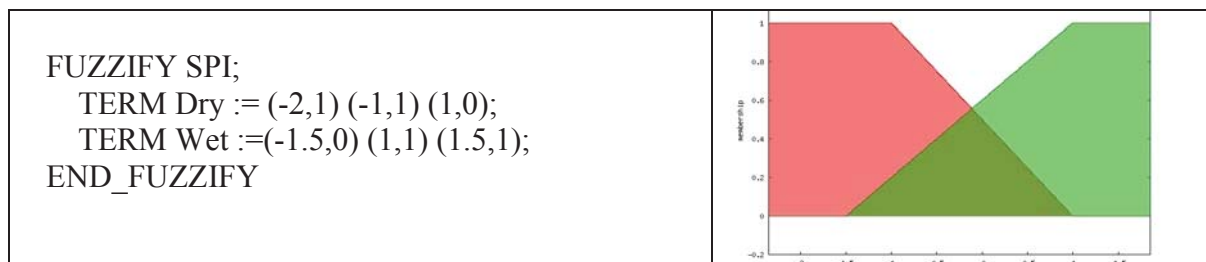


Figure 6.5: Membership function for SPI with four linguistic terms

Annual soil erosion calculated by the Revised Universal Soil Loss Equation (RUSLE) represents the vulnerability of soil to erosion as the indicator of desertification. Estimating soil loss tolerance (T-value) is the threshold criterion for the sustainability of land production, which determines permissible soil loss. According to Baja et al. (2005) based on USDA-SCS, T-value for soils with 0.5 meter depth is approximately one ton per hectare per year; therefore, the selected T-value relates to maximum erosion for the study area.

For partitioning RUSLE, according to regular clustering, three categories are designated three linguistic terms {low, average, high} as shown in Figure 6.6.

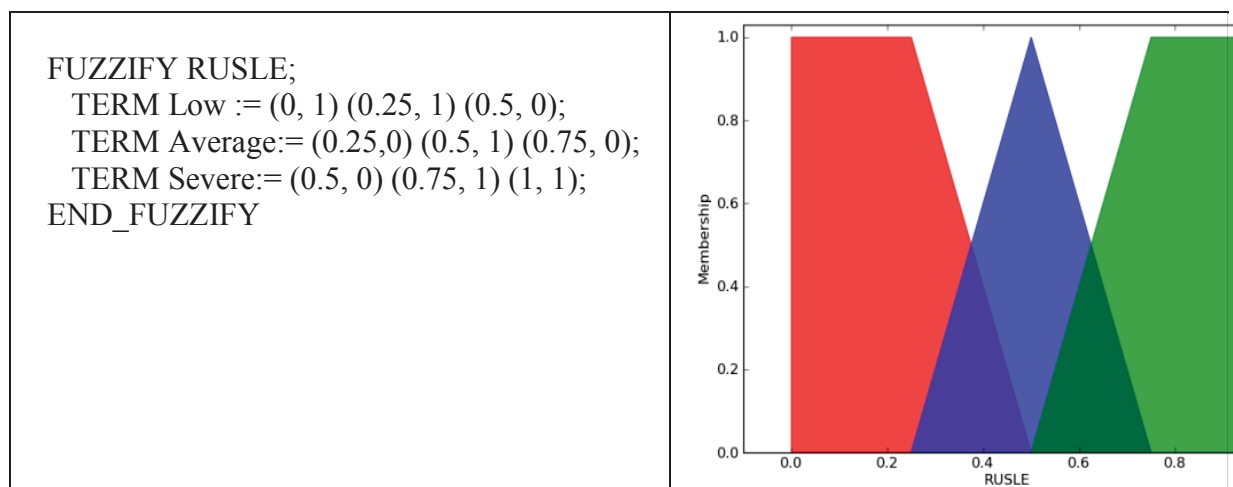


Figure 6.6: Membership function for soil erosion (RUSLE) with three linguistic terms

For flooding or overflow the linguistic variable (Q) is chosen with three fuzzy terms, shown in Figure 6.7.

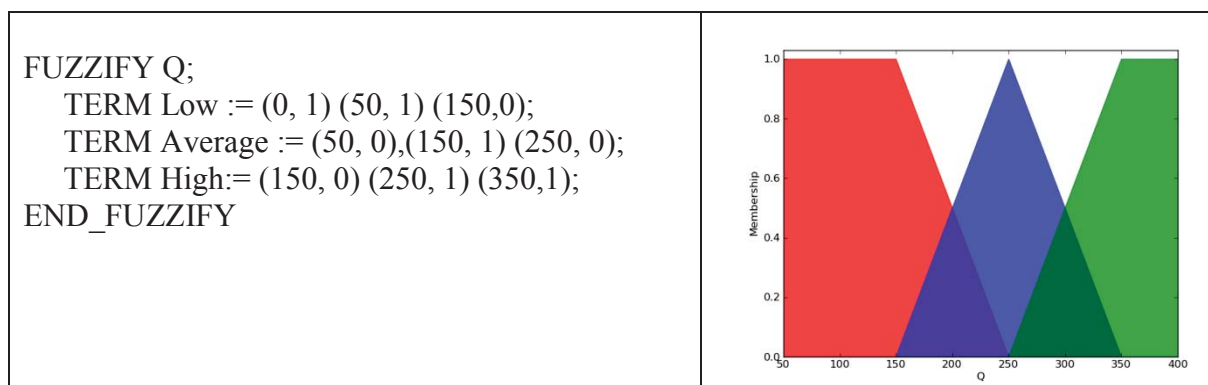


Figure 6.7: Membership function for flooding (Q) with three linguistic terms

6.2.3 Step III -Rule Block (Rule Base)

The third step, or Rule Block (RB), is the signal part of a fuzzy inference system that contains rules, defined by the empirical knowledge of experts and the knowledge learnt from data. In other words, the prepared fuzzy sets in the previous step are used in rules-making, which are either by expert rule or by data-based rule (induction method).

The rule block includes fuzzy operators to combine all fuzzy sets of linguistic variables per rule as well as rule accumulation. In computational GIS, simple operators are applied such as OR (maximum) or AND (minimum). The operator infers fuzzy output layer from raster layers for each cell. Therefore, the result of this step is used to create fuzzy output raster layers that contain the vulnerability/susceptibility of each cell to desertification.

6.2.3.1 Vegetation Health Index Rule base

The definition of the thermal-vegetation integration is a knowledge base for Vegetation Health Index (VHI) by function of Thermal Condition Index (TCI) and Vegetation Condition Index (VCI), as shown in Figure 6.8. In other words, the relationship between TC and VCI, shown in Figure 6.8 stands for Vegetation Health Index (VHI). The low value in VHI shows critical vegetation greenness, as the low value of any index either in VCI or TCI will imply low value in VHI. Conversely, the healthier vegetation is, the higher values of VCI, while the lower temperature decrease, the higher values of TCI are.

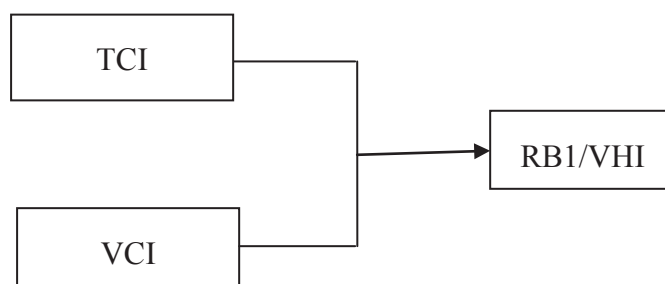


Figure 6.8: Fuzzy model of VHI (RB1).

In order to understand and acquire the interpretable information about land surface features, for visual interpretation of land surface features, samples of features have been obtained and presented. Figure 6.9 shows the relationship VCI and TCI and the position of land classes in

scatter plot as the characteristics of VCI and TCI in different land surfaces, whose attributes are also described in Table 6.1.

Table 6.1: The characteristics of features

Type	Code	Description
Sand dune	S	Sand dunes in the eastern part of Kashan
Rock	R	Bare soil and rock in the highland area
Desert pavement	F	Gravel surface in alluvial fans
Cropland	C	Vegetated area (agricultural land and orchards)
Low wetland	W1	Low wetland and the lowest part of Salt Lake with high moisture, and with salt crust cover in dry seasons
	W2	Salty lands with lower moisture content than W1, with wind and water erosion

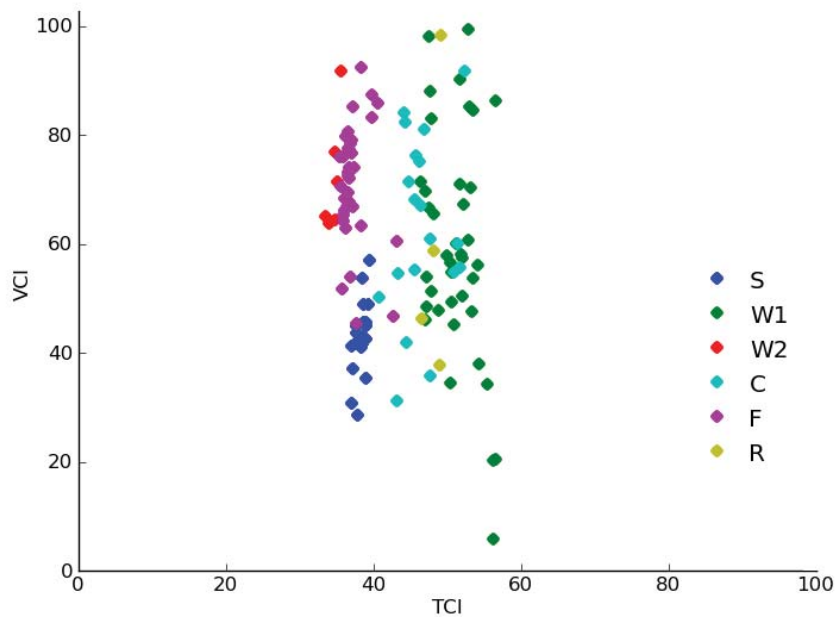


Figure 6.9: The scatter plot of feature values in TCI and VCI

Despite the absence of a statistically significant relationship between VCI and TCI in the study area, the integration of vegetation indices VCI and TCI is recognized as Vegetation Health Index (VHI). In fact, TCI values are relatively dependant on the existence of water or moisture in the

environment; therefore, sand dunes and dry salt crusts have low values of TCI, while VCI is the function of vegetation condition, in turn, VCI is affected by environmental factors such as drought and temperature. The important fact about the integration of TCI and VCI is that the regions near populated areas have low values of vegetation health index (VHI), which proves that these areas are highly susceptible to desertification during the study (Figure 6.10).

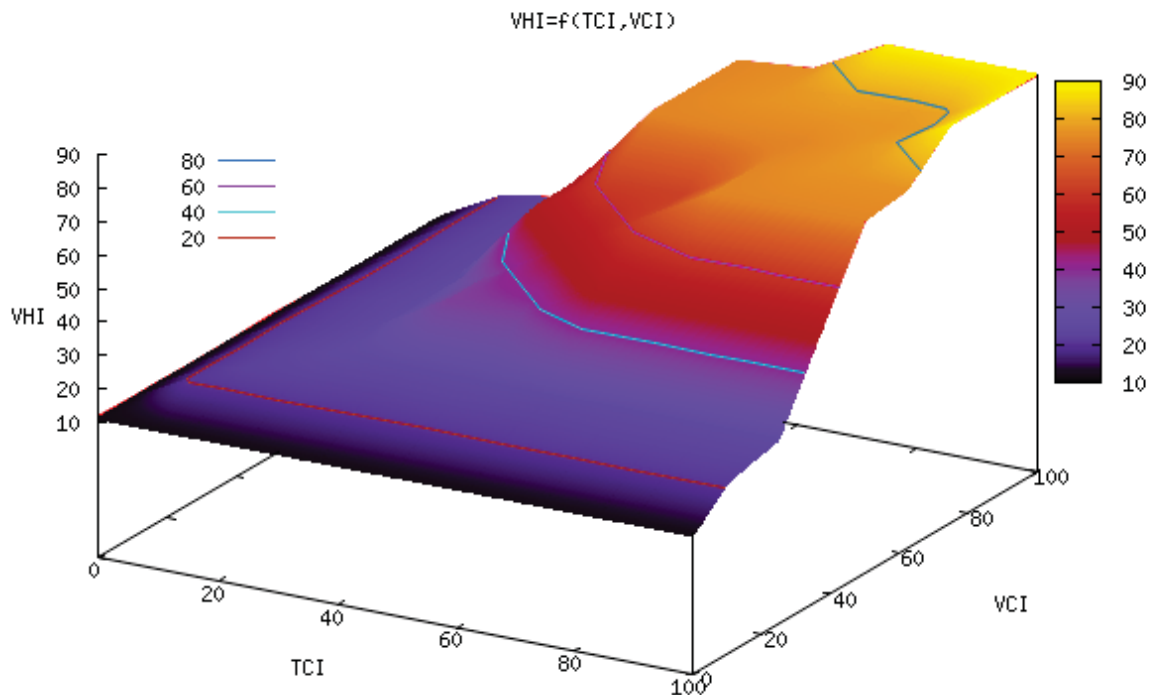


Figure 6.10: Relationship of TCI and VCI in rule base

In relation to VHI and their components, “Law Of Minimum” (LOM) and “Law Of Tolerance” (LOT), are considered for rule-making; in reality, high temperature is an extreme value for vegetation growth and causes drought by increasing evapotranspiration. Consequently, low values of TCI correspond to high temperatures, which are essential in land evaluation, especially evident in low latitude arid lands.

Low value of VCI also relates to low greenness of vegetation in the study period, in other words it shows severely affected areas. Again, considering LOM, the low vegetation condition is a hindrance for productivity and conservation issues. For this reason, experts can determine the importance of lower values, as shown in Table 6.2, in which we have chosen the four rules containing “Low” and “Very low” terms as expert rules. In the event of extreme climatic conditions, such as severe drought, land can become so seriously damaged that normal restoration

takes a long time. When such extremes exceed the critical threshold the damage to land can have severe long-lasting economic and environmental consequences.

Table 6.2 shows expert rules and data-based rules; the latter one is acquired by learning from data based on Wang-Mendel method in Fispro environment. Table 6.3 also shows the rules after simplification.

Table 6.2: Rule base (1) by expert (E=Expert) and Induction Wang-Mendel (I= Induction) after consistency analysis

No.	Type	If TCI	VCI	VHI
1	E		Very Low	Very Low
2	E	Very Low	Not(Very Low)	Very Low
3	E	Low	Low OR Average OR High OR Very High	Low
4	E	Low OR Average OR High OR Very High	Low	Low
5	I	Average	Very High	High
6	I	Average	Average	Average
7	I	High	Average	High
8	I	Very High	Average	High
9	I	High	Very High	Very High
10	I	Average	High	High
11	I	Low	Low	Low
12	I	High	High	High
13	I	Very High	High	Very High

Table 6.3: Rule base (1) after simplification (E=Expert, I= Induction)

No.	Type	If TCI	VCI	VHI
1	E		Very Low	Very Low
2	E	Low	Low OR Average OR High OR Very High	Low
3	E	Low OR Average OR High OR Very High	Low	Low
4	E	Very Low	Not(Very Low)	Very Low
5	I	Average	Average	Average
6	I	High OR Very High	Average	More or Less (High)

According to Figure 6.11, the inference of rule base (RB2) is designed and their rules also brought in Tables (6.4, 6.5, and 6.6); Erosion index and flooding (Q) have positive relationship with desertification, while the values SPI have negative correlation.

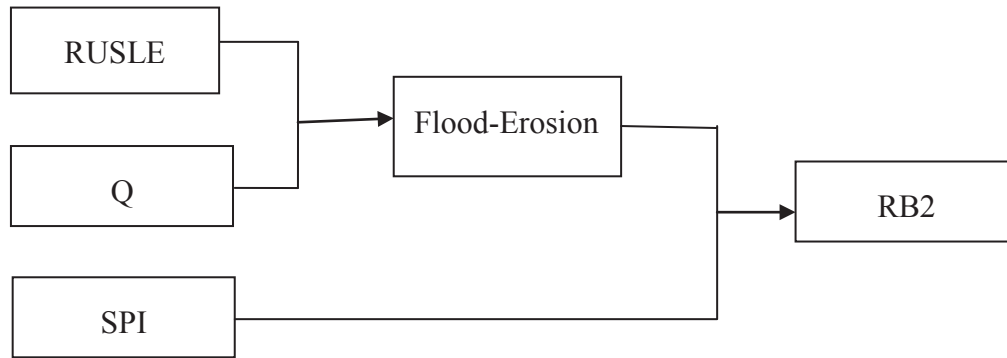


Figure 6.11: Desertification rule bases according to three indicators (Q, RUSLE, and SPI)

Table 6.4: Rules for Flood-Erosion (FE) from erosion index (RUSLE) and flooding (Q)

No.	Type	If RUSLE	Operator	Q	FE
1	E	Low	And	Low	Low
2	E	Average	And	Low	Average
3	E	Low	And	Average	Average
4	E	Average	And	Average	Average
5	E	High	Or	High	High

Table 6.5: Rule base (RB2) for Flood-Erosion (FE) and SPI

No.	Type	If SPI	Operator	FE	RB2
1	E	Dry	Or	High	High
2	E	Wet	And	Low	Low
3	E	Wet	And	Average	Average

Table 6.6: The final Rule base (RB)

No.	Type	If RB1(VHI)	Operator	RB2	Desertification
1	E	Very Low			Very Severe
2	E	Low			Severe
3	E	Average OR High OR Very High	And	High	High
4	I	Average	And	Average OR Low	Severe
5	I	High	And	Low	Low

6.2.4 Step IV - Defuzzification and Output

The fourth stage is to map the fuzzy layers into crisp values to determine a final desertification map as output. In this stage, aggregation operators such as maximum for accumulation and the Centre of Gravity (CoG) to overall input are used, and all fuzzy rules outputs are converted to a crisp (numerical) layer to represent the overall vulnerability map. For a linguistic variable output in desertification, five fuzzy terms are defined, as shown in Figure 6.12.

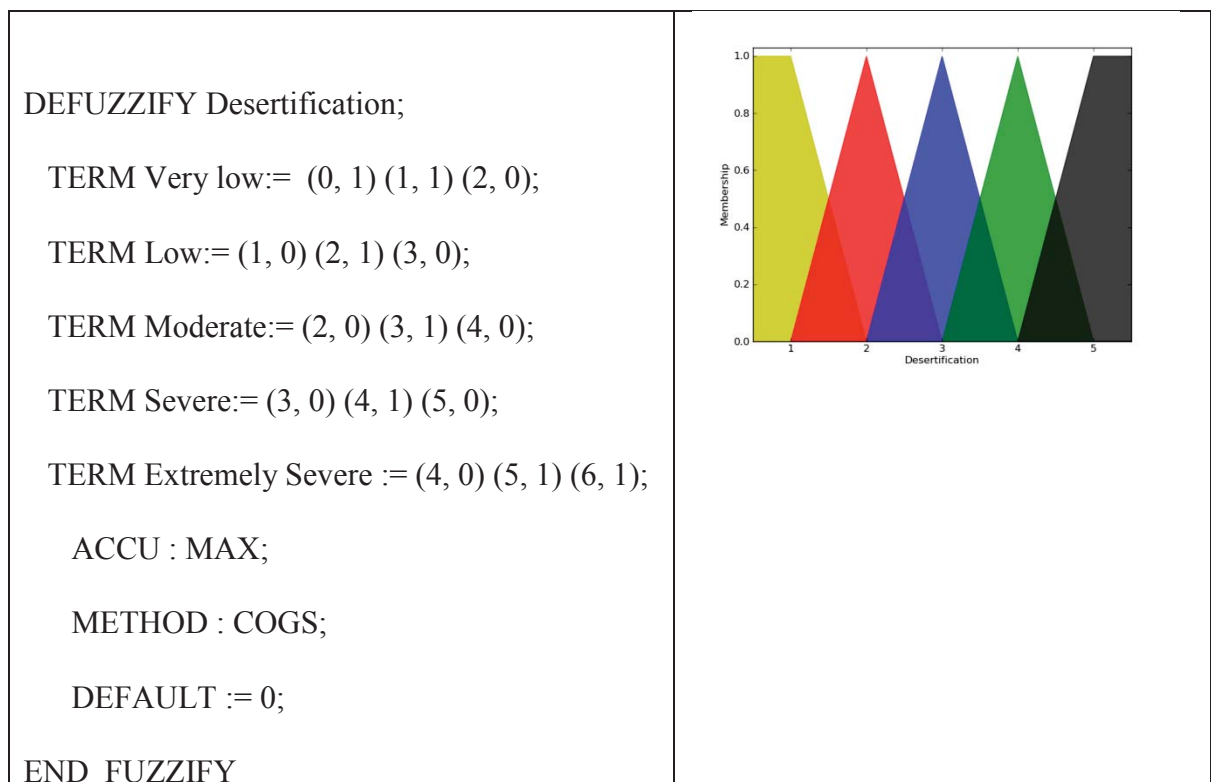


Figure 6.12: Membership function for output with five linguistic terms

In this stage, the layers calculated in the defuzzification stage are represented in two approaches: firstly, for each of the fuzzy sets in a desertification variable, a fuzzy map was designed; and in the second approach of accumulation and defuzzification, only one output is presented.

6.3 Fuzzy Map

Frequently in natural phenomena several factors simultaneously influence the cause of the events, therefore, their variations relate to the affective factors, and the degree of influence; however, each factor is also uncertain. Additionally, there is no sharp and discrete boundary between classes when each factor is classified into separate classes (Jang et al. 1997).

Fuzzy modelling uses linguistic variables and fuzzy sets (adjectives), as shown in Figure 6.13. Because of uncertainty in the value of each pixel, every determined fuzzy set might be validated, according to the membership function. In other words, in susceptibility maps like the desertification map, each pixel shares some characteristics of validity according to severity classes. Depending on the position of the pixel value in membership functions, there will be a degree of overlap in the membership of other fuzzy sets. For example, a pixel with fuzzy term “High” in the desertification map may also have some degree value in other fuzzy term sets, such as “Very High”, “High”, “Moderate”, and even “Low”. Therefore in GIS, according to the fuzzy model, the severity map of each fuzzy set can be shown as a map corresponding to the defined fuzzy sets of the output variable, as shown in Figure 6.14.

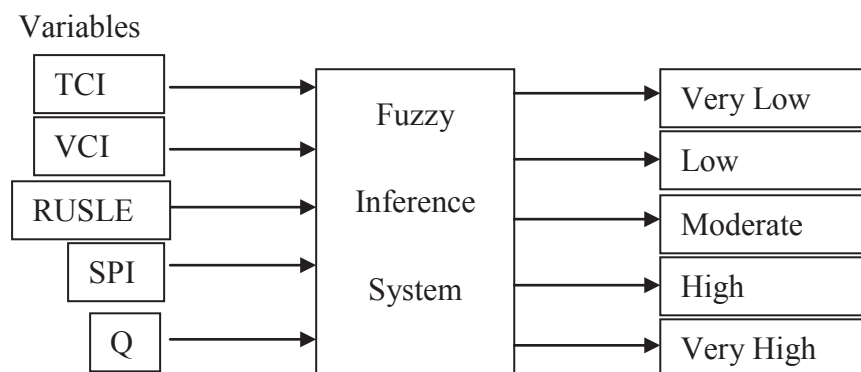


Figure 6.13: Fuzzy model with multiple fuzzy outputs

Figure 6.14 represents the final fuzzy map of the study area, with four maps of fuzzy sets including Low, Moderate, High, and Very High.

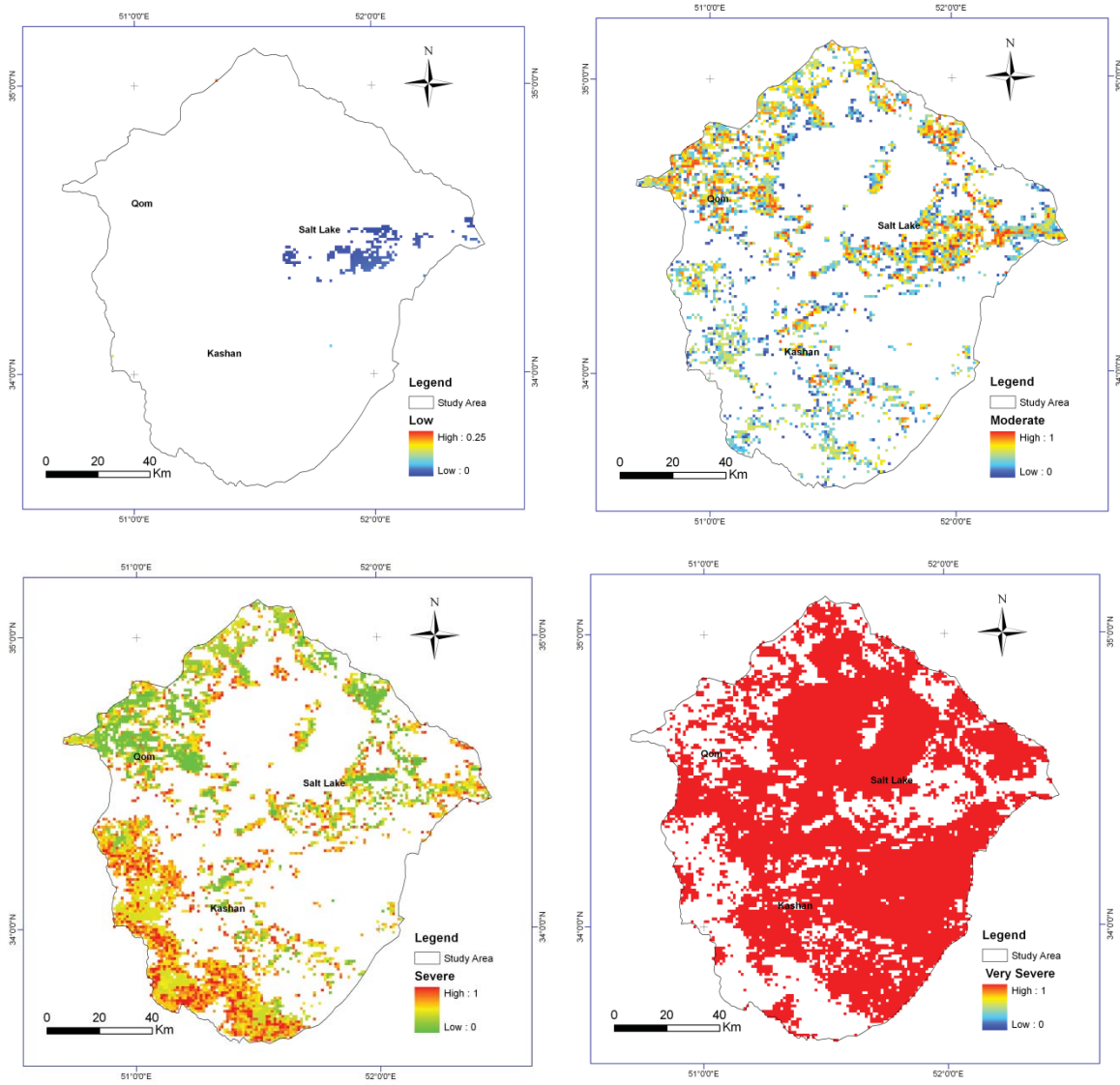


Figure 6.14: Different layouts of fuzzy model of desertification map according to the fuzzy sets

Chapter 7

Conclusion and Recommendations

7.1 Introduction

The Qom-Kashan region is one of the driest areas in central Iran, where, except on the margins of the region, the land is made up of desert. In a swathe of land between mountainous regions and the most affected areas (salt crust and sand dunes), there are some croplands, supported by artificial irrigation systems. In the plain areas, there is sparse vegetation, which is used as pastureland.

In the study area, erosion and drought are the two most active causes of desertification, exacerbated by a growing population and overgrazing. Therefore, the areas near the residential areas are under greater pressure. Additionally, in the study area, there are two land covers: salt crust and sand dunes, which are indexed as extremely severe desertification, deprived of vegetation - so that the former is covered with salt, while the latter is covered with sand, where wind erosion is prevalent.

Studies in geosciences, such as the development of desert features and the phenomenon of desertification, are interdisciplinary, and contribute to other scientific researches in geology, hydrology, and soil science, where each has its own perspective in the study of the desertification process.

Remote sensing is a versatile tool in the investigation of desertification, where satellite images play a key role in the assessment of climatology and geological processes, as well as the study of dryland features. Therefore, digital satellite images, based on reflective and thermal spectra, help recognise the effective factors and their severities in desertification.

In this chapter, the temporal and spatial variations of these variables are examined, in order to acquire enough knowledge of the relevant factors in desertification, and the findings based on spatial analysis and image processing of digital data are discussed.

7.2 Vegetation Indicators and Drought

There is a specific interaction between the condition of vegetation and rainfall. In rainy seasons, the vegetation conditions are favourable; however, there is a time lag in the plant response to rainfall (Schmidt and Karnieli 2000), which is also controlled by soil type. In the use of NDVI, in drought studies, it has been proved that there is a time lag between the onset of drought and its effect on the vegetation index. In order to interpret the interaction of NDVI and precipitation, the study needed to consider a soil's capacity for holding water; because sandy soils are drier they hold less water (Thenkabail et al. 2004).

In the study area, green vegetation exists only in the margins of wetlands, mountain fronts and on the banks of seasonal streams. Because of the artificial irrigation in croplands and artificial forest areas (haloxylon and tamarisk), NDVI variations are also significant. In the westward submontane regions, owing to the west rainy currents, the values of NDVI are high (Figure 7.1).

In order to analyze the vegetation trends, we have taken samples from five geomorphologic units, including the vegetation area (croplands), wetlands (two types; very wet and rarely wet), sand dunes, alluvial fans, rocks (high lands). The time series of monthly spatial average NDVI is plotted in Figure 7.1, in the ten-year period from 2000 to 2009.

NDVI values increase from January until May following rainfall, then, because of aridity, the greenness of vegetation decreases. A maximum value of NDVI shows healthy crops and orchards, and artificial forestlands (mainly in the foothills of mountainous regions near Kashan and Qom) where water is provided by deep subterranean wells or Qanats. The positive values of NDVI relate

to dense, healthy orchards and crops; the NDVI values for vegetation are more than 0.2, while the land surface with NDVI of zero represents bare soils.

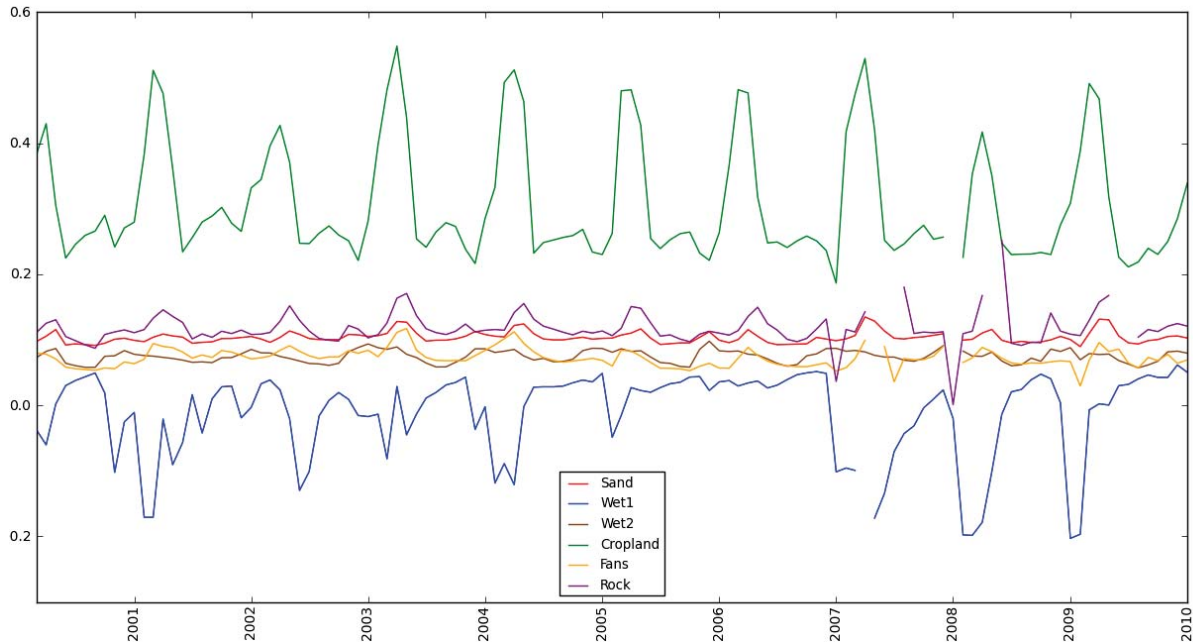


Figure 7.1: The monthly mean NDVI in land cover (2000-2009)

The water bodies and the salt crust in the Salt Lake have negative NDVI values. The negative NDVI values indicate the existence of water or wetlands, especially in the rainy seasons. Wet areas in the playa in January and February show the lowest NDVI in the lowest parts of the wet playa, which is relevant to water. The NDVI values for the very wet area (wet1) are markedly negative. The lowest values of NDVI in spring are undoubtedly linked to the existence of water and the rising of groundwater table.

Because of low-density vegetation, the tamarisk areas have low-NDVI values; however, the extensive natural tamarisk forest can be detected in the north-western parts of Qom Lake, especially on riverbanks.

For immobile sand dunes, the NDVI values are approximately zero. Therefore, the corresponding NDVI pixels around the zero value represent soil, salt crust, and sand dune. Therefore, in the study area, the value of NDVI is low, due to vast-bare lands with sparse vegetation; this condition also affects the VCI trend.

Vegetation Condition Index (VCI) as a function of NDVI is the confirmation indicator to show the deviation of vegetation healthiness in a normal year. In this regard, VCI is derived from the normalization of the NDVI index. When ecological impacts are lessened or eliminated, the VCI trends reflect only the healthy well-being of vegetation.

The findings by Shamsipour (2005) in the Kashan area, based on AVHRR data, showed that the year 2000 experienced the severest drought. In the same year was recorded a high variation in the spatial distribution. The findings also showed that VCI values increased significantly during relative wet years from 2001 to 2004, especially in croplands and planted forest, but VCI values in barren lands were low.

The spatial distribution of VCI values is presented in Figure 7.2. As most of the plants in the study area exist in tension conditions, VCI values are “very low” in the south-eastern region; noticeably, VCI values around residential areas are also very low.

Figure 7.2 shows the mean values of VCI in various land units. In this regard, values of VCI in sand dunes, alluvial fans, croplands, and mountains are lower than 50; there are “very severe” class (0-20) and “severe class” (20-40) of desertification. However the mean value of VCI for wetlands and the salt lakes is more than 50.

In sand dunes, there are many limitations for vegetation, as follows: (1) Land Surface Temperature (LST) is also hot. (2) The rate of wind erosion is high. So land is devoid of vegetation, as a result, the value of VCI is very low (<15) indicating extreme degradation in this area. In hills and alluvial fans, water erosion, coupled with wind erosion, hinders the development of stable vegetation; therefore, these areas are also predominantly of low VCI value. Despite high wind erosion in the plain areas, these areas have a moderate value of VCI, which relates to the interaction of land surface and the low value of NDVI. Regarding severe conditions in saline wetlands, with very little vegetation cover, VCI trends show only the stable condition for the considered period (Figure 7.2).

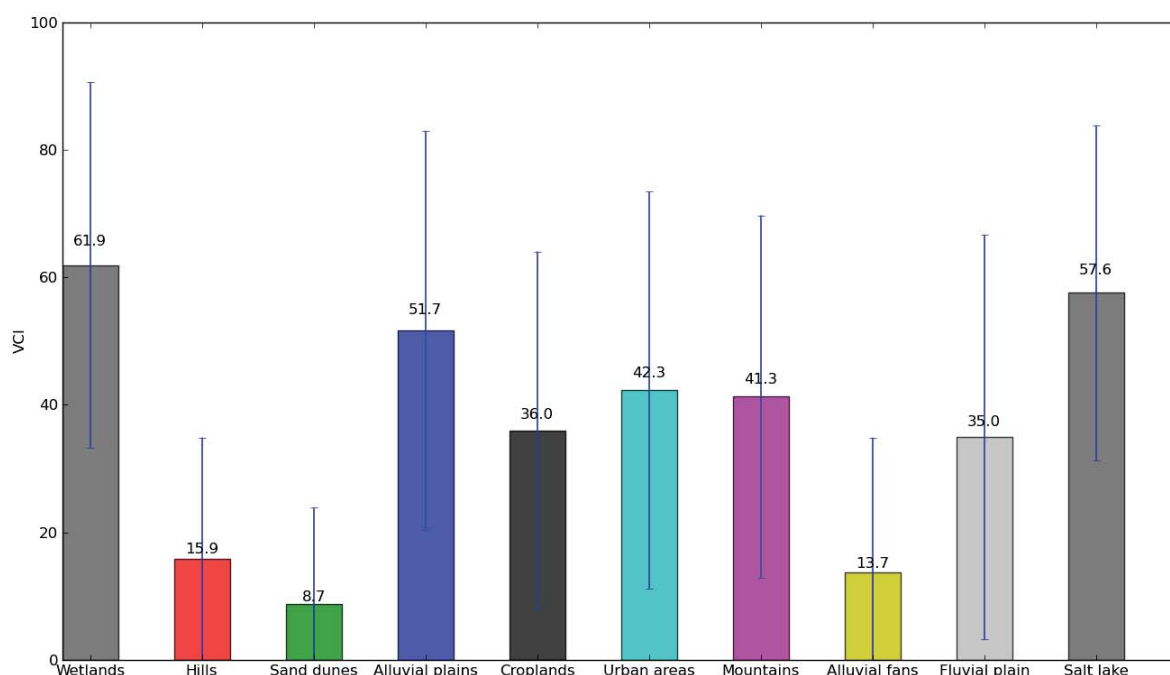


Figure 7.2: VCI variation over land units: vertical blue lines shows the standard deviation of VCI

Table 7.1: the average of VCI value in land units (2006)

Land use	Very severe	Severe	Medium	High	Very high
Alluvial fans	74	13	7	3	2
Alluvial plains	21	17	21	19	23
Croplands	36	22	20	14	8
Fluvial Plain	40	17	17	12	13
Hills	71	18	6	3	1
Mountains	29	20	24	17	10
Salt lake	5	23	30	18	24
Sand dunes	82	12	3	1	1
Urban areas	33	15	20	18	14
Wetlands	11	10	24	24	31

Table 7.1 includes the average value of VCI in 2006. In the sand fields, VCI value is so severe that 82 percent of the area is in the “very severe” class, and only 12 percent of the area is in the “severe” class (Table 7.1). The “very severe” class covers 74 percent of the alluvial fan region and 71 percent of hills. Therefore, according to VCI, sand dunes, alluvial fan, and hills are considered as “very severe” desertification.

7.2.1 Land Surface Temperature (LST) Condition

In the study area, the variation of land surface temperature (LST) over different land features such as plains, wetland, sand field, cropland, alluvial fan and rock, is plotted in Figure 7.3. According to the time series of temperature in Figure 7.3, the study area experiences high escalations in temperature. Even though there are differences between land surface temperature and air temperature in different land covers, the lowest values of land surface temperature occur in months with low air temperature. Therefore, December and January are the coldest months, whereas June and August are the warmest months. The month of January in 2008, having an extreme low temperature, is an exceptional event.

The times series in Figure 7.3 also shows that wetlands have the lowest temperature (the blue line); despite the high air temperature in wetlands and playas, because of moisture, LST (brightness temperature) is low. This fact is instructive in identifying and detecting playa and wetlands. In addition to moisture contents, albedo also controls the surface temperature in salt crusts such as Qom Lake. In this area albedo is high; therefore, land surface temperature is low. In recent years, high variations in salt lake areas, which relate to low water inputs and the high concentration of salts, means a high occurrence of drought. Nevertheless, the spatial distribution of surface temperature in playas is relatively uniform, because of homogeneous salt crust. The water contents of plants also affects the surface temperature of the vegetated area, however, the average temperature in croplands (the green line) is higher than in wetlands.

The features in low-level plains such as sand dunes (red line) and alluvial fans have the highest temperature values among the features in the study area (Figure 7.3); hence, they are hot spots. The characteristics of material in land also influence land surface temperature. For instance, as sand has high quartz content and low specific heat capacity, its temperature fluctuates between extremely high and extremely low. Therefore, sand dunes have high temperature during the day. In remote sensing studies, the thermal spectral characteristic of sand dunes is a leading factor for the monitoring of sand movement as well as its surface condition.

The colour of the surface also controls the value of surface temperature. As the process of oxidation makes the outer layer of surface gravel darker in alluvial fans and desert pavement, land surface temperature is high.

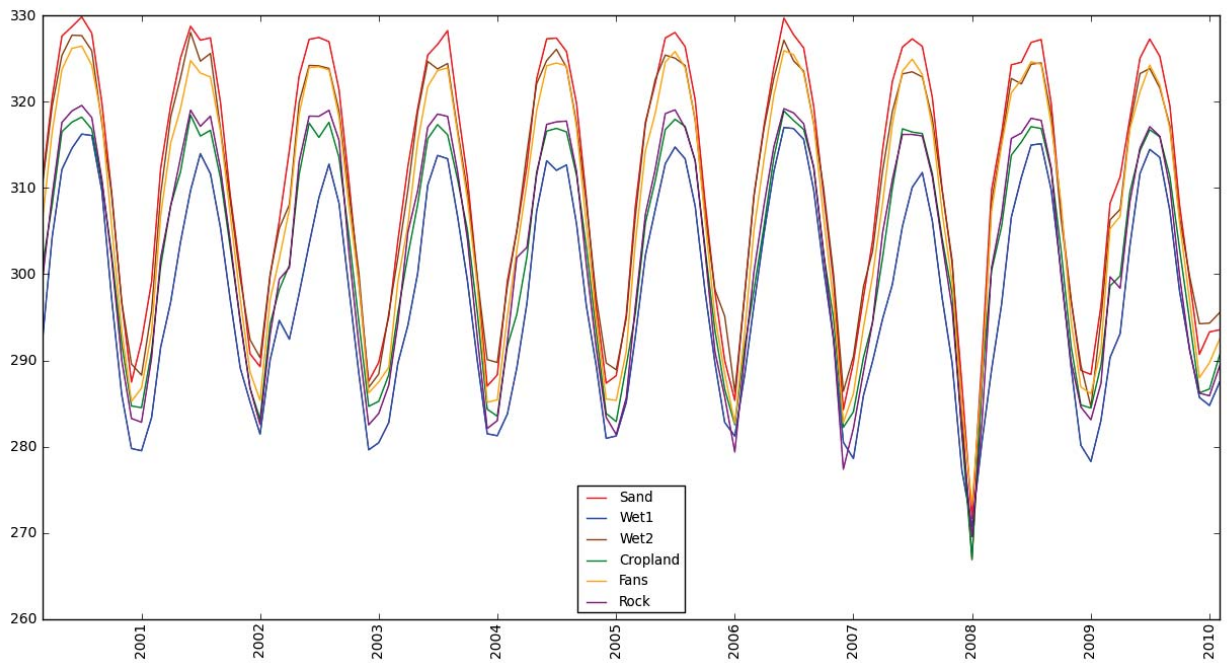


Figure 7.3: The trend of LST in different classes, in the study area, between 2000 and 2009.

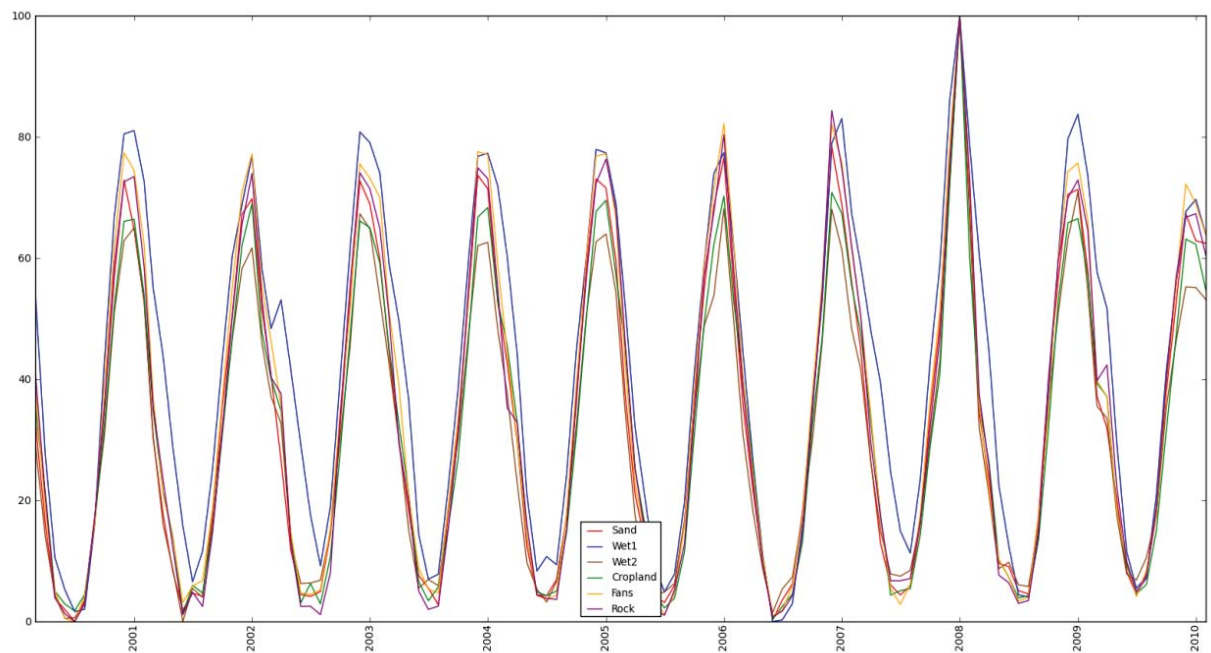


Figure 7.4: The trend of TCI between 2000 and 2009 according to different classes in the study area.

The topography of mountainous regions plays a significant role in the receiving of sunlight, and eventually controls land surface temperatures (LST); consequently, the inhomogeneous areas have varying temperature. As temperature declines dependently on altitude, temperature is low in the

highlands. For instance, the south-west part of the study area has moderate TCI, which are shown in Figure 7.4 and 7.5. As TCI is the deviation of temperature from the highest temperature, its trend is opposite to LST; the low values occur in high temperature, in summer.

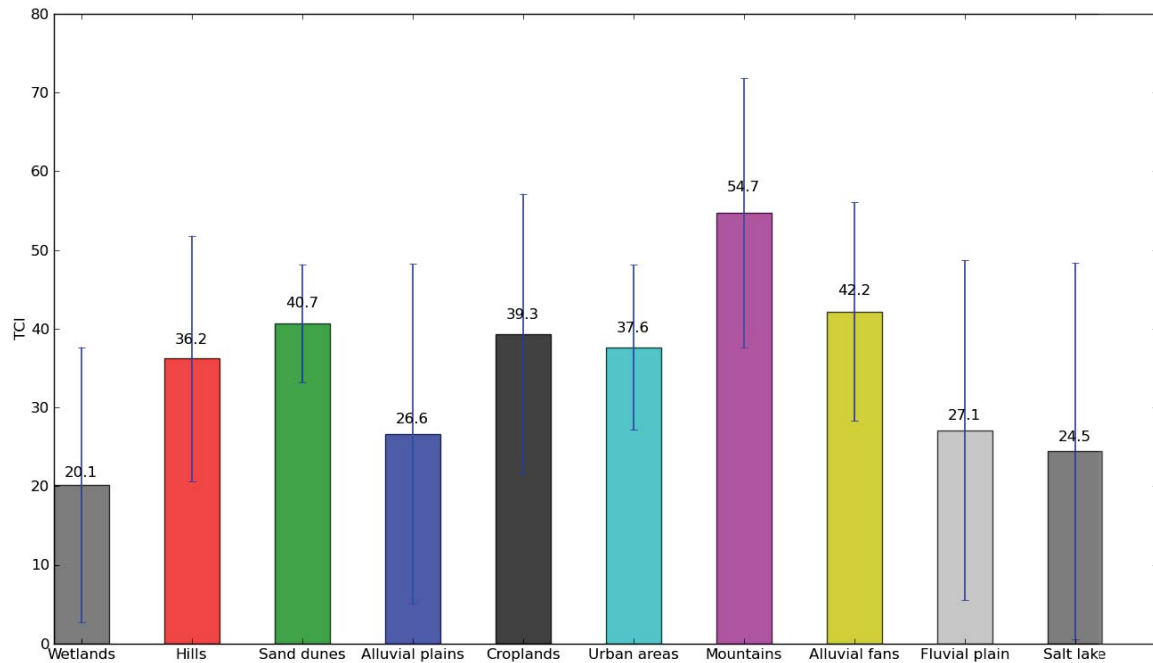


Figure 7.5: Mean of TCI in land units of the study area (2006); vertical blue lines shows standard deviation

TCI intensity in 2006 is divided into five classifications: “very severe”; (0-20), “severe”; (20-40), “moderate”; (40-60), “high”; (60-80), and “very high”; (80-100), and then mean values of TCI in each land unit are plotted in Figure 7.5, and their percentage values also are given in Table 7.2.

According to Table 7.2, TCI classes of “very severe” and “severe” cover more than 50 percent of the land units such as wetlands, salt lakes, alluvial plains, fluvial plains, croplands, and hills. However, these two classes of TCI, “very severe” and “severe”, in mountainous regions, sand dunes, and alluvial fans contain lower than 50 percent of each of the land units.

Contrary to Vegetation Condition Index (VCI), Thermal Condition Index (TCI) in wetlands and salt lakes is low. The major parts of the study area have a low value of TCI, especially wetlands, salt lakes, alluvial fans, and fluvial plains which have TCI values lower than 30 (Figure 7.5).

Table 7.2: The percentage of TCI classes in land units of the study area (2006)

	Very severe	Severe	Medium	High	Very High
Alluvial fans	8	31	55	6	
Alluvial plains	44	24	26	5	1
Croplands	9	51	27	9	4
Fluvial Plain	44	22	28	5	
Hills	18	38	40	4	
Mountains	3	18	36	40	3
Salt lake	50	21	21	8	1
Sand dunes	2	37	61		
Urban areas	6	46	47		
Wetlands	56	28	15	2	

7.2.2 Vegetation Health Index (VHI) Analysis

In order to evaluate the proposed model and explain evidences between TCI and VCI indices, the time series of these indices with precipitation is shown in Figure 7.6. The spatial distribution of precipitation was interpolated from the monthly precipitation point data in meteorological station. The spatial mean of each temporal layer was used for the comparison. The time series of the indices is brought with histograms, which is illustrated in Figure 7.6. As a result, the land surface humidity is affected by precipitation, and then the mean monthly TCI trend follows the (mean monthly) precipitation events. Despite of being sparsely vegetated and relatively highly extent of bare lands in the study area, the VCI trend also is affected by precipitation. Therefore, this shows lag time response between VCI and rainfall. The highest values occur after the end of cold season, that is, the growing of plant occurs in rainy period till the beginning of warm period. In croplands irrigation also might affect the values of VCI during the summer season.

Temperature Condition Index (TCI) and Vegetation Condition Index (VCI) have a positive association with vegetation health, in other words, TCI and VCI show thermal and drought influences over plants. Healthy vegetation is found in places with the high values of VCI and TCI; while the low values of VCI and TCI are in the places where water deficiency or thermal pressure effects vegetation. In fact, high or low thermal conditions affect vegetation in arid land. Although during January and February, water is available, there is a decline in the VCI index of the study area, because of low temperature.

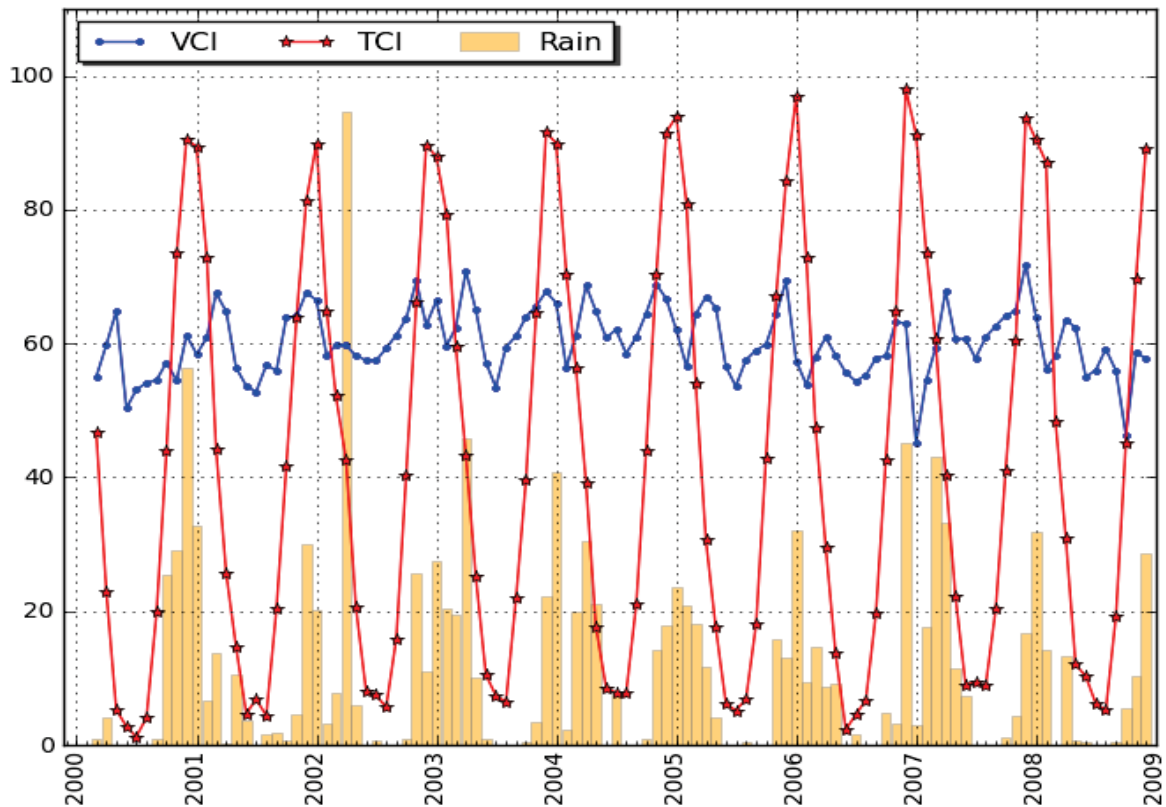


Figure 7.6: Time series of spatial mean monthly VCI, TCI, and precipitation in the study area between 2000/3 to 2008/12.

7.2.3 Standardised Precipitation Index (SPI) Analysis

Standardised Precipitation Index (SPI) is a method that uses precipitation data to determine drought or wet events in different timescales. Positive values show wet years, and negative values indicate dry years. SPI is not only useful in determining the temporal and spatial extent of drought, but is also helpful in finding the onset and severity of drought.

Precipitation deficiency has different effects on groundwater, soil moisture and river currents. In this regard, 1 and 3 months long timescales of SPI show short-term drought that only affects soil (agricultural drought). There is a significant relationship between NDVI and SPI during a growing season; the 3-monthly timescale of SPI correlated with NDVI. Therefore, the 3-month SPI indicates the agricultural drought. As a result, SPI is a useful indicator to record the time lag between drought and vegetation response (McKee et al. 1993; Ji and Peters 2003).

While the 6 and 12 long month timescales of SPI indicate the medium period that influences stream and river currents, reservoir levels and even groundwater levels. Meanwhile, the 12 and 24 months long timescales of SPI, which maps long-term drought, are linked to groundwater levels over longer timescales. Since a long drought reduces groundwater and increases the sensitivity of land, it causes desertification (Boken et al. 2005).

The 38-year long-term meteorological data (1967-2008) are applied to estimate the Standardised Precipitation Index (SPI) for the meteorological station in Kashan. The time series of SPI for the different scales is shown in Figure 7.7. The frequencies for dry conditions are tabulated in Table 7.3. According to this table, the number of drought events is increasing.

According to Table 7.3, SPI in Kashan meteorology station shows that more than 55 percent of the measured months has “near normal” drought conditions including “mild wet” and “mild dry” conditions, within one unit of standard deviation. There is no “extremely dry” drought in a one-month period (SPI 1) - on the contrary, no “extremely wet” condition is recorded in this scale. These trends also reveal that dryness increases by the length of period, so that the frequency of a “severely dry” month in the 24-monthly timescale of SPI is about 8.1 percent, and the frequency of a “moderately dry” month in a 12-month timescale reaches 14.6 percent (Figure 7.7). In fact, the distribution of drought events in the Kashan station shows that the region has been experiencing long and more intensive periods of drought.

The lowest 24-month drought intensity in Kashan occurred in January 1986, with a value of -2.79. The longest drought, which began in 1988 and ended in 1992, was followed by the wettest years for approximately two years (Figure 7.7).

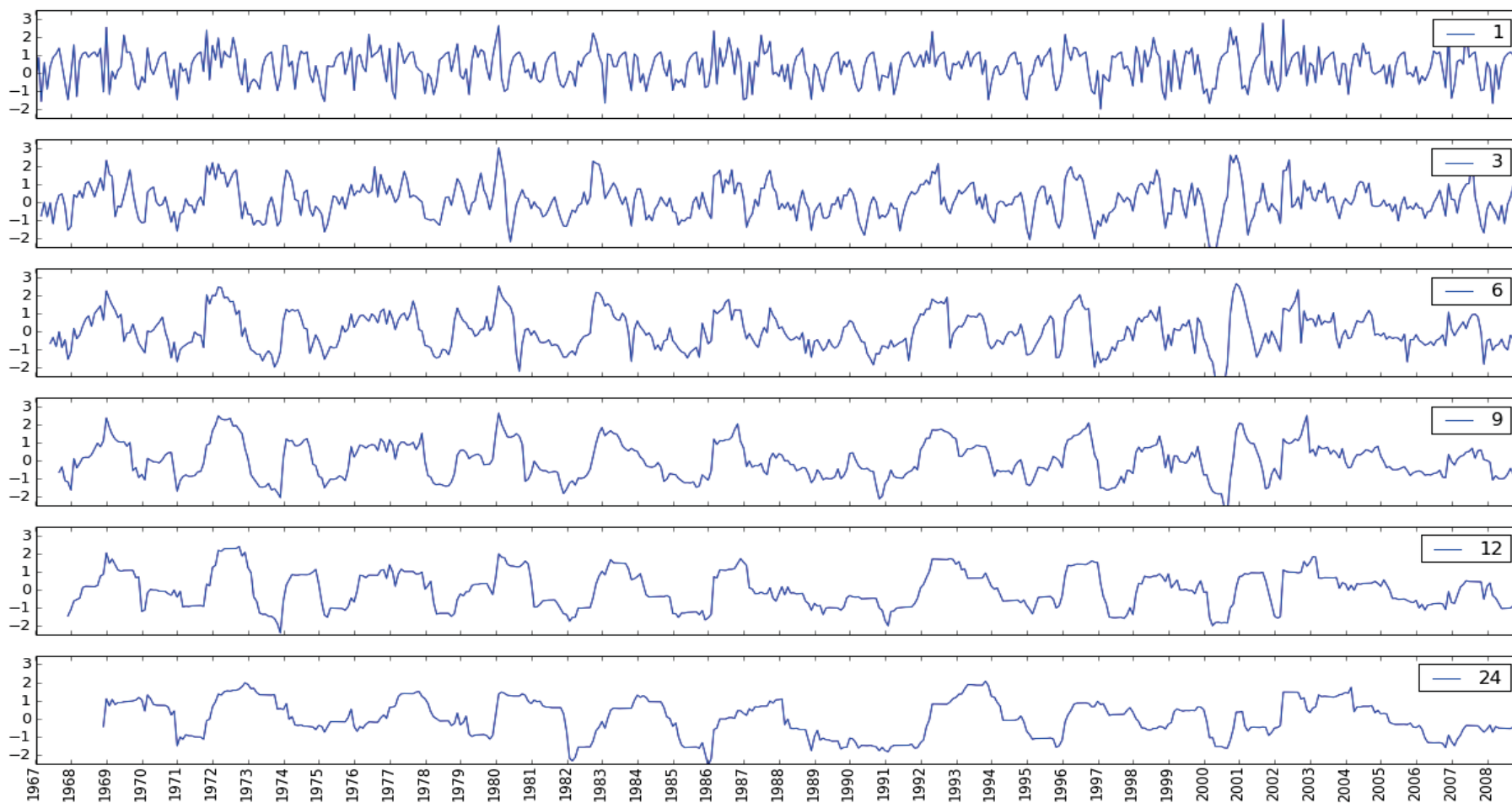


Figure 7.7: The diagrams of Standardised Precipitation Index (SPI) for Kashan meteorology station, from top to bottom for 1, 3, 6, 9, 12, and 24-monthly timescale periods, respectively, from 1967 to 2008.

Table 7.3: Drought frequency recorded by Kashan meteorology station, from 1967 to 2008

Drought Category	1 Month SPI	3 Month SPI	6 Month SPI	9 Month SPI	12 Month SPI	24 Month SPI
Mild (0 to -1)	130	177	185	171	154	146
Moderate(-1 to -1.49)	32	44	57	61	72	55
Severe (-1.5 to -1.99)	6	10	18	20	24	39
Extremely severe (< -2)	-	6	5	4	3	5

In 2000, severe drought occurred with the lowest values of SPI intensity for three, nine, and twelve-monthly timescale periods (with all values approximately -2.7); hence, this particular year is the most recently severe drought experienced in the Kashan region, which corresponds to the agricultural and hydrological drought categories.

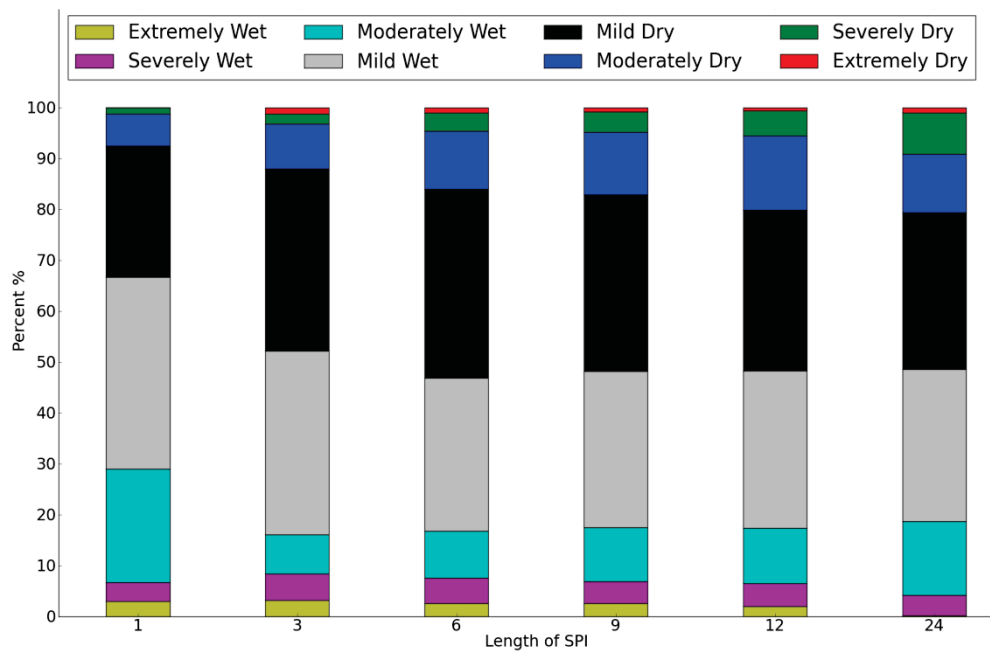


Figure 7.8: SPI frequency for the Kashan meteorology station

Results have also shown that recent droughts tend towards higher intensity and over longer periods. Given the increasing demand for water in agriculture and industry, amongst a growing population, incidence of drought will prove to be extremely costly. Shamsipour (2005) also applied a simple normalized model (Z) to study drought in the Kashan regions, also concluded that the years 2000 and 2001 were dry years.

7.3 The Extent and Severity of Desertification

The land cover units are classified into mountain, hill, plain, cropland, alluvial fan, wetland, salt crust, and sand dune (Figure 4.5 in Chapter 4), which are used as a base map. Considering the criteria mentioned in Tables 5.9, 5.10, 5.11, and 5.12, the severity map of desertification is estimated in the study area, where “moderate”, “severe”, and “very severe” desertification are 1,661 (10 percent), 6,268 (40 percent), and 8,010 (50 percent) square kilometres, respectively. The desertification map of the study area is illustrated in Figure 5.11, which shows the area of the study dominated by “severe” and “very severe” classes of desertification, which are the affected areas such as wetlands, salt crusts, sand dunes and sparsely-vegetated areas.

According to Figure 5.11, the high salinity of soil, harsh climate, and the rise of groundwater levels account for the high severity and susceptibility in playa, salt crust, and wetlands. In the study area, wind erosion is also a major problem, due to the sensitivity of soil to wind erosion and the low holding capacity of soil. Croplands in plain areas, especially near populated areas, have been given a relatively moderate degree of severity, helped by artificial irrigation and some positive land management. In mountainous regions, water erosion is high with harsh occurrences - so these areas are allocated “severe” class.

The severely affected area, which has exhausted vegetation and harsh thermal conditions, constitutes more than half of the study region; therefore, according to Table 7.5, 70-90 percent of the study area experiences moderate desertification and severe desertification. A small portion of the area severely affected by erosion and flooding, accounts for about 10 percent, while moderate flooding impacts on 54.4 percent of the study area.

Table 7.4: Percentage of affected area according to Erosion (RUSLE), flooding (Q), drought (SPI), Vegetation Condition Index (VCI), and Thermal Condition Index (TCI)

Criteria	Class	Area (sq km)	Percent
SPI	Wet	7458	46.8
	Dry	8479	53.2
RUSLE	Low	13283	83.6
	Moderate	861	5.4
	Severe	1738	10.9
Q	Low	5242	32.9
	Moderate	8667	54.4
	Severe	2026	12.7
VCI	Severe	8812	55.3
	Moderate	2861	18
	Good	4253	26.7
TCI	Severe	8348	52.4
	Moderate	5570	35
	Good	2010	12.6

The statistical result of this study, based on fuzzy modelling according to chapter six, shows the severity of desertification in Table 7.5 and Figure 7.9. Almost all the area is subject to desertification, mainly through the vegetation and environmental degradation process, where 83.4 percent of the study area is affected severely (high) and very severely (very high) by desertification. This clearly demonstrates that the majority of the study area is under threat of extremely severe desertification, which covers 65.8 of the study area (Figure 7.10).

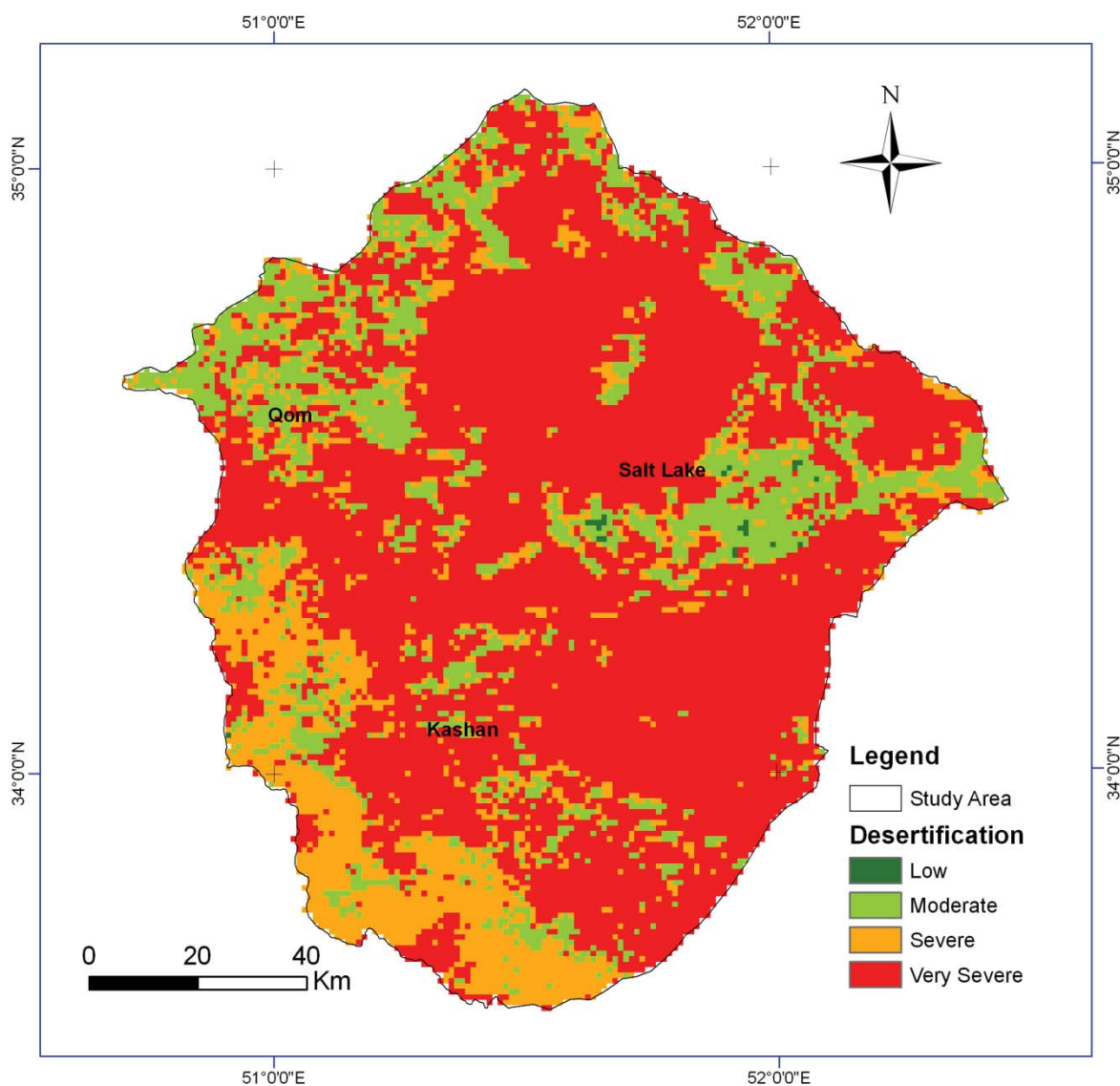


Figure 7.9: Desertification map based on fuzzy modelling

Table 7.5: Severity of desertification based on fuzzy modelling

Class	Low	Moderate	Severe	Very Severe
Area (sq km)	24	2621	2805	10476
Percent	0.2	16.5	17.6	65.8

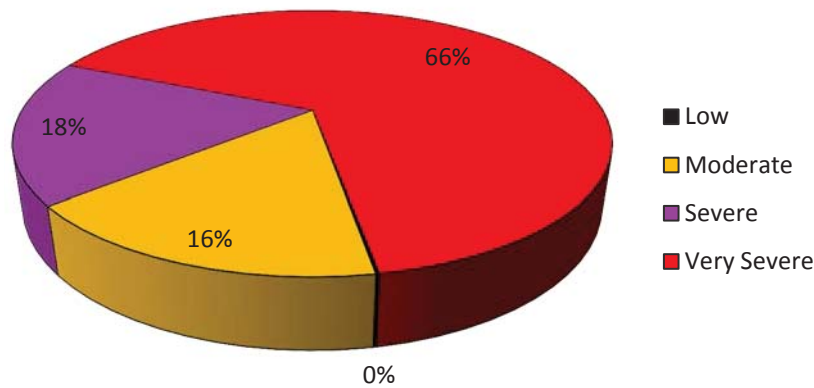


Figure 7.10: Desertification percentage based on fuzzy modelling

According to the result of fuzzy modelling, as shown in Figure 7.10, the “low” severity of desertification covers a small part of the study area, while the severity classes of “severe” and “very severe” are the prevalent classes in the study area. So that, except in the mountainous regions, the majority of severity classes in the study area are ranked “very severe”, in regard to desertification. As shown in Table 7.6, the “very severe” class consists mainly of sand dune, i.e. 90.6 percent. The occurrence of other land features in the “very severe” class is also high, where percentages of land units such as hill, alluvial fans, and fluvial plains are 83.1, 82.1, and 76.2, respectively.

Although Qum Lake is covered with salt crust, which is typical desert, two classes of “severe” and “very severe” desertification cover 70 percent of this land unit: “very severe” desertification is 60.9 percent and “severe” desertification is 9.1 percent. “Severe” desertification in the mountainous regions is the main type of desertification, but when considering the two classes of desertification (severe and very severe) as one class, the sum of these two classes amounts to 87.9 percent overall. This shows how much of the mountainous regions are under threat of “severe” and “very severe” desertification. According to the severity classes of desertification, only 50.6 percent of cropland has “very severe” desertification, but “severe” class and moderate” classes are 21 percent and 28.4 percent, respectively. Again, the sum of the two classes of “severe” and “very severe” desertification reaches 71.9 percent (Table 7.6).

Table 7.6: The percentages of desertification severity in land units of the study area

		Desertification Severity Classes			
		Low	Moderate	Severe	Very Severe
Land units	Alluvial fans	0.0	10.7	7.2	82.1
	Alluvial Plains	0.0	19.0	8.9	72.1
	Croplands	0.0	28.4	21.0	50.6
	Fluvial Plain	0.0	13.1	10.7	76.2
	Hills	0.0	5.6	11.3	83.1
	Mountains	0.0	11.3	52.9	35.8
	Salt Lake	1.2	28.8	9.1	60.9
	Sand dunes	0.0	3.5	5.9	90.6
	Wetlands	0.0	17.8	8.0	74.2

7.4 Accuracy Evaluation of the Desertification Map

The overall accuracy of the FOA-based model, in referring to the reference map, is about 73.3 percent, and the Kappa coefficient, K_{hat} , is also about 0.52, while the measured overall accuracy for the fuzzy model is about 61 percent, and K_{hat} is also around 0.25. According to Koutroumpas et al. (2010), K_{hat} is “moderate” for FOA-based models and “fair” for fuzzy models.

The commission error for the “very severe” class is low; that is, 10 percent in the FAO-based model and 28.4 percent in fuzzy model, while the commission error of the “moderate” class in two models is very high. Approximately 66 percent of samples of the “moderate” class are brought from other classes in the FAO-based model, whereas its value is 87.1 percent in fuzzy modelling. In contrast to the commission error, the user’s accuracy of two models is low; its value in the FAO-based model and the fuzzy model is 34 percent and 12.9 percent, respectively.

In contrast, as shown in Table 7.7 and Table 7.8, the omission error, as with commission error, is also low in two models of the “very severe” class; explicitly, its value reaches 25.4 percent and 23.2 percent in FAO-based model and fuzzy modelling, respectively.

Omission errors in the “moderate” and “severe” classes of the FAO-based model are significantly lower than in the fuzzy model. According to Table 7.7 and Table 7.8, they are 26.1 percent and 29.6 percent in “moderate” and “severe” classes in the desertification map, derived

from the FAO model, respectively. Omission errors in the “moderate” and “severe” classes of the fuzzy model are 65.2 percent and 63 percent, respectively.

Table 7.7: Confusion matrix result of the FAO model; errors and accuracies are shown in percent

		Reference map					
		<i>Moderate</i>	<i>Severe</i>	<i>Very Severe</i>	Total	User's Accuracy	Error of Commission
Result of FAO Model	<i>Moderate</i>	17	21	12	50	34.0	66.0
	<i>Severe</i>	1	88	52	141	62.4	37.6
	<i>Very Severe</i>	5	16	188	209	90.0	10.0
	Total	23	125	252	400		
	Producer's Accuracy	73.9	70.4	74.6			
	Error of Omission	26.1	29.6	25.4			

Table 7.8: Confusion matrix result of the fuzzy model; errors and accuracies are shown in percent

		Reference map					
		<i>Moderate</i>	<i>Severe</i>	<i>Very Severe</i>	Total	User's Accuracy	Error of Commission
Result of Fuzzy Model	<i>Moderate</i>	8	12	42	62	12.9	87.1
	<i>Severe</i>	4	44	16	64	68.8	31.3
	<i>Very Severe</i>	11	65	192	268	71.6	28.4
	Total	23	121	250	394		
	Producer's Accuracy	34.8	36.4	76.8			
	Error of Omission	65.2	63.6	23.2			

7.5 Conclusion

According to field trip analysis and the visual interpretation of satellite images, most of the study area is confronted with severe or very severe desertification, a fact also confirmed by the statistically computerized models, such as GIS-integrated fuzzy models and the traditional FOA-based model in this project. The “very severe” class of desertification, being the most predominant

type of desertification in the study area, reaches 65.8 percent of the area according to the fuzzy model.

The results of thermal and spectral properties, particularly TCI and VCI, also show the advantages of these data in the evaluation of desertification as a dynamic phenomenon. TCI and VCI represent the variations in the wetness of the surface area and the greenness of vegetation. As a result, the fuzzy model derived from these parameters also confirms this information.

Nonetheless, as shown in this project, satellite images play a significant role and are effective in the diagnosis of land features as well as the phenomena in desert regions. A visual interpretation, based on key elements of interpretation, is useful for the diagnoses of dryland features. Additionally, satellite images are useful in the calculation of indicators such as the remote sensing-based indices of TCI and VCI, where such indicators show the relative variations of land surface status. Thermal images, in addition to the estimation of land surface temperature, can provide valuable information in the diagnosis of natural phenomena such as desertification.

7.6 Research Limitations

The contrasting results and conflicting views over the rate of desertification in the study area are the main constraints in the study of desertification; without clearly confirmed methods, the evaluation of accuracy, related to desertification maps, is difficult. Other research constraints, which exist usually in desert studies, are as follows:

- Administrative affairs

Time-consuming administrative process within government delays access to primary data such as meteorological data from the local organisations. Sometimes it is impossible to acquire up-to-date data.

- Data constraints

Many national research institutions and organisations which are producing and collecting data, seldom manage to cooperate in desert study research. Unfortunately, many of these data organisations are often not publicly accessible, especially for young volunteer researchers and students.

- Field accessibility

To undertake fieldwork study is one of the most important yet problematic areas in desert-related researches. Difficulties in accessing the study area minimise field work activity.

7.7 Recommendations

This study represents the indicators based on remote sensing and GIS data. However, for a more comprehensive study of desertification, evidence from field work must be gathered and indicators evaluated by field surveys and field observation.

Inevitably, any new method in environmental studies has its own limitations and is subject to drawbacks, which affect the efficiency and reliability of the methodology. Therefore, in this research, the inaccessibility to the study area in drylands presents an obstacle to field studies and the evaluation of results. Paucity of data also limits the information about the environment in question. These comments highlight the need to establish a database for dryland studies, which should be freely and easily available to students and researchers. Furthermore, the accessibility of up-to-date data helps researchers to accomplish studies in a short time, with low cost.

The reliability of remote sensing studies needs detailed information concerning factors and environments; therefore, to analyse and interpret the remote sensing images, a knowledge of other disciplines would prove useful. Disciplines such as physiology, soil science, climatology, hydrology, chemistry and physics provide invaluable information about the desertification processes.

Scientific researches, it must be said, investigate the causal factors and consequences of phenomena such as desertification. Such results should be made public, as society plays a significant role in combating desertification; coordination between governmental and professional executives and their inhabitants are vital factors in any successful project.

Furthermore, a disturbance in the natural balance of a dryland has many aftermaths. For instance, an imbalance in hydrology causes deficiency in surface moisture (drought) and increases the susceptibility of dryland to sandstorms. Frequent drought and consumption of water destroys the natural balance of watersheds, the surface of drylands becomes dry where fine

sediments are deposited. As a result, wind can blow dust away, creating sandstorms and causing high erosion.

In recent years, many sandstorms in Iran have impacted heavily on the country's economy. Therefore, in the implementation of development plans, such as reservoir construction, hydrological imbalance should be considered.

Finally, this research has been carried out by using MODIS images, therefore, it is suggested that this framework should be evaluated regionally throughout Iran, and complemented by further satellite data to understand the problems of desertification.

Bibliography

- Abbaspour, R. A., M. R. Delavar, and R. Batouli, 2003: The Issue of Uncertainty Propagation in Spatial Decision Making. *Proceedings of the 9th Scandinavian Research Conference on Geographical Information Science*, Espoo, Finland, Department of Surveying, Helsinki University of Technology, 57–65.
- Abramowitz, M., and I. A. Stegun, 1965: *Handbook of Mathematical Functions: with Formulas, Graphs, and Mathematical Tables*. Dover Publications,
- Agnew, C., and A. Warren, 1996: A Framework for Tackling Drought and Land Degradation. *Journal of Arid Environments*, **33**, 309–320.
- Ahmadi, H., 1998: *Applied Geomorphology (Desert: Wind Erosion)*. Tehran University Publication, 395 pp.
- Alavipanah, S. K., H. Ahmadi, and C. B. Komaki, 2004: A Study of the Geomorphological Facies of Yardang Area of Lut desert Based upon Photomorphic Unit Analysis of Satellite Images. *Iranian Journal of Natural Resources*, **57**, 21-34.
- Alavipanah, S. K., C. B. Komaki, A. Goorabi, and H. R. Matinfar, 2007a: Characterizing Land Cover Types and Surface Condition of Yardang Region in Lut Desert (Iran) Based upon Landsat Satellite Images. *World Applied Sciences Journal*, **2**, 212–228.
- Alavipanah, S. K., M. Saradjian, G. R. Savaghebi, C. B. Komaki, E. Moghimi, and M. K. Reyhan, 2007b: Land Surface Temperature in the Yardang Region of Lut Desert (Iran) Based on Field Measurements and Landsat Thermal Data. *J. Agric. Sci*, **9**, 287–303.
- Alonso Moral, J., L. Magdalena, and S. Guillaume, 2008: HILK: A New Methodology for Designing Highly Interpretable Linguistic Knowledge Bases Using the Fuzzy Logic Formalism. *International Journal of Intelligent Systems*, **23**, 761–794.
- Alonso Moral, J. M., 2007: Interpretable Fuzzy Systems Modeling with Cooperation between Expert and Induced Knowledge (Modelado de sistemas borrosos interpretables con cooperación entre conocimiento experto e inducido). Universidad Politécnica de Madrid-E.T.S.I. Telecommunication (UPM), 1-244 pp. <http://oa.upm.es/588/>.
- Altman, D., 1994: Research Article. Fuzzy set theoretic approaches for handling imprecision in spatial analysis. *International Journal of Geographical Information Systems*, **8**, 271-289. <http://www.informaworld.com/10.1080/02693799408902000>.
- American Meteorological Society, 1997: Meteorological drought-Policy statement. *Bull. Amer. Meteor. Soc.*, **78**, 847–849.
- Anarmar, E. R., M. R. Feyzi, and M. T. Hagh, 2010: Hierarchical fuzzy controller applied to multi-input power system stabilizer. *Turk J Elec Eng & Comp Sci*, **18**.
- Aubreville, A., 1949: *Climats, forets et désertification de L'Afrique tropicale*. Société D'Éditions Géographiques, Maritimes et Coloniales, Paris, 351 pp.
- Baja, S., M. Ramli, and M. Jayadi, 2005: Fuzzy Decision Analysis in Land Suitability Evaluation: A Tool for Precision Land Management Interpretation. Conference Proceedings of Map Asia 2005, Jakarta, Indonesia, GIS Development.
- Bartlett, J. E., J. W. Kotrlik, and C. C. Higgins, 2001: Organizational research: Determining appropriate sample size in survey research. *Information Technology Learning and*

- Performance Journal*, **19**, 43–50.
- Boken, V. K., A. P. Cracknell, and R. L. Heathcote, 2005: *Monitoring and Predicting Agricultural Drought: A Global Study*. Oxford University Press, USA,
- Bone, C., S. Dragicevic, and A. Roberts, 2005: Integrating high resolution remote sensing, GIS and fuzzy set theory for identifying susceptibility areas of forest insect infestations. *International journal of remote sensing*, **26**, 4809–4828.
- Bouchon-Meunier, B., R. R. Yager, and L. A. Zadeh, 1995: *Fuzzy logic and soft computing*. World Scientific, 512 pp.
- Brandtberg, T., 2002: Individual tree-based species classification in high spatial resolution aerial images of forests using fuzzy sets. *Fuzzy sets and systems*, **132**, 371–387.
- Burrough, P. A., 1989: Fuzzy mathematical methods for soil survey and land evaluation. *European Journal of Soil Science*, **40**, 477–492.
- Burrough, P. A., R. A. MacMillan, and W. Deursen, 1992: Fuzzy classification methods for determining land suitability from soil profile observations and topography. *European Journal of Soil Science*, **43**, 193–210.
- Casillas, J., O. Cordón, and F. Herrera, 2000: Improving the Wang and Mendel's fuzzy rule learning method by inducing cooperation among rules. *Proceedings of the 8th Information Processing and Management of Uncertainty in Knowledge-Based Systems Conference*, 1682–1688.
- Castillo, O., and P. Melin, 2008: *Type-2 Fuzzy Logic: Theory and Applications*. Springer, 252 pp.
- Chopra, P., 2006: Drought Risk Assessment using Remote Sensing and GIS: A case study of Gujarat. ITC, Faculty of Geo-Information Science and Earth Observation of the University of Twente, 67 pp.
- Chortaria, C., A. Karavitis, and S. Alexandris, 2010: Development of the SPI drought index for Greece using geo-statistical methods. BALWOIS : Water Observation and Information System for Balkan Countries, Ohrid, Republic of Macedonia.
- Congalton, R. G., L. K. Fenstermaker, J. R. Jensen, K. C. McGwire, and L. R. Tinney, 1991: Remote sensing and geographic information system data integration: error sources and research issues. *Photogrammetric Engineering & Remote Sensing*, **57**, 677–687.
- Cordón, O., F. Herrera, and F. Hoffmann, 2001: *Genetic fuzzy systems: evolutionary tuning and learning of fuzzy knowledge bases*. World Scientific, 492 pp.
- Davidson, D. A., S. P. Theocharopoulos, and R. J. Bloksma, 1994: A land evaluation project in Greece using GIS and based on Boolean and fuzzy set methodologies. *International Journal of Geographical Information Systems*, **8**, 369–384.
- Dervos, N., E. A. Baltas, and M. A. Mimikou, 2006: Rainfall-Runoff Simulation in an Experimental Basin Using Gis Methods. *Journal of Environmental Hydrology*, **14**, 1-14.
- Dohrenwend, J., and A. Parsons, 2009: Pediments in Arid Environments. *Geomorphology of Desert Environments*, pp. 377-411, Springer the Netherlands.
- Dregne, H. E., and N. T. Chou, 1992: Global desertification dimensions and costs. *Degradation and Restoration of Arid Lands*, pp. 249-281, International Center for Arid and Semiarid Land Studies, Lubbock: Texas Tech. University.

- Eastman, J. R., and M. A. Worcester, 2001: Guide to GIS and Image processing Volume 2. *Idrisi Manual*, 144 pp.
- Emam, A. R., F. Fakhri, A. Rafiei Emam, and A. Ahmadian, 2003: Desertification vulnerability in Varamin Plain, Central of Iran. *Gis Development, The Geospatial Resource Portal, Geospatial Application Papers*.
- Emberger, L., 1963: *Bioclimatic map of the Mediterranean zone: explanatory notes*. UNESCO-FAO, 58 pp.
- Erwig, M., M. Schneider, and F. Hagen, 1997: Vague Regions. *5th Int. Symp. on Advances in Spatial Databases (SSD)*, Vol. 1262 of, Springer Verlag, 298--320.
- Eswaran, H., R. Lal, and P. F. Reich, 2001: Land degradation: an overview. *Responses to Land degradation. Proc. 2nd. International Conference on Land Degradation and Desertification, Khon Kaen, Thailand. Oxford Press, New Delhi, India*, 20--35.
- Farajzadeh, M., and M. N. Egbal, 2007: Evaluation of MEDALUS model for desertification hazard zonation using GIS; study area: Iyzad Khast plain, Iran. *Pak. J. Biol. Sci.*, **10**, 2622-2630. <http://www.ncbi.nlm.nih.gov/pubmed/19070073>.
- Feiznia, S., A. N. Gooya, H. Ahmadi, and H. Azarnivand, 2001: Investigation on desertification factors in Hossein-Abad Mish Mast Plain and a proposal for a regional model. *Biaban*, **6**, 1-14.
- Fullér, R., 1995: *Neural fuzzy systems*. Springer, Berlin/Heidelberg, 289 pp.
- fuzzyTECH, 2001: User's Manual for all fuzzyTECH 5.5 Editions. www.ee.ui.ac.id/~muis/import/ft531man.pdf.
- Garavelli, A. C., M. Gorgoglione, and B. Scozzi, 1999: Fuzzy logic to improve the robustness of decision support systems under uncertainty. *Computers & Industrial Engineering*, **37**, 477-480.
- Geist, H. J., and E. F. Lambin, 2004: Dynamic causal patterns of desertification. *Bioscience*, **54**, 817--829.
- Gerrits, R., and S. Spreeuwenberg, 2000: VALENS: a knowledge based tool to validate and verify an Aion knowledge base. *ECAI 2000, Proceedings of the 14th European Conference on Artificial Intelligence*, Ed. W. Horn, Berlin, Germany, IOS Press, 731--735.
- Glantz, M. H., and N. S. Orlovsky, 1983: Desertification: A review of the concept. *Desertification Control Bulletin*, **9**, 15--22.
- Glöckner, I., 2006: *Fuzzy Quantifiers: A Computational Theory*. 1st ed. Springer,
- Guillaume, S., B. Charnomordic, and J. L. Lablée, 2002: FisPro (Fuzzy Inference System Professional): An open source portable software for designing fuzzy inference systems. Available in <http://www.inra.fr/internet/Departements/MIA/M/fispro>.
- Guyot, G., and X. F. Gu, 1994: Effect of radiometric corrections on NDVI-determined from SPOT-HRV and Landsat-TM data. *Remote Sensing of Environment*, **49**, 169--180.
- Hammouri, N., and A. El-Naqa, 2007: Hydrological modeling of ungauged wadis in arid environments using GIS. *Revista mexicana de ciencias geológicas*, **24**, 185.
- Heim, R. R., 2002: A Review of Twentieth-Century Drought Indices Used in the United States. *Bulletin of the American Meteorological Society*, **83**, 1149-1165.

- Hemphill, J., and J. E. Estes, 2003: History of Aerial Photographic Interpretation. *RSCC Volume 1 Introduction to Photo Interpretation and Photogrammetry*, Vol. 1, the International Center for Remote Sensing Education (ICRSE).
- Hodges, J., S. Bridges, and S. Yie, 1996: Preliminary results in the use of fuzzy logic for a radiological waste characterization expert system. *Mississippi State Univ., MS, Tech. Rep. MSU-960626*.
- Huete, A., C. Justice, and W. van Leeuwen, 1999: MODIS vegetation index (MOD13) algorithm theoretical basis document. *Link: http://modis.gsfc.nasa.gov/data/atbd/atbd_mod13.pdf*,
- Jang, J. R., C. Sun, and E. Mizutani, 1997: *Neuro-Fuzzy and Soft Computing: A Computational Approach to Learning and Machine Intelligence*. US ed. Prentice Hall, 614 pp.
- Jensen, J. R., 1995: *Introductory Digital Image Processing: A Remote Sensing Perspective*. 2nd ed. Prentice Hall, 316 pp.
- Ji, L., and A. J. Peters, 2003: Assessing vegetation response to drought in the northern Great Plains using vegetation and drought indices. *Remote Sensing of Environment*, **87**, 85–98.
- Jiang, B., 1998: Visualisation of Fuzzy Boundaries of Geographic Objects. *Cartography: Journal of Mapping Sciences Institute, Australia*, **27**, 31–36.
- Jomehpour, M., 2009: Qanat irrigation systems as important and ingenious agricultural heritage: case study of the qanats of Kashan, Iran. *International Journal of Environmental Studies*, **66**, 297–315.
- JRC (Joint Research Centre), 2010: European Soil Portal. <http://eusoils.jrc.ec.europa.eu/library/themes/Salinization>.
- Kassas, M., 1995: Desertification: a general review. *Journal of Arid Environments*, **30**, 115–128.
- Khalili, A., 1992: The long-term three-dimensional variation of annual temperature: case study of Iran. *Nivar*, **32**, 13-25.
- Klein, L. A., 1999: *Sensor and data fusion concepts and applications*. Society of Photo-Optical Instrumentation Engineers (SPIE) Bellingham, WA, USA,
- Kogan, F., R. Stark, A. Gitelson, L. Jargalsaikhan, C. Dugrajav, and S. Tsooj, 2004: Derivation of pasture biomass in Mongolia from AVHRR-based vegetation health indices. *International Journal of Remote Sensing*, **25**, 2889.
- Kogan, F. N., 1995: Droughts of the late 1980s in the United States as derived from NOAA polar-orbiting satellite data. *Bulletin of the American Meteorological Society*, **76**, 655–668.
- Kogan, F. N., 1997: Global drought watch from space. *Bulletin of the American Meteorological Society*, **78**, 621–636.
- Koutroumpas, A. C., I. S. Alexiou, M. Vlychou, and L. I. Sakkas, 2010: Comparison between clinical and ultrasonographic assessment in patients with erosive osteoarthritis of the hands. *Clinical rheumatology*, **29**, 511–516.
- Krinsley, D. B., 1970: *A Geomorphological and Paleoclimatological Study of the Playas of Iran. Part I*. US Government Printing Office, Washington, DC, 227 pp.
- Lal, R., 2001: Soil degradation by erosion. *Land Degradation & Development*, **12**, 519–539.
- Lal, R., T. Iivari, and J. M. Kimble, 2003: *Soil Degradation in the United States: Extent, Severity, and Trends*. 1st ed. CRC Press, 224 pp.

- Ledeneva, Y., R. G. Hernandez, and A. Gelbukh, 2008: Automatic Estimation of Parameters of Complex Fuzzy Control Systems. *New Developments in Robotics Automation and Control*, pp. 475-504, Sciyo d.o.o.
- Lee, G. S., and K. H. Lee, 2006: Application of fuzzy representation of geographic boundary to the soil loss model. *Hydrology and Earth System Sciences Discussions*, **3**, 115–133.
- Lloyd-Hughes, B., 2002: The long-range predictability of European drought. Department of Space and Climate Physics; University College London, 203 pp.
- Loukas, A., and L. Vasiliades, 2004: Probabilistic analysis of drought spatiotemporal characteristics in Thessaly region, Greece. *Natural Hazards and Earth System Science*, **4**, 719–731.
- van Lynden, G. W. J., 2004: European and world soils: present situation and expected evolution. I International Conference on Soil and Compost Eco-biology, León - Spain, soilACE, 55-63.
- Mahler, R. P. S., 1995: Combining ambiguous evidence with respect to ambiguous a priori knowledge. Part II: Fuzzy logic. *Fuzzy Sets and Systems*, **75**, 319-354.
- Mamdani, E., 1974: Application of fuzzy algorithms for control of simple dynamic plant. *Proceedings of IEEE*, **121**, 1585-1588.
- Mangimeli, J., 2010: Geology of sand dunes: White Sands National Monument. *US National Park Service (NPS)*, <http://www.nps.gov/whsa/naturescience/index.htm>.
- Mather, P., 2004: *Computer processing of remotely sensed images: an introduction*. 3rd ed. John Wiley & Sons, Chichester West Sussex England, Hoboken NJ, 442 pp.
- Matinfar, H. R., 2005: Evaluation of sensor data, ASTER, LISS-II, ETM +, TM, MSS to identify soil based on field studies and geographic information systems. University of Tehran, 301 pp.
- Mbagwu, J., 2003: Aggregate stability and soil degradation in the tropics. *Invited presentations College on Soil Physics*, 245–252.
- McKee, T. B., N. J. Doesken, and J. Kleist, 1993: The relationship of drought frequency and duration to time scales. *Eighth Conference on Applied Climatology*, Anaheim, CA, American Meteorological Society, Boston, MA, 179-184.
- Metternicht, G., 2001: Assessing temporal and spatial changes of salinity using fuzzy logic, remote sensing and GIS. Foundations of an expert system. *Ecological Modelling*, **144**, 163–179.
- Mian, T. M., 1999: Fuzzy Logic Based Automotive Airbag Control System. University of Windsor, 170 pp.
- Middleton, N., and D. Thomas, 1992: *World Atlas of Desertification*. United Nations Environment Programme / Edward Arnold.
- Mishra, S. K., and V. P. Singh, 2003: *Soil conservation service curve number (SCS-CN) methodology*. Kluwer Academic Publishers, 536 pp.
- Mitasova, H., and L. Mitas, 1999: Modeling soil detachment with RUSLE 3d using GIS. *University of Illinois at Urbana-Champaign*, Available online at: <http://www2.gis.uiuc.edu>, **2280**.
- Moameni, A., 2000: Impact of Land Utilization Systems on Agricultural Productivity. the APO Seminar on Impact of Land Utilization Systems on Agricultural Productivity, Islamic Republic of Iran, Tokyo, Japan, Asian Productivity Organization(APO), 186-210.
- Morgan, L. A., 2007: *Integrated geoscience studies in the greater Yellowstone area [electronic*

- resource] : volcanic, tectonic, and hydrothermal processes in the Yellowstone geocosystem / edited by Lisa A. Morgan. U.S. Dept. of the Interior, U.S. Geological Survey, [Reston, Va.].*
- Murray, S., L. Burke, D. Tunstall, and P. Gilruth, 1999: *Drylands Population Assessment II*. Global land degradation information system (LADA), UN Development Programme, New York.
- Myneni, R., F. Hall, P. Sellers, and A. Marshak, 1995: The interpretation of spectral vegetation indexes. *IEEE Trans. Geosci. Remote Sensing*, **33**, 481-486.
- National Electrical Manufacturers Association (NEMA), I. T., 2005: *IEC 61131-7 Ed. 1.0 b:2000, Programmable controllers - Part 7: Fuzzy control programming*, Multiple. Distributed through American National Standards Institute (ANSI), Rossly, USA.
- Okin, G. S., D. A. Roberts, B. Murray, and W. J. Okin, 2001: Practical limits on hyperspectral vegetation discrimination in arid and semiarid environments. *Remote Sensing of Environment*, **77**, 212-225.
- Pakparvar, M., 1998: Desert research and control of desertification in Iran. *Proceedings of the Intl. Symposium New Technologies to Combat Desertification*, Tehran, Iran, 25-34.
- Parida, B. R., 2006: Analysing the effect of severity and duration of Agricultural drought on crop performance using Terra/MODIS Satellite data and Meteorological data. ITC - Faculty of Geo-Information Science and Earth Observation of the University of Twente, 92 pp.
- Pashiardis, S., and S. Michaelides, 2008: Implementation of the Standardized Precipitation Index (SPI) and the Reconnaissance Drought Index (RDI) for regional drought assessment: a case study for Cyprus. *European Water Publication*, **23**, 57-65.
- Quiring, S. M., and T. N. Papakyriakou, 2005: Characterizing the spatial and temporal variability of June-July moisture conditions in the Canadian prairies. *International Journal of Climatology*, **25**, 117-138.
- Rasmussen, K., B. Fog, and J. E. Madsen, 2001: Desertification in reverse? Observations from northern Burkina Faso. *Global Environmental Change*, **11**, 271-282.
- Renard, K. G., and J. R. Freimund, 1994: Using monthly precipitation data to estimate the R-factor in the revised USLE. *Journal of Hydrology*, **157**, 287-306.
- Renard, K. G., G. R. Foster, G. A. Weesies, D. K. McCool, and D. C. Yoder, 1996: Predicting soil erosion by water: a guide to conservation planning with the revised universal soil loss equation (RUSLE), USDA Agriculture Handbook Number 703. *Washington, DC*,
- Robinson, V. B., 2003: A perspective on the fundamentals of fuzzy sets and their use in geographic information systems. *Transactions in GIS*, **7**, 3-30.
- Rubio, J. L., and E. Bochet, 1998: Desertification indicators as diagnosis criteria for desertification risk assessment in Europe. *Journal of Arid Environments*, **39**, 113-120.
- Sasikala, K. R., and M. Petrou, 2001: Generalised fuzzy aggregation in estimating the risk of desertification of a burned forest. *Fuzzy Sets and Systems*, **118**, 121-137.
- Schmidt, H., and A. Karnieli, 2000: Remote sensing of the seasonal variability of vegetation in a semi-arid environment. *Journal of Arid Environments*, **45**, 43-59.
- Seiler, R. A., F. Kogan, and J. Sullivan, 1998: AVHRR-based vegetation and temperature condition indices for drought detection in Argentina. *Advances in Space Research*, **21**, 481-484.

- Sepaskhah, A. R., and P. Sarkhosh, 2005: Estimating storm erosion index in southern region of IR Iran. *Iranian Journal of Science & Technology, Transaction B, Engineering*, **29**.
- Sepehr, A., A. M. Hassanli, M. R. Ekhtesasi, and J. B. Jamali, 2007: Quantitative assessment of desertification in south of Iran using MEDALUS method. *Environ Monit Assess*, **134**, 243-254.
- Shamsipour, 2007: Analysis of Drought Events for Kashan Area with NOAA-AVHRR Data. University of Tehran, 300 pp.
- Sobrino, J. A., V. Caselles, and C. Coll, 1993: Theoretical split-window algorithms for determining the actual surface temperature. *Il Nuovo Cimento C*, **16**, 219–236.
- Soto, M., L. Giddings, and B. Rutherford, 2009: Standardized precipitation index zones for México. *Atmósfera*, **18**.
- Symeonakis, E., and N. Drake, 2004: Monitoring desertification and land degradation over sub-Saharan Africa. *International Journal of Remote Sensing*, **25**, 573.
- Tang, X., 2004: Spatial object modelling in fuzzy topological spaces: with applications to land cover change. ITC, Faculty of Geo-Information Science and Earth Observation of the University of Twente, 218 pp.
- Thenkabail, P. S., M. S. D. Gamage, and V. U. Smakhtin, 2004: *The use of remote sensing data for drought assessment and monitoring in Southwest Asia*. International Water Management Institute (IWMI), Clolombo, Sri Lanka,
- Toy, T. J., and G. R. Foster, 1998: Guidelines for the Use of the Revised Universal Soil Loss Equation (RUSLE) version 1.06 on Mined Lands, Construction Sites and Reclaimed Lands. *Office of Surface Mining, Denver, CO*, 103 pp.
- Tsakiris, G., and H. Vangelis, 2004: Towards a drought watch system based on spatial SPI. *Water Resources Management*, **18**, 1–12.
- Tucker, C. J., 1979: Red and photographic infrared linear combinations for monitoring vegetation. *Remote sensing of Environment*, **8**, 127–150.
- Unganai, L. S., and F. N. Kogan, 1998: Southern Africa's recent droughts from space. *Advances in Space Research*, **21**, 507–511.
- United Nations & International Strategy for Disaster Reduction, 2004: *Living with risk: a global review of disaster reduction initiatives / International Strategy for Disaster Reduction, United Nations*. United Nations, New York, <http://www.unisdr.org/eng/about%5Fisdr/bd-lwr-2004-eng.htm>.
- Vermote, E. F., and S. Kotchenova, 2008: Atmospheric correction for the monitoring of land surfaces. *Journal of Geophysical Research-Atmospheres*, **113**, 12.
- Wang, F., 1990: Improving remote sensing image analysis through fuzzy information representation= Amélioration de l'analyse d'images de la télédétection à l'aide de la représentation floue d'information. *Photogrammetric Engineering and Remote Sensing*, **56**, 1163–1169.
- Wang, L. X., and J. M. Mendel, 1992: Generating fuzzy rules by learning from examples. *IEEE Transactions on systems, man and cybernetics*, **22**, 1414–1427.
- Werner, J., N. Woodward, R. Nielsen, R. Dobos, and C. Hoefl, 2007: Hydrologic Soil Groups. *National Engineering Handbook*, 7:1-5, United States Department of Agriculture(USDA),

- Natural Resources Conservation Service(NRCS), Washington, DC.
- Werner, J., N. Woodward, D. Q. Quan, R. Nielsen, C. Kluth, A. Plummer, J. Van Mullem, and C. Conaway, 2004: Estimation of Direct Runoff from Storm Rainfall. *Part 630 National Engineering Handbook*, pp. 10:1-51, United States Department of Agriculture (USDA), Natural Resources Conservation Service (NRCS), Washington, DC.
- Wilhite, D. A., 2000: Drought as a natural hazard: Concepts and definitions. Drought: A Global Assessment. *Hazards Disasters Ser*, **1**, 3–18.
- Wischmeier, W. H., 1962: Storms and soil conservation. *Journal of Soil and Water Conservation*, **17**, 55–59.
- Wischmeier, W. H., 1974: New developments in estimating water erosion. *24th. Annual Meeting of the Soil Conservation Society of America*, Syracuse, New York, 179–186.
- Wischmeier, W. H., and D. D. Smith, 1978: *Predicting Rainfall Erosion Losses. A Guide to Conservation Planning. Agriculture Handbook No. 537.* , Science and Education Administration, U.S. Department of Agriculture (USDA), Washington, 58 pp.
- Zadeh, L., 1965: Fuzzy sets. *Information and Control*, **8**, 338-353.
- Zadeh, L., 1975: The concept of a linguistic variable and its application to approximate reasoning-- I. *Information Sciences*, **8**, 199-249.
- Zhan, X., and M. L. Huang, 2004: ArcCN-Runoff: an ArcGIS tool for generating curve number and runoff maps. *Environmental Modelling & Software*, **19**, 875–879.
- Zhu, A. X., B. Hudson, J. Burt, K. Lubich, and D. Simonson, 2001: Soil mapping using GIS, expert knowledge, and fuzzy logic. *Soil Science Society of America Journal*, **65**, 1463.

CURRICULUM VITAE

Chooghi Bairam Komaki



Date of Birth: August 6, 1973, Gonbad-e-kavous, Iran

Citizenship: Iranian

Marital Status: Married

1991- 1995	Secondary School (high school), Gonbad-e-kavous, Iran
1995-1999	Agricultural Engineering , Soil Science at University of Gorgan, Iran
1999-2002	Natural Resources Engineering, Desert Zones Management at University of Tehran, Iran

Professional Career

May 2000 to May 2002	Project on Study of Yardangs in the Lut Desert using Satellite Image Processing, Desert Research Center, Tehran University
January 2005 to January 2006	Identification and Organization of Irrigation System and Drainage Projects to Develop and Cultivate Crops in the Atrak Catchment, Mojab Engineering Consulting Company, Gorgan

Teaching Experience

- Teaching of training courses of Geographic Information System (GIS) softwares at Tarbiat Modares University, Tehran and Tarbiat Moallem Centre, Gonbad-e-kavous, Iran
- Teaching at the University of Shahroud, Iran:
 - Remote Sensing (RS)
 - Geographic Information System (GIS)

Honours and Awards

- First position in M.Sc. National Entrance Exam ,Iran,1999
- Third position in Ph.D. National Entrance Exam, Iran, 2001

Languages

Language	Spoken	Written	Reading
Turkmen	Mother tongue	Mother tongue	Mother tongue
Farsi	Excellent	Excellent	Excellent
English	Very good	Very good	Excellent
Turkish	Excellent	Fair	Fair
Arabic	Poor	Poor	Fair
German	Poor	Poor	Fair

LIST OF PUBLICATIONS

Scientific Publications

- Alavi Panah, S. K., and C. B. Komaki, 2003: Investigation of Land Surface Temperature in Lut Desert. *Journal of Biaban*, **7**.
- Alavipanah, S. K., H. Ahmadi, and C. B. Komaki, 2004: A Study of the Geomorphological Facies of Yardang Area of Lut desert Based upon Photomorphic Unit Analysis of Satellite Images. *Iranian Journal of Natural Resources*, **57**, 21-34.
- Alavipanah, S. K., C. B. Komaki, A. Goorabi, and H. R. Matinfar, 2007a: Characterizing Land Cover Types and Surface Condition of Yardang Region in Lut Desert (Iran) Based upon Landsat Satellite Images. *World Applied Sciences Journal*, **2**, 212–228.
- Alavipanah, S. K., M. Saradjian, G. R. Savaghebi, C. B. Komaki, E. Moghimi, and M. K. Reyhan, 2007b: Land Surface Temperature in the Yardang Region of Lut Desert (Iran) Based on Field Measurements and Landsat Thermal Data. *Journal of Agricultural Science and Technology (JAST)*, **9**, 287–303.
- Komaki, C. B., and S. K. Alavi Panah, 2006: Study of Spectral Separability of the Lut Desert Classes Based on Remotely Sensed Data. *Geographical Researches*, **37**, 13-27.